December 2012

Evaluation of a Microwave Receiver Based on a Track and Hold Amplifier

Joseph William DiChiara
Worcester Polytechnic Institute

Julian Alexander DeZulueta
Worcester Polytechnic Institute

REL MQP 4711

Evaluation of a Microwave Receiver Based on a Track and Hold Amplifier

A Major Qualifying Project Report
Submitted to the Faculty of the
WORCESTER POLYTECHNIC INSTITUTE
in partial fulfillment of the requirements of the
Degree of Bachelor of Science in
Electrical and Computer Engineering

By:

Julian De Zulueta
Joseph William Dean DiChiara

On Site Advisors:	Academic Advisors:
Naomi Marcus	Dr. Reinhold Ludwig
Brian McHugh	Dr. Sergey Makarov
John Putnam	
Eric Renda	

Abstract

Our project objective was to evaluate a new circuit topology to explore if it could be integrated into an existing superheterodyne receiver chain, making a smaller and simpler RF front-end. A traditional superheterodyne receiver was built and measured so we could easily compare and contrast characteristics between the two models. Using the same parameters, we evaluated the new wideband track-and-hold amplifier and compared the two models. Our testing and research has shown that while the device does work, the following significant problems must be overcome for the track-and-hold amplifier to be implemented in the superheterodyne chain: rotating IF frequency, poor linearity, instability at integer multiples of the clock, and precise phase locking.

Table of Contents

Table of Figures

Executive Summary

The superheterodyne architecture has been the most popular choice for radio frequency (RF) receivers for the past 70 years, but the rise of high-speed sampling devices has caused experts to question the dominance of this architecture in receiver design. Ideally, the goal of all receiver designers is to connect the antenna directly to the digital signal processor (DSP), but our current level of technology cannot achieve this goal. The use of high-speed sampling devices works toward this goal: it shortens the analog portion of the RF front end of the receiver and moves the antenna closer to the DSP. The goal of this project was to build a new receiver architecture around a high-speed sampling device and compare it to the superheterodyne architecture currently deployed by our sponsor. To determine which architecture is superior, we used the following list of parameters: linearity, signal to noise ratio, noise figure, cost and size. Using the comparison, we compiled a final list of recommendations for the use of the THA architecture.

The new receiver architecture was built around a track-and-hold amplifier (THA) made by Hittite Microwave. This device samples at 4 GS/s and has an input frequency range from DC to 18 GHz. This device was used to under-sample an X-band (8-12 GHz) signal; it reproduces a low frequency output signal that can be fed into an analog to digital converter (ADC). A generic block diagram of our implementation of this new architecture can be seen in Figure 1. Our analysis of the THA system raised important issues relative to phase locking and signal instability.

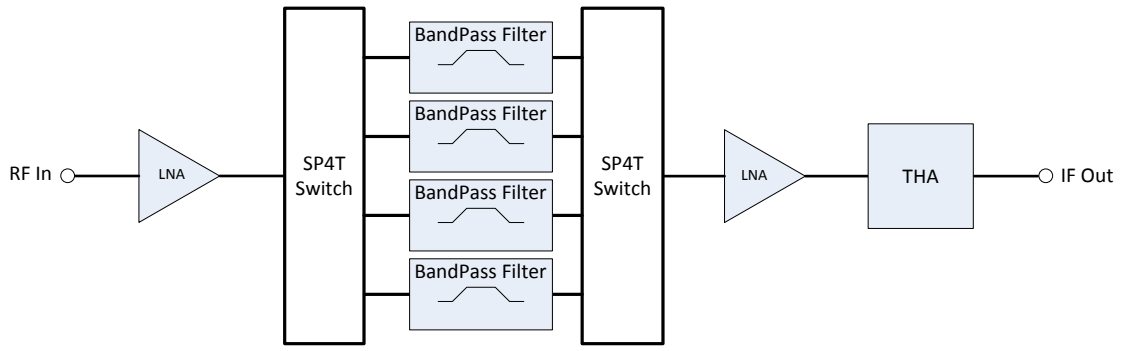

Figure 1: Track-and-hold architecture

We determined that the THA had a precise absolute sample accuracy requirement. To verify the device samples at the accurate time, we provided a 10 MHz reference signal between the clock and RF signal generator. The large slew rate of the X-band signal created a need for a precise phase lock between the referencing signals of the clock and the input signal. The accuracy needed between these two devices for a $1V_{pp}$, 10 GHz signal was approximately 159 fs. The limitations of the signal generator made the sample accuracy of 159 fs impossible to achieve. The inability to achieve the needed sample accuracy did not affect our measurements since no data was being processed, however this is a very important finding for future applications.

One of our THA setups witnessed instability using a 10 GHz signal and a 500 MHz clock. We determined that when the signal frequency was a whole number multiple of the clock frequency, the device became unstable. The instability of the output frequency appears to be a consequence of how the THA was designed. Specifically, when the signal divided by the clock is a whole number, the output frequency is reduced to 0 Hz, which means that the input signal cannot be reconstituted. Implementing the THA design was difficult due to the instability, but avoiding the unstable sets of clock and frequency is possible.

The gain compression, signal to noise ratio, and noise figure of the two architectures are all sufficient for a receiver design, but there are differences between the linearity, cost and size parameters. The linearity in the THA architecture was approximately 20 dB lower than the superheterodyne design. The linearity parameter alone is not sufficient enough to rule out the THA architecture, since more linearity can be achieved in other ways. Therefore, the cost and size comparisons for the two architectures must be factored into the overall decision. The THA architecture is both smaller and cheaper than the superheterodyne receiver due to removal of the local oscillator and the image rejection mixer, which also reduced the cost of the design by approximately $5,000. Using these comparisons, a list of recommendations was created. These recommendations are based on the problems that must be overcome to create the most optimized THA architecture. The key five recommendations include:

1. The THA device must have only 1 output frequency for all 4 channels.
2. There can be no instability across any of the 4 channels.
3. More linearity in the receiver may be needed depending on the application.

4. The large noise figure of the device must be suppressed using some method.
5. When operating with X-band signals, the signal and clock of the THA must be phase locked to approximately 159 fs.

If these 5 recommendations can be implemented, then the THA architecture will become a more cost-effective receiver design with competitive technical performance parameters when compared to the conventional superheterodyne design.

Chapter 1 : Introduction

In the field of electrical engineering and communications, the radio frequency (RF) receiver is an important device that allows for the acquisition of information collected by an antenna. The first method implemented was super-heterodyne (superheterodyne) receiver that converts an RF signal to at least 1 intermediate frequency before the final conversion to 0 Hz (baseband) for digital processing. While there have been many other architectures, the superheterodyne design is preferred due to certain advantages and is most widely implemented for receiver architecture [1]. However, one of the disadvantages to using the superheterodyne architecture is the relatively high level of cost and complexity. For decades, system designers have worked towards simplification of RF receivers. Direct connection of a wideband and high dynamic range analog to digital converter to the output of an antenna represents the ultimate in receiver simplification, eliminating the RF components found in an RF receiver. However, the bandwidth and dynamic range of ADCs are not adequate for this approach at RF frequencies [2].

Recently, new track and hold amplifiers (THAs) were introduced by Hittite Microwave [5]. These components are ultra-wideband, external versions of the THAs that are typically found in the input of ADCs. With bandwidths up to 18 GHz and high dynamic range, these components offer the possibility of moving the digital interface in a receiver closer to the antenna output and simplifying receiver architecture.

1.1 : Background

The background material in this section gives a brief introduction into how superheterodyne architectures were discovered and the minimum information needed to understand what is being tested. Signal-to-noise ratio, dynamic range, and third-order products are the most important things that will be tested throughout this project. The background material on these tests is repeated in the appendix for receiver parameters. Finally, this section goes into the different architecture that will be analyzed and how we expect the result to turn out.

1.2 : History

The signal processing technique of heterodyning was first invented in 1901 by Reginald Fessenden. This technique generates new frequencies based on the multiplication of two input frequencies. The two frequencies, f_1 and f_2, are injected into a mixer where the non-linear characteristic of the mixer produces new frequencies nf_1 +/- mf_2, where n and m are any integers.

The sum and difference of the two input frequencies, $f_1 + f_2$ and $f_1 - f_2$, are known as the mixing products and are the lowest order of these new frequencies. Ideally, undesired mixing products are filtered out of the mixer's output, leaving only the desired signal. The desired signal in receivers is typically the difference, $f_1 - f_2$, and is called the intermediate frequency (IF).

The superheterodyne receiver was invented by US Army Major Edwin Armstrong in 1918 during World War I with the purpose of improving early radio communications. The main issue with previous receivers was that vacuum tubes were only able to process signals at lower frequencies but could not be used for higher frequencies. Armstrong began to develop a method for improving the previous design by translating higher frequencies to a lower frequency that could be handled by the vacuum tubes effectively. This frequency translation technique was named heterodyning.

The superheterodyne receiver allowed for the same IF to be produced amongst the different frequencies used throughout different stations. Previously, the amplification and filtering stages needed to be adjusted in order to produce the desired IF. During the 1920s, the superheterodyne receiver was being heavily used by the military, but less frequently for commercial purposes due to higher cost and greater learning curve required to use it. Armstrong sold his patent rights to Westinghouse who in turn sold it to the Radio Corporation of America (RCA). Many engineers at both Westinghouse and RCA were trying to develop a method for making this receiver more effective for commercial use. They provided extra audio frequency amplification to ensure proper functionality especially within city limits and steel buildings. These areas provided far weaker signals than signals being transmitted through suburban areas. By the mid-1930s, the cost to implement the superheterodyne began to fall due to improvements in the design, requiring fewer tubes. During this time period, an increase in the number of broadcasting stations led to the need for higher performance receivers as more signals being broadcasted required greater selectivity from receivers. This increase in broadcasting stations in addition to the lower cost eventually led to the superheterodyne becoming the most widely used technique for commercial receivers. The superheterodyne receiver essentially began as a design used primarily by the military, but it eventually became the standard receiver everywhere [3].

A basic superheterodyne receiver consists of several stages beginning with the antenna. The antenna is required in order to collect a signal wirelessly. The output of the antenna is then

amplified by an RF amplifier. After amplification, the input signal enters a mixer, where it is multiplied with a second signal, known as the local oscillator (LO), to produce the IF signal. The LO signal can be generated by one of any number of different signal generators or oscillators. The frequency of the LO depends on the input signal frequency and is tuned to produce a constant IF. Equation (1) illustrates how multiplying, or mixing, two sine waves produces two new signals with the frequencies set as the sum and difference of the two fundamental frequencies where f_{RF} is the frequency of the input RF signal and f_{LO} is the frequency of the LO.

$$\sin(2\pi f_{RF}t) * \sin(2\pi f_{LO}t) = \frac{1}{2}\{\cos[(2\pi f_{RF} - 2\pi f_{LO})t] - \cos[(2\pi f_{RF} + 2\pi f_{LO})\,t]\} \quad (1)$$

If, however, the frequency from the LO is greater than the input frequency, it is called high-side injection. If the input frequency is greater than the LO frequency, this is considered to be low-side injection. The difference of high-side versus low-side is important because high-side injection causes the frequency spectrum of the original RF signal to be inverted. This phenomenon occurs because the input frequencies in the lower band became the upper band in the output. These signals are then sent through an IF band-pass filter leading to the removal of all the undesired signals. The IF band-pass filter is designed to be very selective and generally provides high attenuation of any unwanted signals while providing low insertion loss for the desired IF signal.

1.3 : Receiver Parameters

The following sections are an overview of the important performance parameters that will be tested throughout the project. These parameters are also summarized in the appendix.

1.3.1 : Signal to Noise Ratio and Noise Figure

Noise in a receiver is very important to consider when receiving a signal. By comparing the desired signal power to the noise power in a particular system, one can determine whether the noise in the system will allow the desired signals to be processed. The parameter used to define the ratio is called the signal to noise ratio (SNR). The SNR is defined as the root-mean-square (RMS) signal amplitude divided by the average root-sum-square (RSS) of the noise, excluding DC, harmonics and other spurious signals. Noise power is defined over a certain frequency range or bandwidth. The exact formula for calculating SNR can be seen in Equation (2), where Pout and $Pout_{noise}$ are in Watts.

$$SNR = 10 * \log \frac{Pout}{Pout_{noise}} \quad (2)$$

In general, SNR for a receiver degrades as the bandwidth increases. Figure 2 below shows a typical receiver output at an IF frequency of 1.05 GHz. Assuming we are operating at room temperature with a bandwidth of 200 MHz, the SNR of the figure below is approximately 70 dB. Our noise floor is defined in Equation (3) where k is the Boltzmann constant, which is 1.3806e-23JK^{-1}, and T is the room temperature in Kelvin. Using a bandwidth (BW) of 100kHz, the noise floor will be -120 dBm. The signal in Figure 3 is contained in an ideal system where all the harmonics and intermodulated products are filtered out. Otherwise, these distorted products would affect the SNR.

$$Pout_{noise} = 10 * \log(k * T * BW) = -174 + 10 * \log(BW) \quad (3)$$

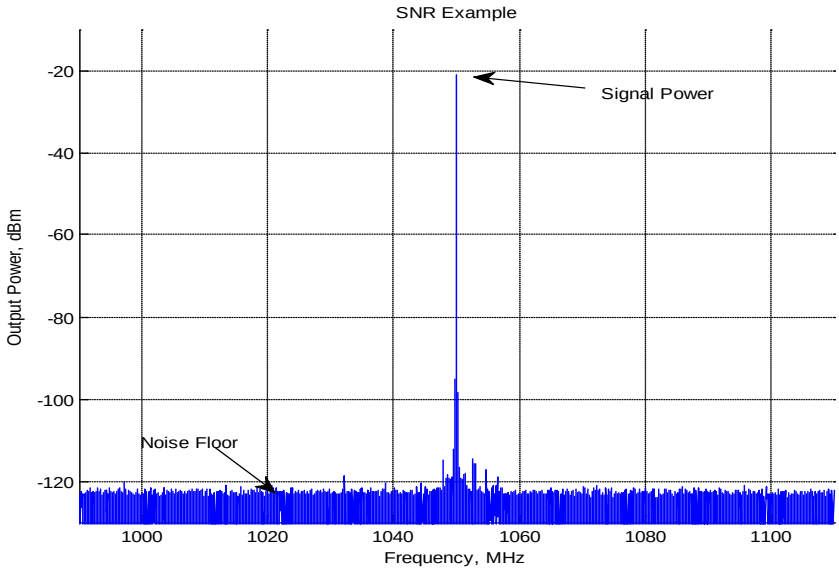

Figure 2: Typical output for receiver at IF stage

SNR is not the only parameter that determines relative strength of the signal versus the noise. One of the other parameters to consider is the signal to noise and distortion ratio (SINAD). This test takes into account the harmonics and other distortion products that could exist in the system and includes them in the noise calculations. When two signals at frequencies f_1 and f_2 pass through a non-linear component in a receiver, the non-linear characteristic produces frequencies at nf_1 +/- mf_2 where n and m are integers. Harmonics are the nf_1 or mf_2 integer multiples of f_1 and f_2, while other distortion products where both n and m $\neq$ 0, are referred to as intermodulation products. The two-tone third order intermodulation products $2f_1 - f_2$ or $2f_2 - f_1$ are particularly troublesome, since they can fall directly within the IF passband and cannot easily

be filtered out. The power ratio of harmonic or intermodulation distortion products to the desired signal is in units of decibels with respect to the carrier (dBc). While SNR disregards distortion products when calculating the signal to noise ratio, SINAD does not and is therefore a more accurate representation of the system performance. The formula for calculating the SINAD ratio in decibels can be seen in Equation (4) [4].

SNR is used in calculating the noise figure (NF) of a receiver. Noise figure is a ratio of the signal to noise ratio at the input of a receiver divided by the signal to noise ratio at the output of a receiver, which is seen in Equation (5). Note that the signal, noise, and distortion values in Equation (4) and Equation (5) are all power levels while SINAD and NF are recorded in decibels.

$$SINAD = 10 * \log \frac{Pout + Pout_{noise} + Pout_{distortion}}{Pin_{noise} + Pin_{distortion}} \quad (4)$$

$$NF = 10 * \log \frac{SNR_{in}}{SNR_{out}} \quad (5)$$

1.3.2 : Dynamic Range

The dynamic range (DR) of a receiver is the ratio between the maximum input signal level and the minimum detectable signal level. For a receiver system, the dynamic range is bounded by the noise floor ($P_{out_{noise}}$) on the lower side and the 1dB compression point of the RF amplifier (P_{1dB}) on the upper side. If these two values are calculated in decibels (dB or dBm) then the formula for calculating the dynamic range of the system can be seen in Equation (6).

$$DR = P_{1dB} - Pout_{noise} \quad (6)$$

While this is useful, most RF receiver designers use another formula that is called spurious free dynamic range (SFDR). The definition for spurious free dynamic range is the ratio between the maximum output signal power and the highest spur which is generally the third-order intermodulated products [6]. This dynamic range calculation takes into account the undesired intermodulation products or spurs in the system that might be due to undesired, random spurs and are greater than the noise floor. SFDR is calculated as the output power ($P_{\omega 1}$) for a desired signal frequency divided by the output power of the third-order intermodulation products ($P_{2\omega 1-\omega 2}$). Equation (7) shows the formula for calculating the SFDR, note that everything is calculated in dB. As noted earlier, intermodulation distortion (IMD) involves the generation of new signals that are not just at harmonics. “Third-order IMD (IM_3) results, for an

input consisting of two signals ω_1 and ω_2, in the production of new signals at $2\omega_1 \pm \omega_2$ and $2\omega_2 \pm \omega_1$ [7].” The third-order IMD products at $2\omega_1 - \omega_2$ and $2\omega_2 - \omega_1$ can be quite troublesome, since for two signals ω_1 and ω_2 that are closely spaced and within the input signal range, the IMD products can appear within the IF passband and cannot easily be filtered out.

$$SFDR = P_{\omega 1} - P_{2\omega 1-\omega 2} \tag{7}$$

1.3.3 : Design

MITRE has recently been exploring ways to simplify the superheterodyne receiver architecture, reducing receiver cost and complexity. Seen in Figure 3 is a block diagram of the existing superheterodyne architecture that was modified. This project assisted MITRE in evaluating a new integrated circuit (IC) created by Hittite Microwave that can be implemented in the superheterodyne architecture. Typical high speed analog to digital converters (ADC’s) can sample signals reliably at a maximum of 3-4 GHz sampling rate with a bandwidth of 1-2 GHz. However, this new component from Hittite is a track and hold amplifier (THA) that can sample signals at input frequencies up to 18 GHz. The new THA can then be used as a master sampler at the front end of an ADC taking in a high frequency input signal and outputting a low bandwidth held wave-form to be processed by the ADC. One of our main objectives included creating a block diagram for the microwave receiver based on the new THA.

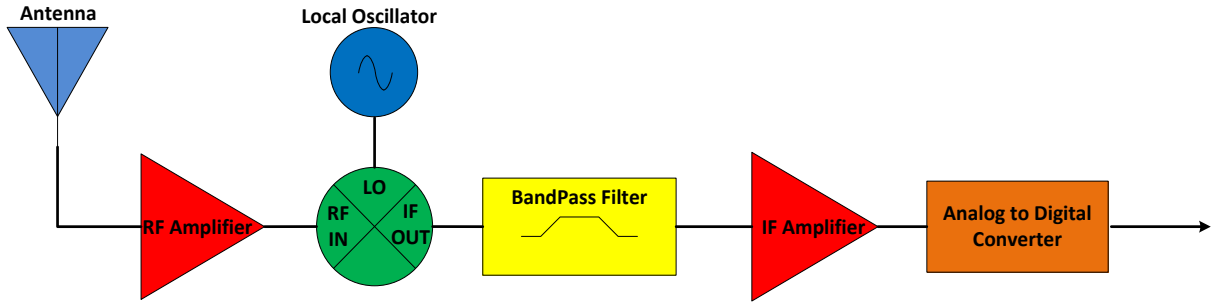

Figure 3: Superheterodyne block diagram

This new component from Hittite Microwave does not affect the overall sampling speed of the ADC, but allows sampling signals at a much higher frequency. Figure 4 shows a graph of how the THA in conjunction with a high speed ADC performed versus the same ADC by itself. Note that the units of dBFS stand for decibels at full scale range where 0dBFS implies that the device is operating at full scale range. Notice how the traditional ADC has a large loss in

amplitude starting at 2 GHz, while the THA with the ADC performs significantly better, with a decrease in amplitude of only a few dB up to 16 GHz. One of the other advantages of using the Hittite THA as the master sampler is linearity. At higher input frequencies the, "ADC converter linearity limitations… are also mitigated because the settled THA waveform is processed with the optimal low frequency linearity of the ADC [5]." The improved linearity of the ADC will also cause a better signal-to-noise ratio, which will be discussed in later sections.

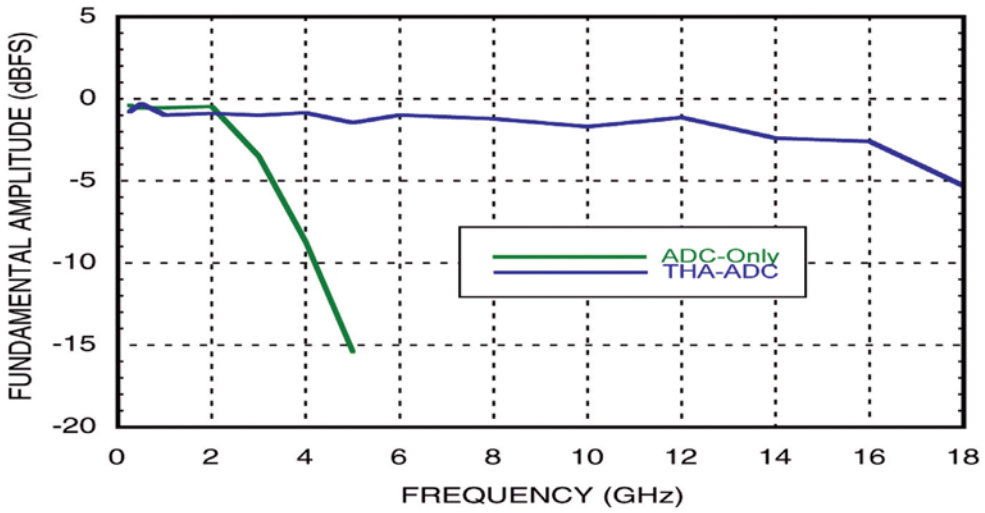

Figure 4: Signal amplitude versus input bandwidth of ADC alone and ADC with THA [5]

Seen in Figure 5 is the block diagram of how the superheterodyne architecture was modified to test the new Hittite track-and-hold amplifier. Overall, the design became much simpler since there is no external frequency mixing. The THA takes in the signal from the antenna and under samples the signal and outputs it directly into the ADC. As stated before, the goal of all RF designers is to hook and antenna directly to a high dynamic range ADC, and this new THA.

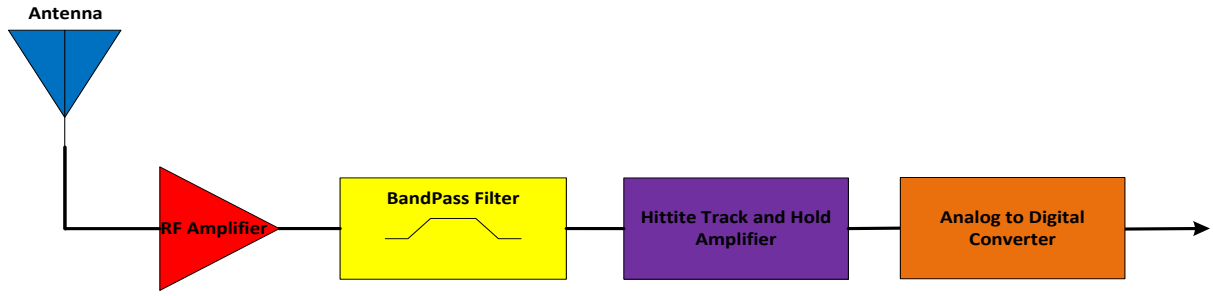

Figure 5: Track-and-hold Architecture

Chapter 2 : Objective

The main objective of this project was to compare a typical superheterodyne RF receiver already built by MITRE to a prototype based on the Hittite Microwave THA setup that was constructed by us. The goal was to initially use evaluation boards to test the performance of the THA. Development and evaluation of a prototype receiver based on the THA is the ultimate objective of this project. By comparing the traditional superheterodyne design to our prototype, we intended to confirm the reported data by Hittite Microwave and determine its viability for inclusion in the traditional superheterodyne design.

Chapter 3 : Approach

For this project, we evaluated and compared the performance between two different receiver designs. The first design included Hittite's 18GHz Ultra Wideband Track-and-Hold Amplifier, while the second was a traditional superheterodyne receiver. The traditional superheterodyne receiver operated in the X-band, which is 8-10 GHz, and the receiver based on the THA operated at the same frequency. They were compared on the basis of several parameters including third-order intercept point (IP3), dynamic range (DR), signal-to-noise ratio (SNR), noise figure (NF), and 1-dB Compression (1dB). A variety of equipment was used to carry out this project such as signal generators, power supplies, digital multi-meters, oscilloscopes, signal analyzers and network analyzers.

One of the major disadvantages with current ADCs is their inability to sample signals above a few GHz while maintaining reasonable dynamic range or SNR. Hittite Microwave's 18GHz Ultra Wideband Track-and-Hold Amplifier has the potential to allow sampling at very high frequencies while maintaining good dynamic range. This could allow simplification of a receiver, resulting in fewer steps or processes between the output of a receiver antenna and the input of an ADC. The THA was implemented in a receiver design and the parameters noted above were measured for the system and compared to the parameters for the traditional receiver.

When comparing these two receivers against each other, the goal was to see a major difference between the two designs. Some of the more important parameters that we focused heavily on are SNR, IP3, NF and 1 dB Compression. The increase in high frequency linearity offered by the THA should cause the ADC to have a higher dynamic range and SNR. The third-order products that is so troublesome for receivers should have less power due to the increased linearity. The major question was whether or not the ADC performed significantly better while operating in conjunction with the THA. A cost analysis of both architectures will be necessary for comparison. Even if the Hittite THA performs significantly better than the traditional superheterodyne architecture, it may not be viable from a cost perspective.

Chapter 4 : Superheterodyne Test Bench

The superheterodyne setup that we evaluated can be seen in Figure 6. The superheterodyne receiver architecture reduces an RF frequency to an IF frequency by mixing two signals from the antenna and the LO. The IF is generally considered to be the absolute difference between the RF and LO frequency. When testing the superheterodyne receivers, there were several issues we needed to troubleshoot before the receivers functioned properly. We performed a basic test on these receivers by connecting a signal generator to the input of the receiver and measured to see if the IF at the output was at an appropriate power level using a spectrum analyzer. When testing Rx02, we noticed that the output power level was much lower than the output power level from Rx01. This power level difference was attributed to the quadrature hybrid being connected in reverse with respect with the two IF ports from the mixer. Another issue was found when measurements we had taken previously were inconsistent with newer measurements. After measuring the signal at several stages within the superheterodyne chain, we found an amplifier that was actually attenuating the signal. The attenuating amplifier was shorted from power to ground, which led to it attenuating 10 dB instead of amplifying 25 dB. We used two different superheterodyne receivers, Rx01 and Rx02, in order to measure any difference in results between the two receivers. The two receiver setup allows us to have some diversity and allows us to perform comparisons. Note that this chapter will only show graphs for Rx01, but all of the complimentary graphs for Rx02 can be seen in the appendix.

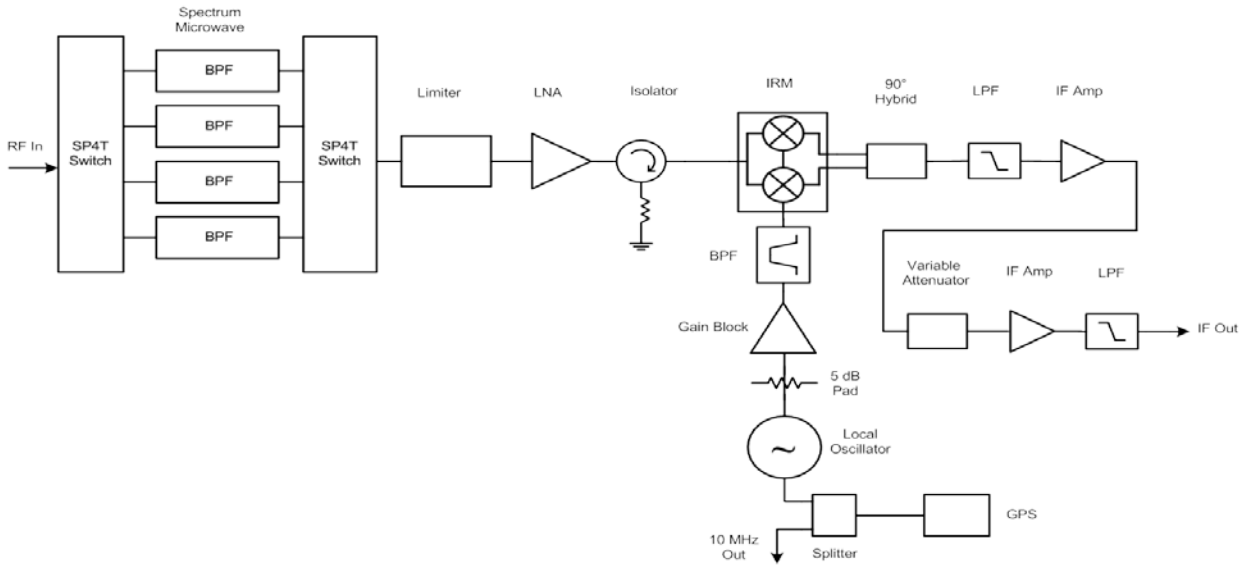

Figure 6: Superheterodyne architecture setup

4.1 : Output 1dB Compression Point

The procedure and the results for how we measured and calculated the 1dB compression point can be seen in the following sections.

4.1.1 : Procedure

The procedure for how we setup our test bench is listed below. An image of the entire test arrangement can be seen in Figure 7.

1. Secure the following equipment for use:
    a. Anritsu MG3692B 20 GHz Signal Generator
    b. Agilent 8564EC 30Hz- 40 GHz Spectrum Analyzer
2. Connect to Spectrum Analyzer, and set the center frequency to that of correct output channel and have the span set at 200 MHz.
3. Connect the input of the receiver up to the signal generator using the other SMA cable and set the power level down very low (something on the order of ~ -70dbm). Figure 7 shows our test bench for this measurement.
4. Calculate the compression of the amplifier and find where the 1dB compression point occurs.

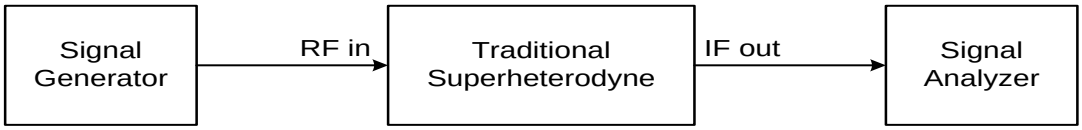

Figure 7: Superheterodyne 1dB test bench

4.1.2 : Results

The data for Rx01 can be seen below. Figure 8 (Figure 46 for Rx02) below shows the output amplifier over its linear range before it begins to compress. The compression is caused by the amplifier operating beyond its normal range. The graph shows how at one point the amplifier is no longer in a linear range. The system begins to compress and the real output power begins to deviate from the idealized output power. The point at which the real power is 80% of the ideal output power is what we are trying to find. Table 1 shows the 1dB compression point data for both receivers.

Table 1: 1-dB compression measurements

1-dB Compression	Rx01 In (dBm)	Rx01 Out (dBm)	Rx02 In (dBm)	Rx02 Out (dBm)
Ch0	-50.836	9.537	-51.743	9.794
Ch1	-50.414	9.682	-51.100	9.789
Ch2	-49.992	9.617	-51.531	9.811
Ch3	-49.831	9.638	-51.279	9.856

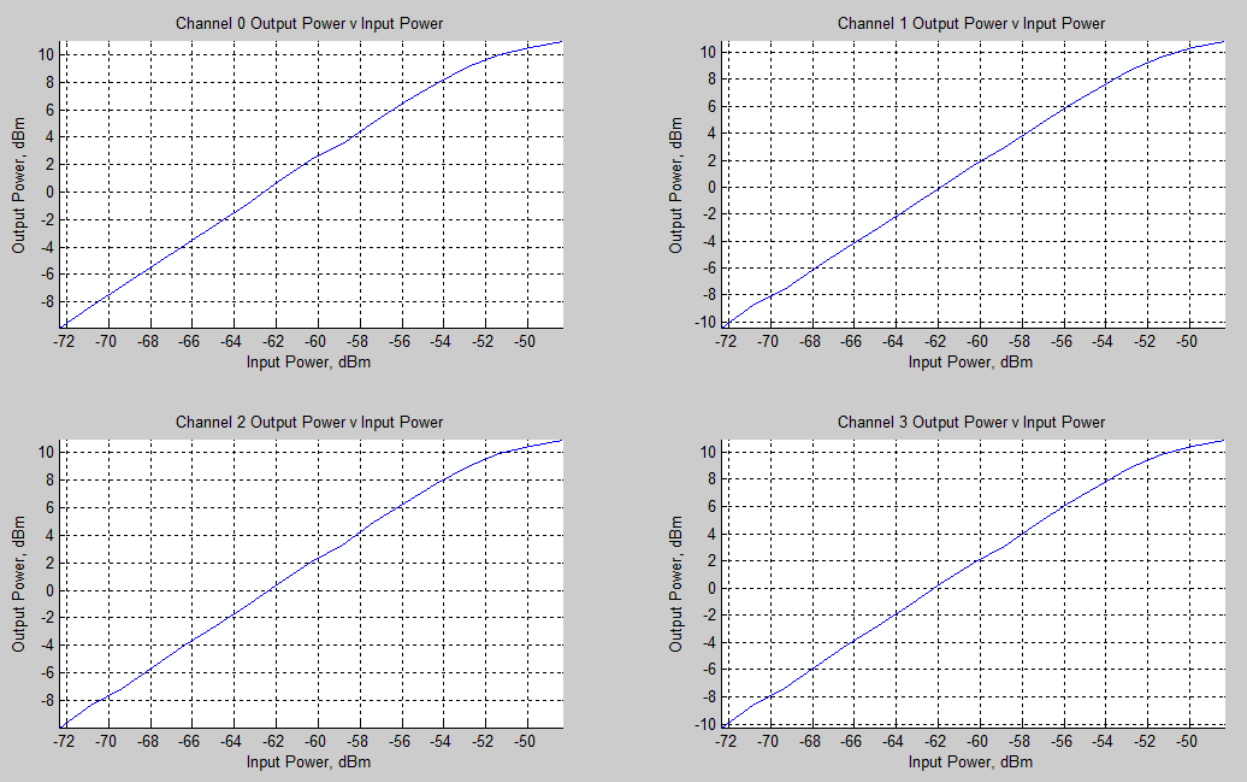

Figure 8: Output Power versus input power for Rx01

4.2 : Group Delay

In this section, we are looking for the variation over the band of S21. This will calculate the change in phase with respect to frequency, or group delay, of our device.

4.2.1 : Procedure

The procedure for how we setup our test bench is listed below. An image of the entire test arrangement can be seen in Figure 9.

1. Secure the following equipment for use and setup according to Figure 9:
    a. Anritsu MG3692B 20 GHz Signal Generator
    b. Agilent E8364C Network Analyzer
    c. 4-Port Quadrature Hybrid
    d. 4-Port Mixer
    e. 50 Ohm Termination
2. Connect port 1 of the network analyzer up to the input of the receiver.
3. Next, connect the IF output of the receiver up to the input hybrid.
    a. Make sure the 50 Ohm termination is connected to the ISO port of the Hybrid.
    b. The Hybrid produces to IF signals 90 degrees out of phase with each other.
4. Connect the two outputs of the hybrid into IF1 and IF2 input ports of the mixer.
5. The signal generator needs to be connected to the LO port of the LO.
    a. The Signal generator needs to be set to Ch0 at +20 dBm.
6. Port 2 of the network analyzer needs to be connected to the RF port of the mixer
    a. Calibrate the NA to view across all for channels
    b. Set the input power level to -30 dBm
    c. Measure S21 and Delay

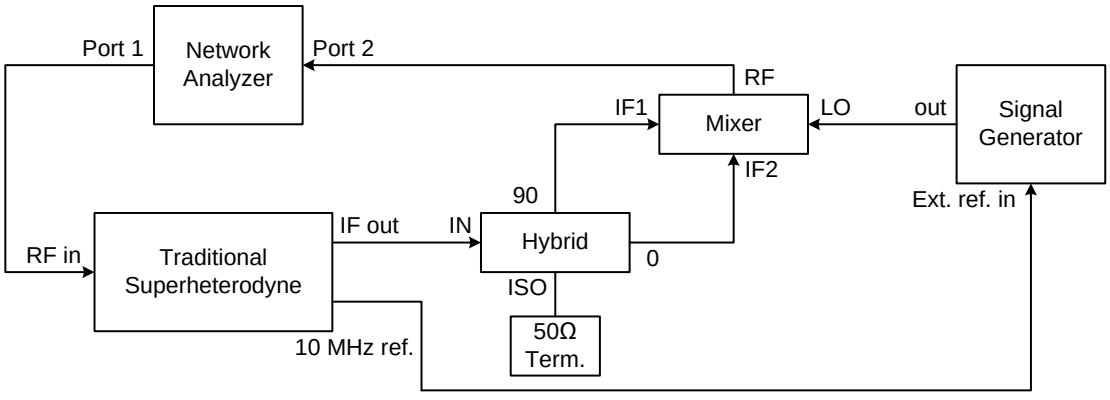

Figure 9: Superheterodyne group delay test bench results

4.2.2 : Results

For group delay variation, what needs to be investigated is how much the phase varies over the bandwidth of the signal. The network analyzer was calibrated for the whole range of all four

channels to make measurements quicker. Figure 10 (Figure 47 for Rx02) below shows all four channels for Rx01 displayed side by side in a sub plot. Over the bandwidth of each channel a 'bowl' shape can be seen. Each channel has a bandwidth of 200 MHz, which the data cursors show on the graphs. At the two extreme points of the channel we observed the time it takes for the signal to propagate through the receiver. Using these we generated the group delay for each channel and displayed it below in Table 2. The goal of the receiver was to have a group delay that was less than 3 ns for all channels.

Table 2: Group delay measurements for superheterodyne Rx01 and Rx02

	Channel 0 Group Delay	Channel 1 Group Delay	Channel 2 Group Delay	Channel 3 Group Delay
Rx01	1.69 ns	1.81 ns	0.51 ns	2.14 ns
Rx02	1.26 ns	1.42 ns	1.3 ns	1.27 ns

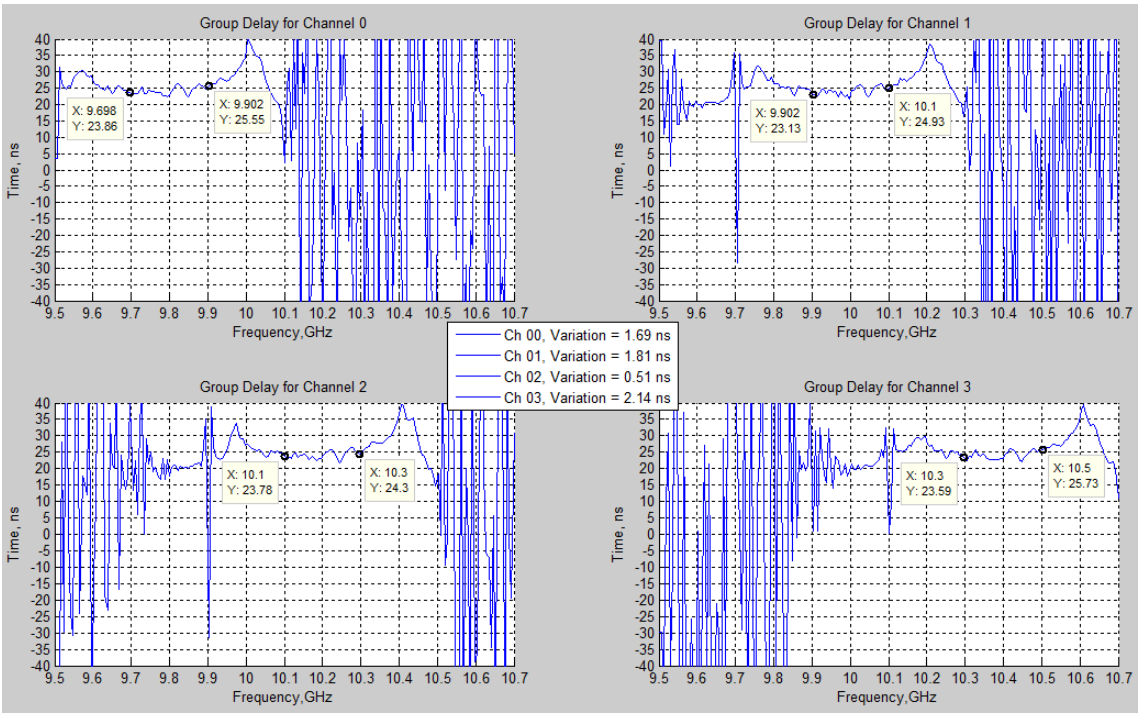

Figure 10: S21 parameter measuring delay across all four channels for Rx01

4.3 : In-Band Spurs

In-band spurs are random signals that can leak through into the bandwidth of your signal. They can be created by a variety of things, and they can distort the data be transmitted in the signal. They need to be marked and measured to determine if they will have any influence on the signal.

4.3.1 : Procedure

The procedure for how we setup our test bench is listed below. An image of the entire test arrangement can be seen in Figure 11.

1. Secure the following equipment for use:
    a. Anritsu MG3692B 20 GHz Signal Generator
    b. Agilent 8564EC 30Hz- 40 GHz Spectrum Analyzer
    c. 6 inch SMA-SMA cables
2. Connect the input of the receiver to the signal generator and set it to channel 0, with a power level of ~ -70 dBm.
3. Connect the output of the receiver up to the spectrum analyzer and center it at the IF band. Figure 7 shows our test bench for this measurement.
    a. Reduce the bandwidth of the analyzer to lower the noise floor
        i. The spurs can easily be seen, but reducing the bandwidth will help to isolate a correct power level.
4. Record any spurs within the bandwidth of the channel.

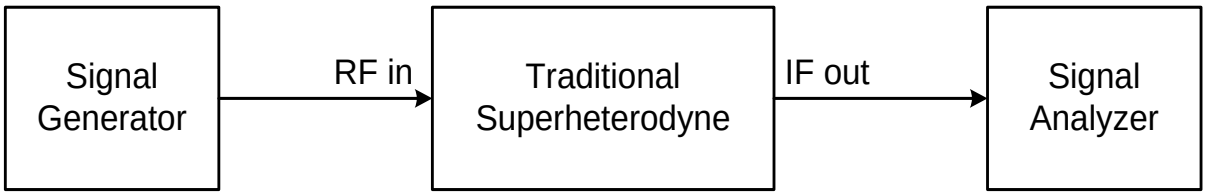

Figure 11: Superheterodyne general test bench

4.3.2 : Results

The purpose of recording all the spurs in the domain is to determine if any spurs exist in the band. If there are spurs at a semi high power level, then this can cause distortion in the data. This test simply determines where the in-band spurs are and what their power levels are. SNR and SINAD are very important to consider when reconstructing a signal and can distort the data. A spur with high power level can easily disrupt the data. Figure 7 (Figure 8 for Rx02) seen below shows the largest spurs within the signal and labels the power level. The X and Y

coordinates of each data cursor represents the frequency in MHz and the output power level of the spur in dBm, respectively. Table 3 below displays the highest spur power level for each channel.

Table 3: Highest output spur for each channel of Rx01 and Rx02

	Channel 0 In-Band Spurs	Channel 1 In-Band Spurs	Channel 2 In-Band Spurs	Channel 3 In-Band Spurs
Rx01	-58.42 dBm	-66.26 dBm	-70.41 dBm	-68.49 dBm
Rx02	-64.36 dBm	-64.97 dBm	-63.89 dBm	-63.67 dBm

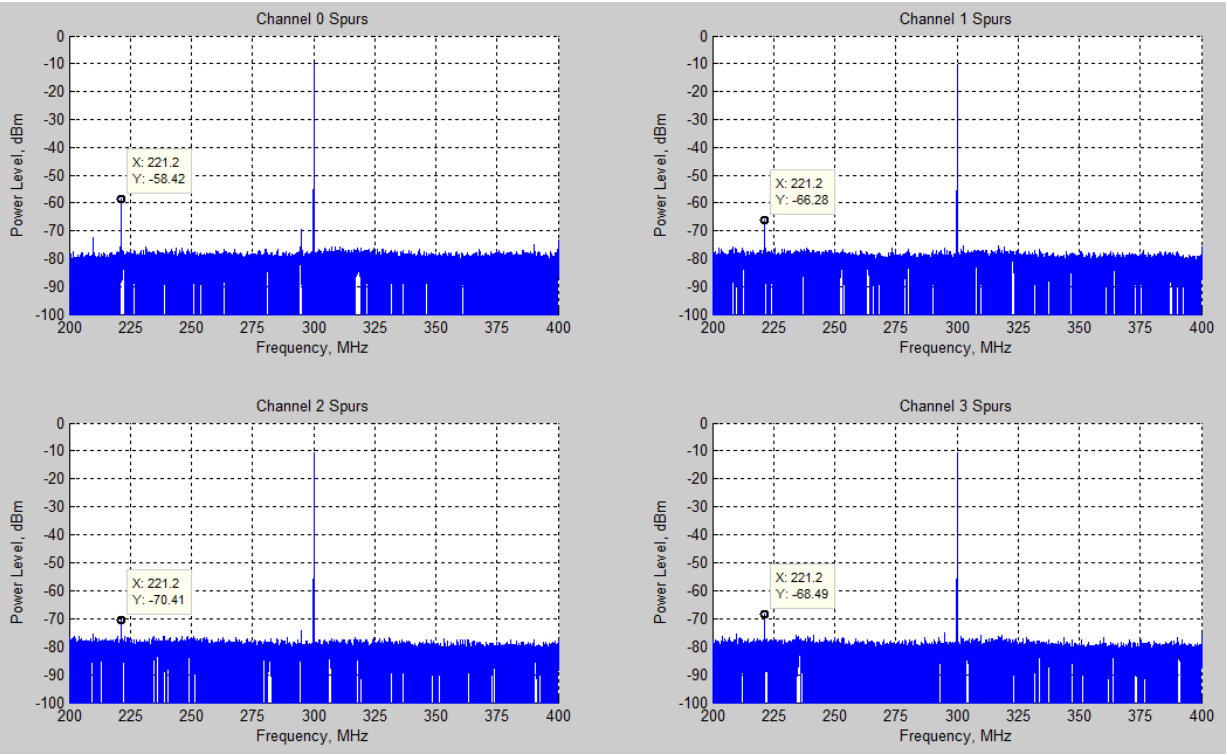

Figure 12: Output power level versus frequency for the In-band spurs of Rx01

4.4 : Input VSWR

The voltage standing wave ratio helps to determine that amount of reflections input of the receiver. A high VSWR will have large reflections and cause some power to be sent back along the line. It is important to minimize the VSWR at both input and output to reduce reflections along the line.

4.4.1 : Procedure

The procedure for how we setup our test bench is listed below. An image of the entire test arrangement can be seen in Figure 13.

1. Secure the following equipment for use:
    a. Agilent E8364C Network Analyzer
    b. 6 inch SMA-SMA cable
2. Connect port 1 of the network analyzer to the input of the receiver. Figure 13 demonstrates our test bench for this measurement.
    a. Calibrate the NA to view across channel 0
    b. Set the number of points to 201
    c. Set the input power level to -30 dBm
    d. Measure S11 and SWR

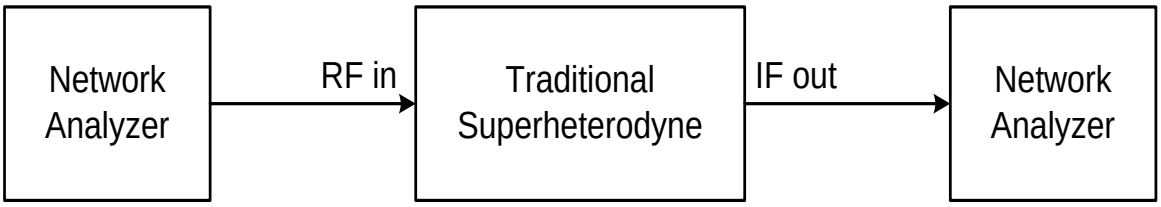

Figure 13: Superheterodyne VSWR test bench

4.4.2 : Results

Input or output VSWR is a 1-port measurement when using a network analyzer. Using the network analyzer we can see the S11 parameter, which can be used to determine the input reflections and VSWR. Input VSWR measurements can be seen below. Figure 14 (Figure 49 for Rx02) shows the input VSWR across all four channels for Rx01. The red line seen in all the graphs is the average value across the band. These results show minimal reflections at the input of the device allowing for almost 100% power transfer. Each channel has 200 MHz bandwidth in these calculations. Table 4 shows the average values for each receiver.

Table 4: Input VSWR measurements for superheterodyne

Input VSWR	Rx01	Rx02
Ch0	1.25	1.22
Ch1	1.33	1.44
Ch2	1.35	1.27
Ch3	1.37	1.23

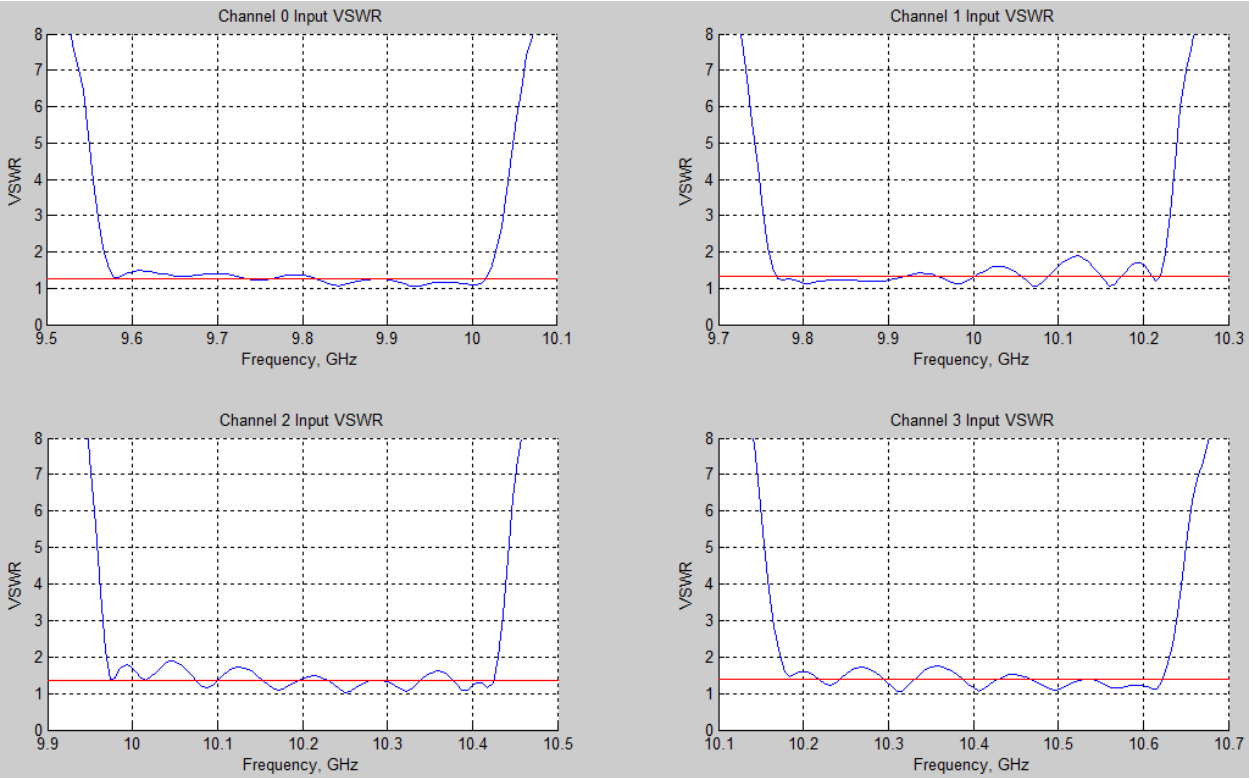

Figure 14: Input VSWR versus frequency for Rx01

4.5 : Noise Figure

The noise figure is a measurement that views the degradation of the signal through the device. The input SNR of the device will be degraded and have a smaller output SNR. The noise figure takes the ratio of these two items to determine how much degradation takes place in the chain. The following is the procedure we used to calculate the noise figure and the results that we got from our measurements.

4.5.1 : Procedure

The procedure for how we setup our test bench is listed below. An image of the entire test arrangement can be seen in Figure 15.

1. Requires the following instruments:
    a. Agilent N8973A Noise Figure Meter and Noise Source
    b. 6 inch SMA-SMA cables
2. Set digitally-controlled variable attenuator to 0 dB.
3. Set noise figure meter to measure the noise figure and gain between 200 – 400 MHz and set to downconvert in order to correct data based on the RF frequency. Set LO frequency to desired value (RF – 300 MHz).
4. Calibrate noise figure meter with noise source that can output at the desired RF frequencies.
5. Connect noise source to Rx input. Connect Rx output to noise figure meter. Figure 15 shows our test bench for this measurement.
6. Repeat for attenuation of 21 dB and 31.5 dB.
7. Repeat for all channels.

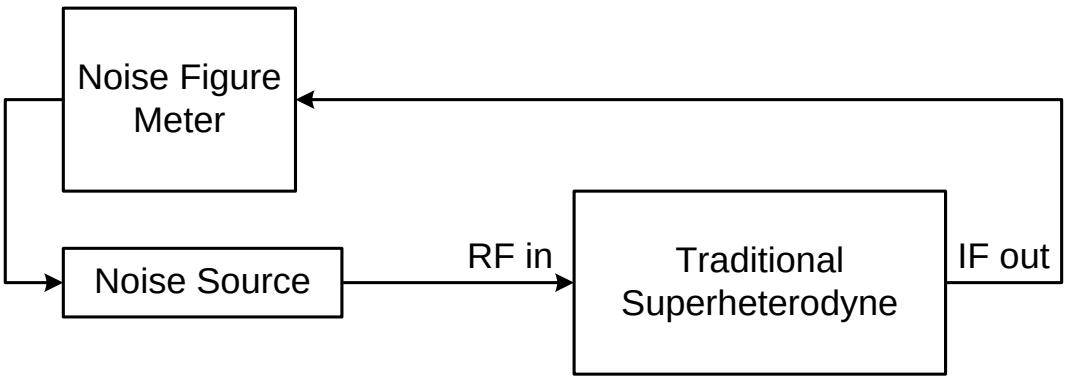

Figure 15: Superheterodyne noise figure test bench

4.5.2 : Results

As stated before, noise figure is a ratio of the signal to noise ratio at the input of a receiver divided by the signal to noise ratio at the output of a receiver. NF is a measurement that

is more heavily affected by the first components in a signal chain. The noise factor for cascaded devices can be determined using the formula as shown in Equation 8 [14]. The following equation is a linear formula, where F is the noise factor. To get the noise figure, take the base 10 logarithm of the noise factor and multiply it by 10, which is the standard formula for turning a number into dB.

$$F = F_1 + \frac{F_2 - 1}{G_1} + \frac{F_3 - 1}{G_1 G_2} + \frac{F_4 - 1}{G_1 G_2 G_3} + \cdots + \frac{F_n - 1}{G_1 G_2 G_3 \ldots G_{n-1}} \quad (8)$$

Our results for the noise figure with different attenuator values are demonstrated in Figure 16 (Figure 50 for Rx02), Figure 17 (Figure 51 for Rx02), and Figure 18 (Figure 52 for Rx02). The average NF for Rx1 with the attenuator at 0 dB ranged between 3.99 dB and 4.1 dB throughout all four channels. The average NF with the attenuator at 21 dB ranged between 4.18 dB and 4.28 dB. The average NF with the attenuator at 31.5 dB ranged between 5.6 dB and 5.95 dB. With the digital attenuator set at 0dB, the goal of the project was to have a noise figure around 4dB. As shown in Table 5 seen below, our goal was achieved.

Table 5: Noise figure for all channels with digital attenuator at 0 dB

	Channel 0 Noise Figure	Channel 1 Noise Figure	Channel 2 Noise Figure	Channel 3 Noise Figure
Rx01	4.08 dB	4.1 dB	3.99 dB	4.07 dB
Rx02	3.41 dB	3.87 dB	3.56 dB	3.71 dB

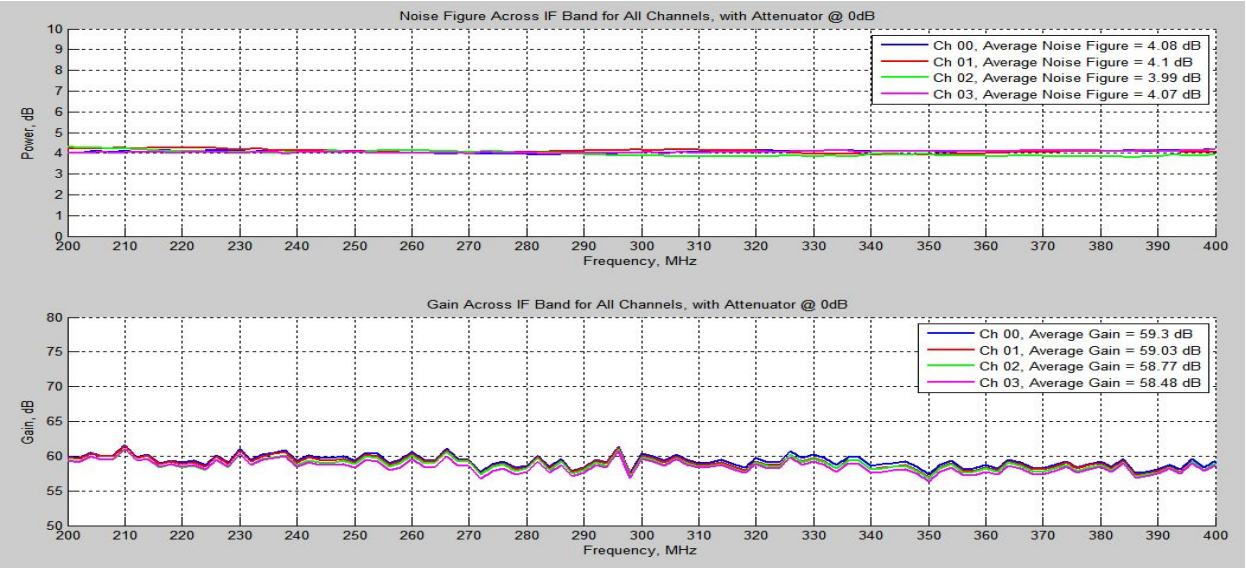

Figure 16: Rx01 noise figure and gain with variable attenuator at 0 dB

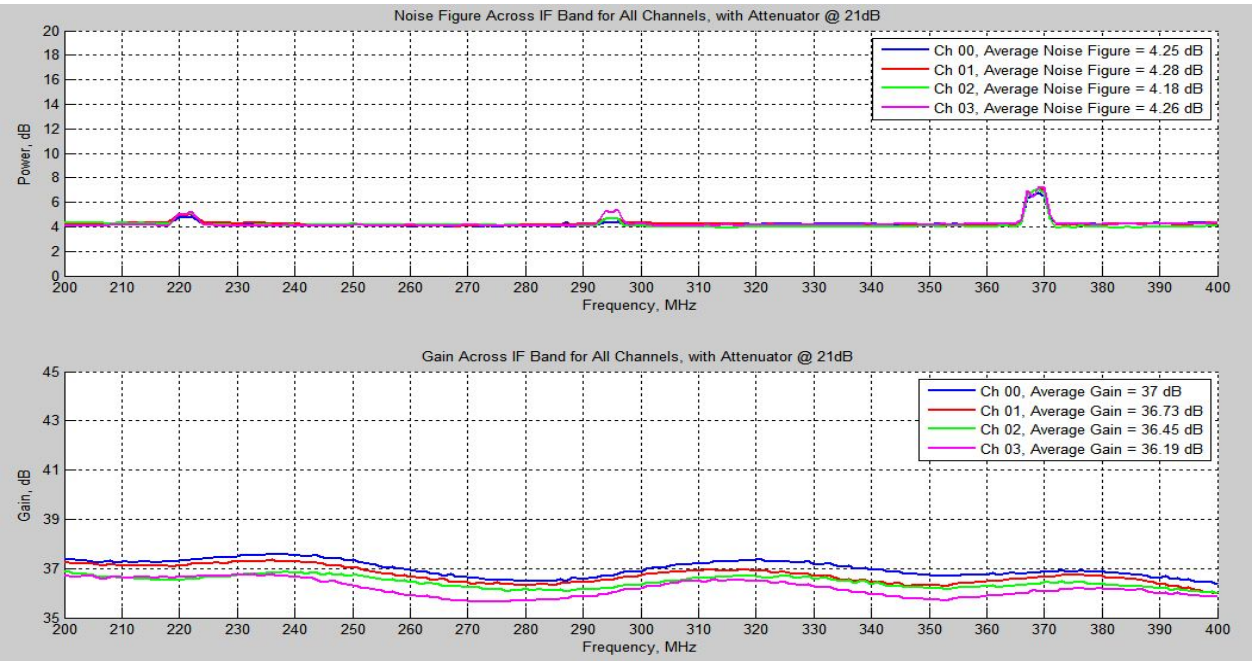

Figure 17: Rx01 noise figure and gain with variable attenuator at 21 dB

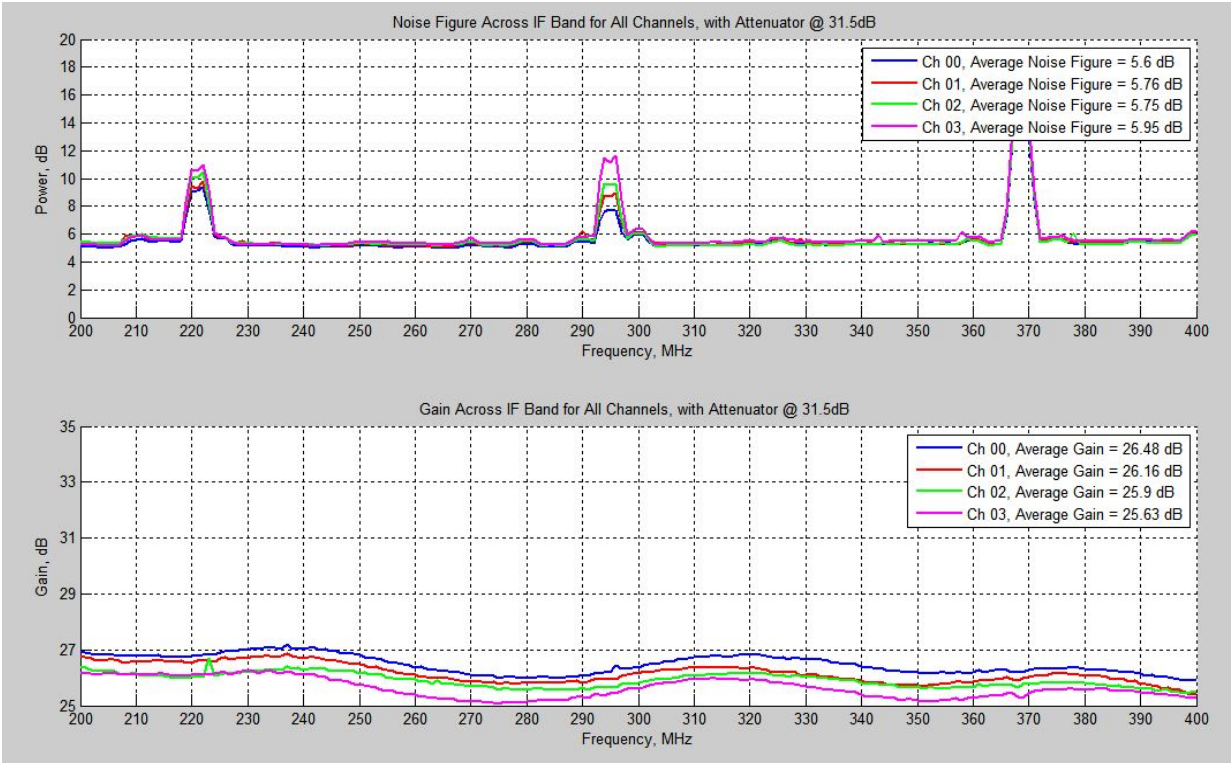

Figure 18: Rx01 noise figure and gain with variable attenuator at 31.5 dB

4.6 : Output Third-Order Intercept (OIP3)

To measure the linearity of the receiver, we observed the third-order intercept point, or IP3. By injecting two signals coupled together at the input, we can view their third order intermodulated products at the output. As you increase the fundamental tone, the third order product should increase by a factor of three. By taking measurements at multiple points, one can perform a linear regression for the two lines. One will have a slope of 1 while the other will have a slope of 3. The y coordinate of where these two lines cross is the output IP3 values that we are looking for.

4.6.1 : Procedure

The procedure for how we setup our test bench is listed below. An image of the entire test arrangement can be seen in Figure 19.

1. Requires the following instruments and components:
    a. Anritsu MG3692B 20 GHz Signal Generator
    b. Agilent 8564EC 30Hz- 40 GHz Spectrum Analyzer
    c. Isolator
    d. Splitter
    e. 6 inch SMA-SMA cables
2. Set digitally-controlled variable attenuator to 0 dB.
3. Connect signal generator output to the isolator input. Repeat for second signal generator and isolator.
4. Connect isolators to the input ports of the splitter. Connect output of splitter to the input of Rx.
5. Connect output of Rx to signal analyzer. Figure 19 illustrates a setup of our test bench for this measurement.
6. Set first signal generator to the RF frequency with a 1 MHz negative offset with a low power level (~ -70 dBm).
7. Set second signal generator to the RF frequency with a 1 MHz positive offset with a low power level (~ -70 dBm).
8. Set center frequency of signal analyzer to RF with span to reveal both signals.
9. Reduce bandwidth until the third order intermodulation products can be seen.
10. Repeat for all channels

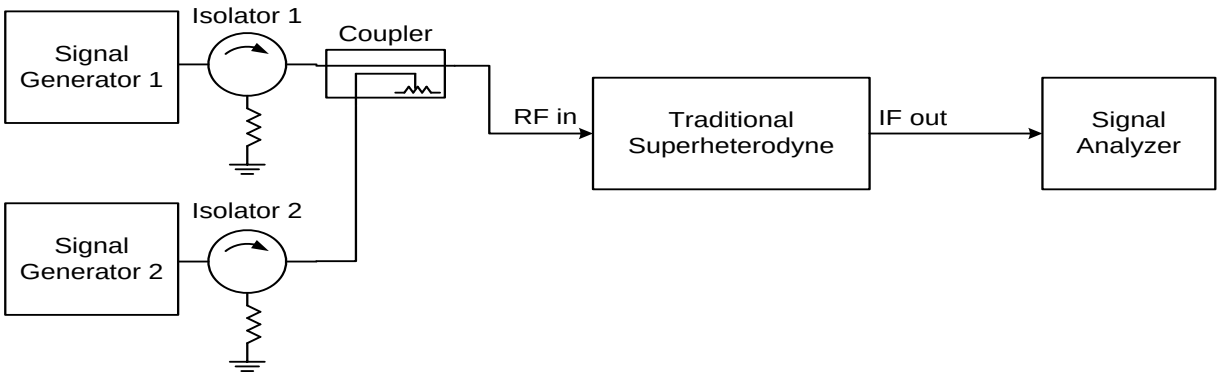

Figure 19: Superheterodyne IP3 test bench

4.6.2 : Results

A greater IP3 illustrates greater linearity in the system. The IP3 is not an observable measurement, but a theoretical point that is generally lying beyond the 1 dB compression point. By observing the third order intermodulated products along with the fundamental tone, we can find where they cross and determine their linearity. The equations for finding where the third order products come out is seen in Equation 9. Instead of performing linear regression we solved for the point where these two crossed and created a formula from it, which can be seen in Equation 10. The results from measuring the output third-order intercept (OIP3) for Rx01 and is shown in Figure 20 (Figure 53 for Rx02), while the IP3 values are displayed in Table 6.

$$f_{third-order} = 2 * f_1 - f_2 \quad and \quad f_{third-order} = 2 * f_2 - f_1 \tag{9}$$

$$\frac{3*P_{out} - P_{third-order}}{2} \tag{10}$$

Table 6: OIP3 measurements for superheterodyne

OIP3	Rx01 (dB)	Rx02 (dB)
Ch0	21.97	25.00
Ch1	22.04	24.90
Ch2	21.93	25.22
Ch3	22.21	25.17

Our goal was for the OIP3 to be no less than +20 dBm which all our results exceeded.

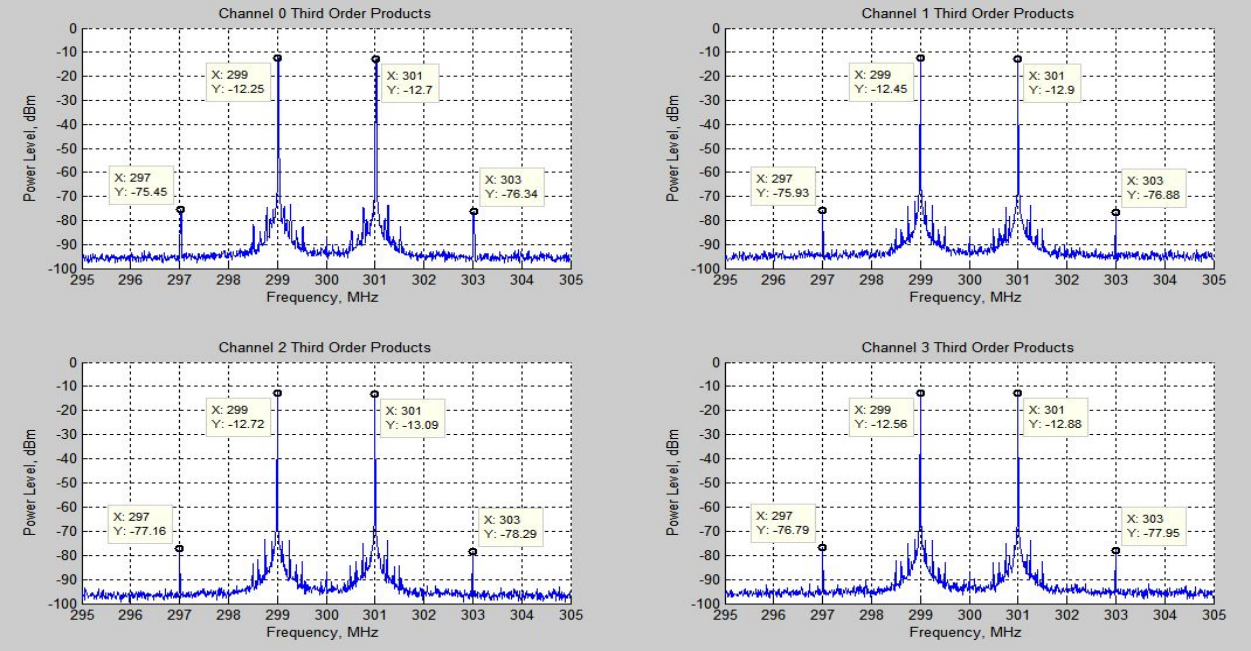

Figure 20: Output third-order intermodulated products versus frequency for Rx01

4.7 : Out of Band Rejection

Out of band rejection is the measurement that determines how effective filters reject the signals that are not wanted.

4.7.1 : Procedure

The procedure for how we setup our test bench is listed below. An image of the entire test arrangement can be seen in Figure 7.

1. Requires the following instruments:
    a. Anritsu MG3692B 20 GHz Signal Generator
    b. Agilent 8564EC 30Hz- 40 GHz Spectrum Analyzer
2. Set digitally-controlled variable attenuator to 0 dB.
3. Connect signal generator to input of Rx and signal analyzer to output of Rx.
4. Set signal generator to output a tone at RF + 300 MHz with a low power level (~ -70 dBm). Figure 7 shows our test bench for this measurement.
5. Set center frequency on signal analyzer to 600 MHz. Reduce the span and bandwidth on signal analyzer until the signal can be seen over the noise.

4.7.2 : Results

The figures demonstrating the out of band signal for Rx01 is shown in Figure 21 (Figure 54 for Rx02). A lower power level for the out-of-band signal is favored due to displaying greater rejection of these signals. The out-of-band-rejection was found based on Equation 11.

$$Out\ of\ Band\ Rejection = P_{out} - P_{out-of-band} \tag{11}$$

The output power level for the fundamental tone used in these calculations for all channels is approximately -12 dB. The output power levels for the rejected signals are displayed in Table 7. These out of band signal power levels led to the out of band rejection values shown in Table 8 below.

Table 7: Out-of-band rejection measurements for superheterodyne

	Channel 0 Output Power Level	Channel 1 Output Power Level	Channel 2 Output Power Level	Channel 3 Output Power Level
Rx01	-106.9 dBm	-103.2 dBm	-109.1 dBm	-104.3 dBm
Rx02	-102.1 dBm	102 dBm	-106.6 dBm	-106.3 dBm

Table 8: Out of band rejection values

	Channel 0 Rejection	Channel 1 Rejection	Channel 2 Rejection	Channel 3 Rejection
Rx01	96.9 dBm	91.2 dBm	97.1 dBm	92.3 dBm
Rx02	90.1 dBm	90 dBm	94.6 dBm	94.3 dBm

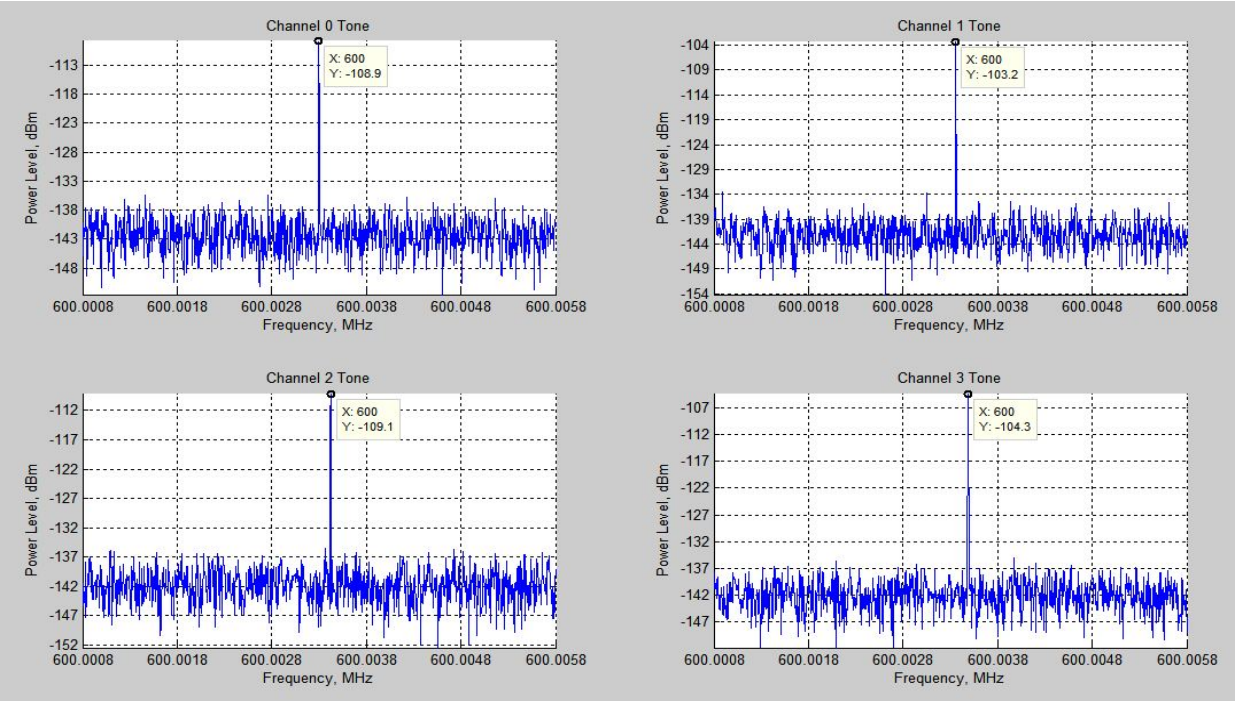

Figure 21: Out-of-band rejection versus frequency for Rx01

4.8 : Output VSWR

The output VSWR observes the reflections at the output of the receiver. By either measuring S11 or S22 (depending on which port is used), one can see how the reflections of the device. If the output VSWR is high, then the power transmitted to the DSP can be reflected back along the line into the output of the receiver. To avoid this, we try to minimize the VSWR so all power is transmitted to the DSP.

4.8.1 : Procedure

The procedure for how we setup our test bench is listed below. An image of the entire test arrangement can be seen in Figure 13.

1. Requires the following instruments:
    a. Agilent E8364C Network Analyzer
    a. 6 inch SMA-SMA cables
2. Calibrate network analyzer to sweep between 10 – 600 MHz with power set to -30 dBm.
3. Connect the network analyzer to the output of Rx. Figure 13 demonstrates our test bench for this measurement.
4. Measure SWR on network analyzer (Measure S11 if connected to port 1 of network analyzer or measure S22 if connected to port 2)

4.8.2 : Results

A graph of output VSWR versus frequency in MHz for Rx01 is shown in Figure 22 (Figure 55 for Rx02). Output VSWR remained the same for all channels for each receiver. The minimum VSWR for Rx01 is approximately 1.03 and the maximum was found to be about 1.23. The average VSWR for Rx01 is 1.13 leading to an average loss of 0.37% or 0.016 dB. The minimum and maximum output VSWR for Rx02 is 1.02 and 1.31. The average VSWR for Rx02 is 1.16 leading to an average loss of 0.55% or 0.024 dB. The goal for this test was for the output VSWR not to exceed a 2:1 ratio equaling a loss of approximately 11%. Our results easily met this goal as they demonstrate a much lower power loss than 11%. Since this measurement is at the output of the device where the frequency is 300 MHz, we would expect to see a rather small VSWR. VSWR only takes effect in high frequency systems, the output IF is not really high enough to experience these kind of reflections.

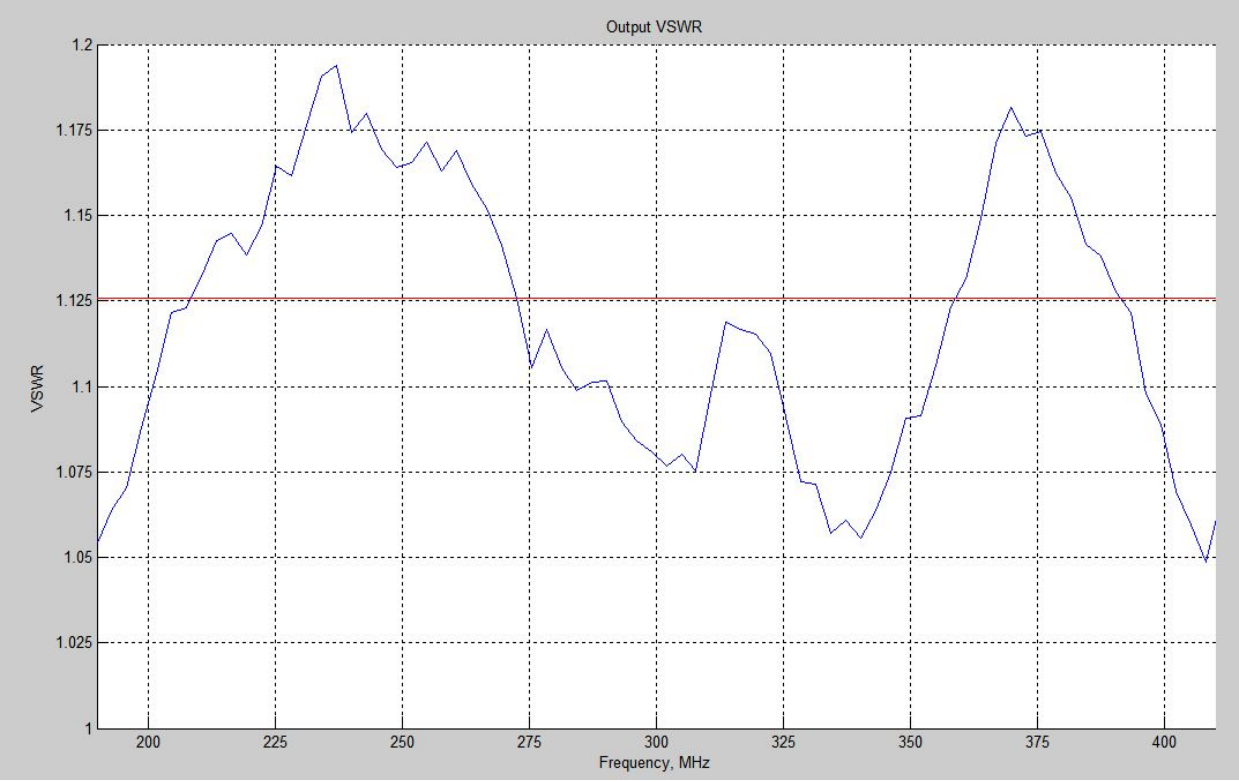

Figure 22: Output VSWR versus frequency for Rx01

4.9 : RF to IF Gain

The RF to IF gain measures the range of the digital attenuator inside the receiver box. To help with power regulations, a digital attenuator was placed inside the receiver to be able to manually change the power level. This can be useful for error protection in circuit schematics, since so many things can happen that is not expected. The measurement tests the digital attenuator range. This test can also be used to ensure that the correct amount of gain is being produced from input output.

4.9.1 : Procedure

The procedure for how we setup our test bench is listed below. An image of the entire test arrangement can be seen in Figure 7.

1. Requires the following instruments:
    a. Anritsu MG3692B 20 GHz Signal Generator
    b. Agilent 8564EC 30Hz- 40 GHz Spectrum Analyzer
    c. 6 inch SMA-SMA cables
2. Connect the signal generator up the input of the receiver.
    a. Set it to channel sweep across the entire channel band (200 MHz bandwidth)
3. Connect the signal analyzer up to the IF output of the receiver. Figure 7 shows our test bench for this measurement.
    a. Set it to view the entire IF band of the receiver
    b. Max sure the system is on max hold to see flatness of the band
4. Repeat for all channels

4.9.2 : Results

The RF to IF gain portion of the testing is used to make sure the receiver has the right amount of gain as a system. The receiver has built in digital attenuator, which also needs to be tested. The digital attenuator can be set anywhere between 0-31.5 dB. Figure 23 (Figure 56 for Rx02) shows the sweep across each channel for Rx01. The range for the digital attenuator for each channel and receiver can be seen below:

Table 9: Digital attenuator range for RF to IF gain for superheterodyne

Digital Attenuator Range	Rx01 (dB)	Rx02 (dB)
Ch0	31.6973	31.4073
Ch1	31.5730	31.3512
Ch2	31.5134	31.4032
Ch3	31.5341	31.4144

Each receiver is supposed to have approximately 60 dB of gain from the RF port to IF port. The input for this test was approximately -70 dBm. Using the known input we used the output power of the device to determine the actual gain in the system. With the output power of the device around -10 dBm, the system has approximately 60 dB of gain as expected.

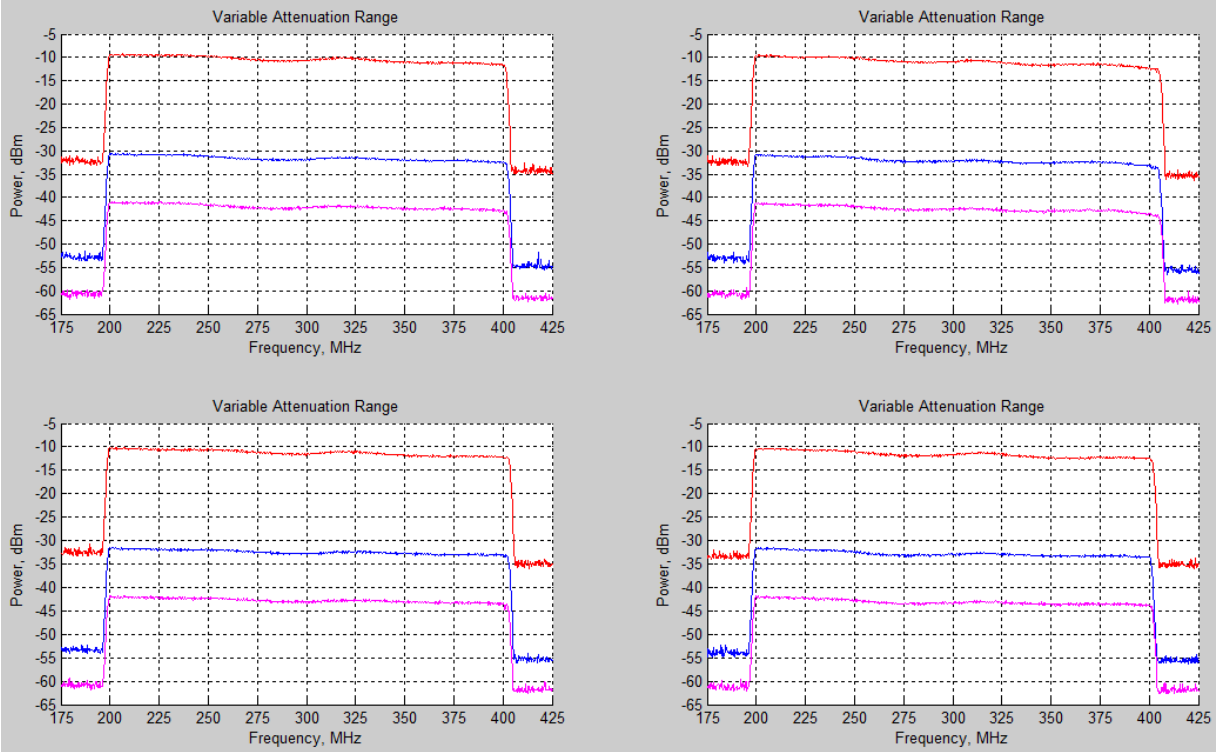

Figure 23: RF to IF gain for Rx01

Chapter 5 : Track and Hold Amplifier Test Bench

The following section shows the setup and procedure for testing the track-and-hold amplifier. The first section walks through the basic setup of the device and what the output wave forms should look like. Beyond that is the test procedure for the receiver parameters used to characterize the device.

5.1 : Basic Setup

The following section walks through the initial setup of the device from start to finish. The first step for testing our device was to create some way to power the device. Figure 24 seen below shows 9 pins at the top of the device that provide the power rails. Table 10 seen below shows that the device needs two different sources 2V and -4.75V. With the devices turned on, we measured the following values seen in Table 11, which correspond with the datasheet values.

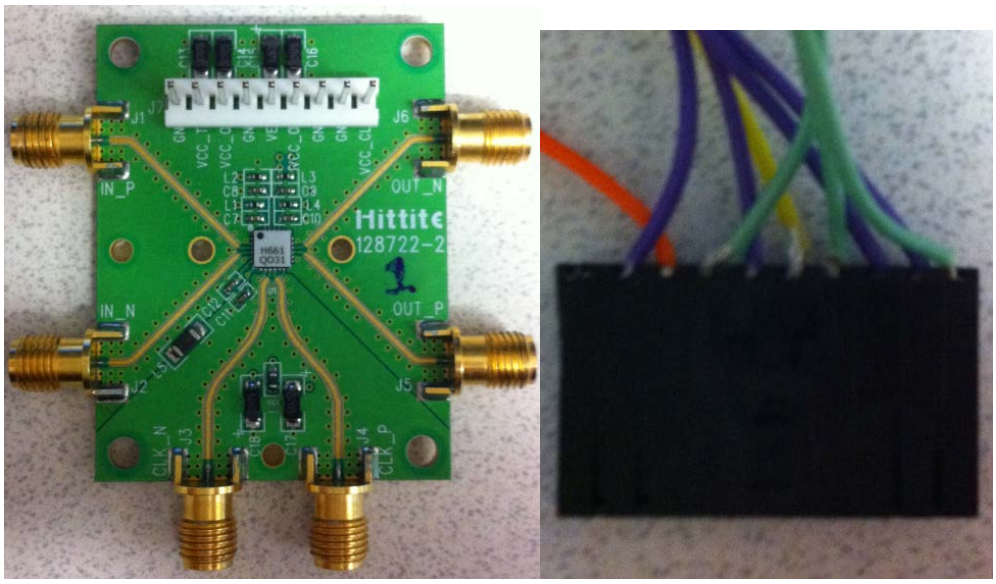

Figure 24: THA device (left) and header (right)

Table 10: THA datasheet specifications

Sources	Voltage (V)	Current (mA)
VccTH	2 ± 0.1V	82
VccOF	2 ± 0.1V	40
VccOB	2 ± 0.1V	73
VccCLK	2 ± 0.1V	26
Vee	-4.75 ± 0.1V	-242

Table 11: THA power measurements

Devices	2 V Source	-4.75 V Source
Device 1	220 mA	-245 mA
Device 2	215 mA	-240 mA

Knowing that the devices were powered properly, we proceeded to try and recreate images in the datasheet. Setting the input signal generator up to 1.125GHz @ +2.00 dBm and the clock signal generator to 500 MHz @ +6.00 dBm, we tried to recreate the image seen in Figure 25. Initially, we ran everything single-ended with 50 Ohm terminations across all the negative portions of the output. With this setup we received the image seen in Figure 26, with ringing at approximately 780 MHz.

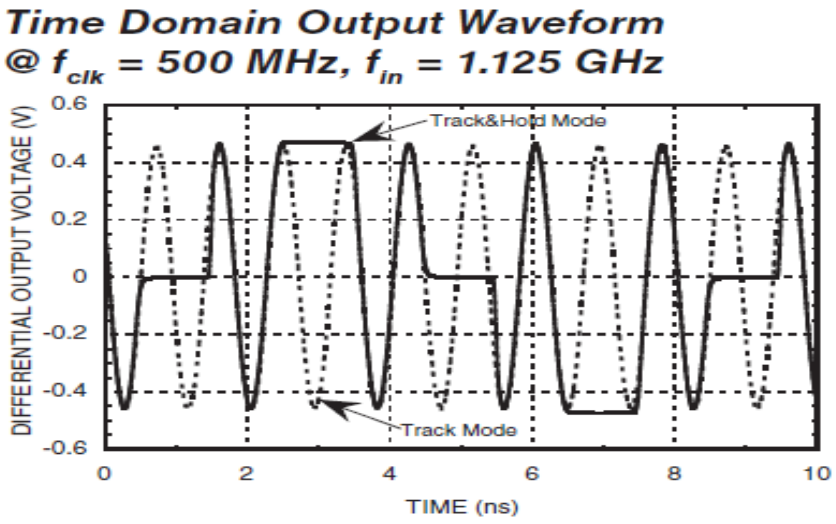

Figure 25: THA datasheet ideal image

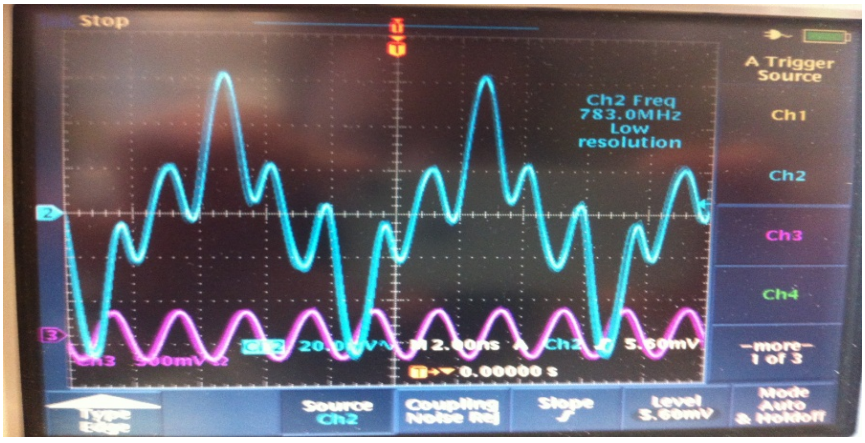

Figure 26: Oscilloscope output (blue is the signal and red is the clock)

Initially, we could not pinpoint the problem, but the people at Hittite Microwave suggested that our oscilloscope, which ran at 1GS/s with an input bandwidth of 500 MHz, could be bandwidth limiting the system and causing Gibbs phenomena. Going according to their suggestion, we obtained a better oscilloscope that could sample at 40GS/s and had an input bandwidth of 8 GHz. At this time we also received a low frequency (4.5 MHz – 3000MHz) unbalanced to balanced transformer (balun). We decided to run the output and input differentially, where the clock has the balun and the output was subtracted inside the oscilloscope. However, due to the extremely high price of X-Band baluns, we still had to run the input single-ended. Using the same setup as before, we ran an input signal of 1.125GHz and a clock of 500 MHz and received Figure 27 at the output. The device seemed to be working properly since we could recreate the exact image seen in the data sheet. However one small problem did crop up when trying to recreate this image over long period of time.

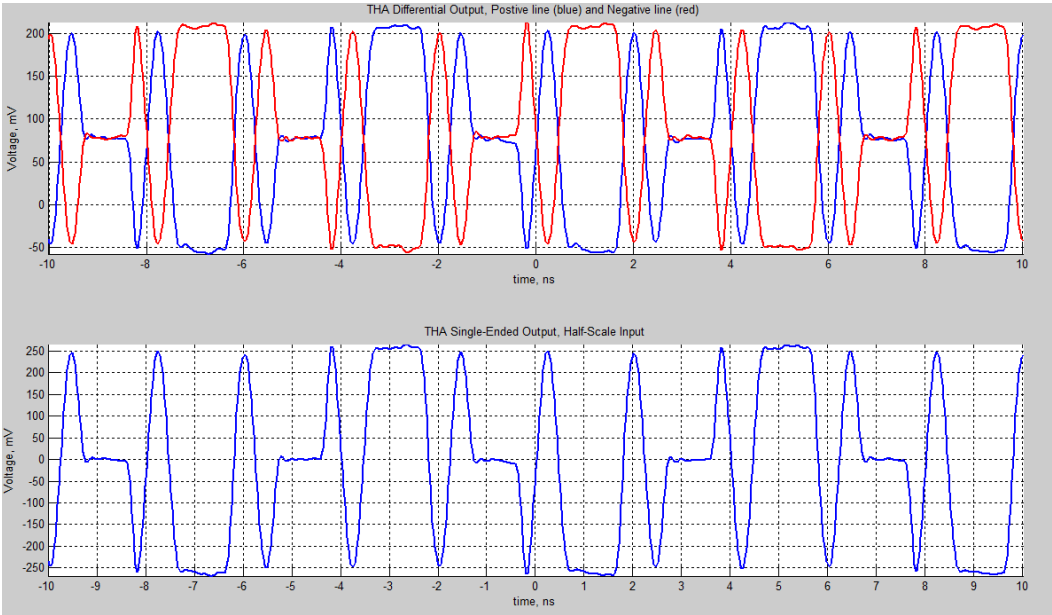

Figure 27: Differential and recombined single-ended output

Over time, the signal suffered from frequency drift where the 'zero samples' would drift part from one another over time. To determine why this was happening we had to look at the slew rate of the signal at that point. Equation 12 seen below shows how to calculate the slew rate (SR) for a given signal, where f is the frequency and A is the amplitude. Using the equation seen below, a signal of 1.125GHz with 500mV amplitude will have a slew rate of 3.53GV/s.

$$SR = 2 * \pi * f * A \tag{12}$$

Using the slew rate we can calculate the level of precision necessary between the phases of the clock and signal. Equation 13 shows the absolute sample accuracy necessary for the two signals to be accurate and experience no frequency drift. We will choose to have the two samples drift no more than ± 10mV on a half scale range of 500mV_{pp}.

$$Sample\ Accuracy = \frac{Precision}{SR} = \frac{10mV}{3.53^{GV}/_{s}} \tag{13}$$

Using the equation seen above, we determined that the sample accuracy for our system was 2.83 ps. Using the oscilloscope the best we could measure was a sample accuracy of at most 1ps. Figure 28 shown below shows the best measurement we could make on the oscilloscope. For the sake of determining feasibility of the device, this aspect will be neglected. Note that the concept of negative time is only a consequence of measuring the phase shift in the time domain. However, it is an extremely important issue that needs to be considered when determining whether or not it could be used in a receiver. Now that we are sure that the device is performing properly, we moved on to testing the X-band signals.

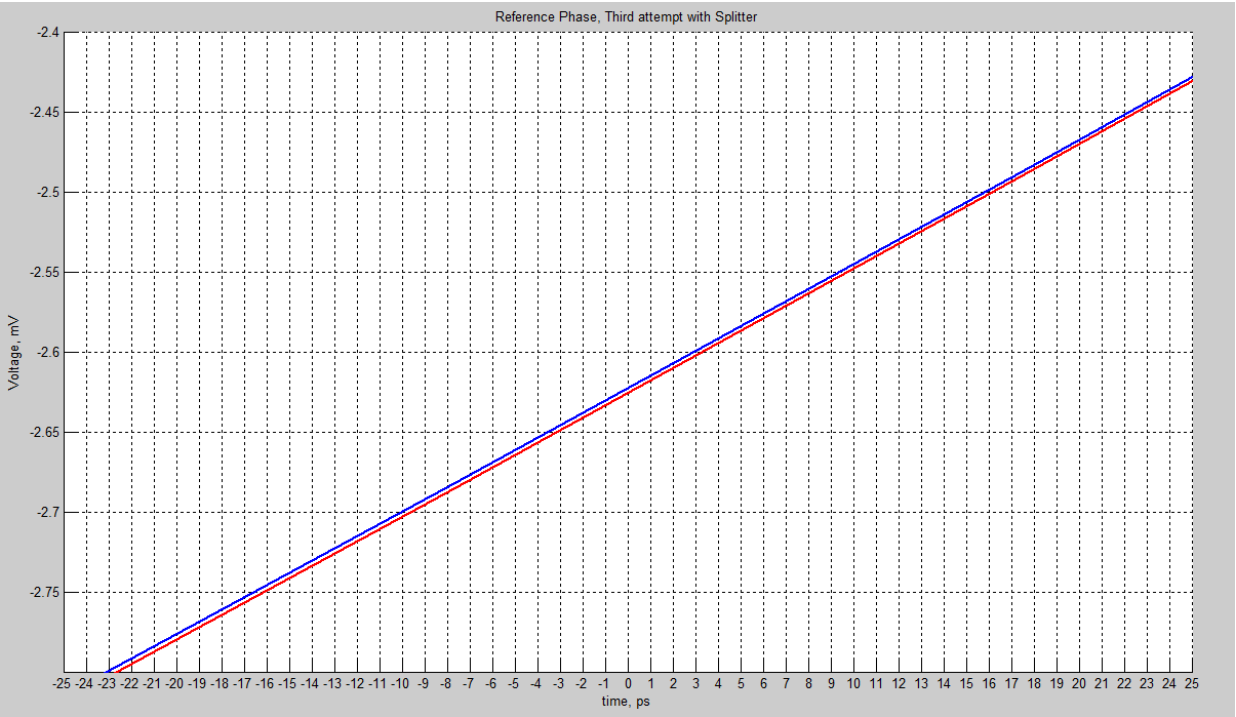

Figure 28: Phase lock between clock and signal

Keeping the same clock as before, which was 500 MHz, we now moved our input signal up into X-band and tested the four different frequencies or channels the traditional receiver

operated at. Our first measurements returned some promising results and interesting flaws. We observed that the device ceased to work when the signal frequency divided by the clock frequency was an integer number. The other three channels were fine, but channel 1 was unstable and could not reconstitute the sine wave. Figure 29 seen below shows the differential output for all four channels. Three of the channels have the possibility of successfully reconstituting the sine-wave, but channel 1 has no chance, which can be seen in Figure 30. As stated before, the instability of the device seems to crop up when the signal frequency divided by the clock frequency is an integer number. To understand why this occurs we need to look at the IF equation for the output frequency. Note that equation 14 uses the frequency of the clock (f_{clk}) and the frequency of the input signal (f_{signal}).

$$f_{IF} = round\left(\frac{f_{signal}}{f_{clk}}\right) * f_{clk} - f_{signal} \tag{14}$$

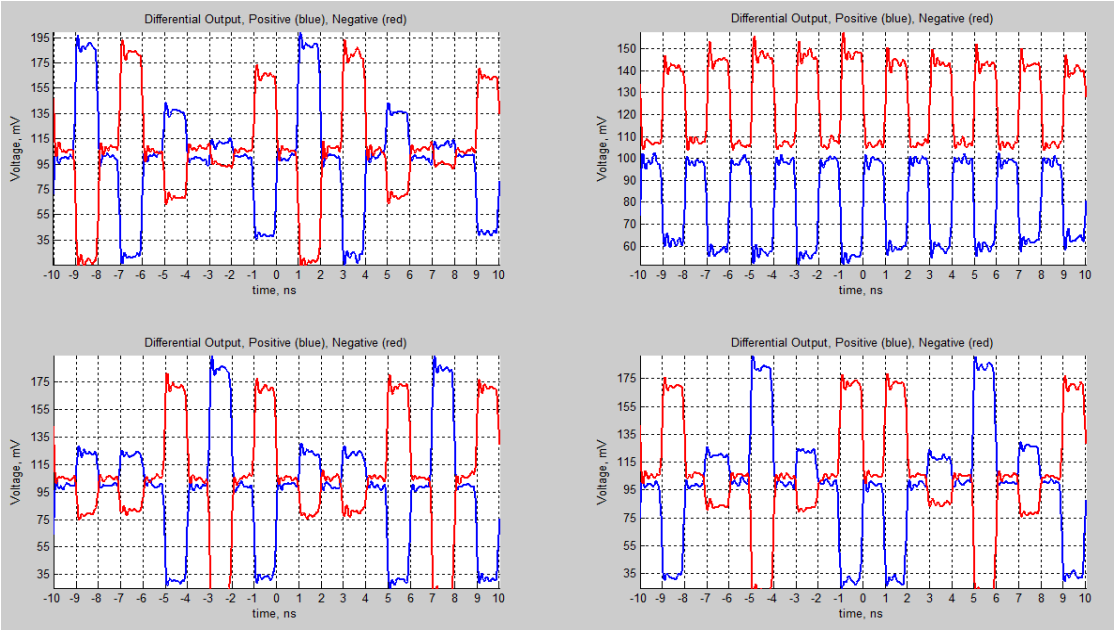

Figure 29: Device 1 differential output for all four X-band channels, positive line (Blue) and negative line (Red)

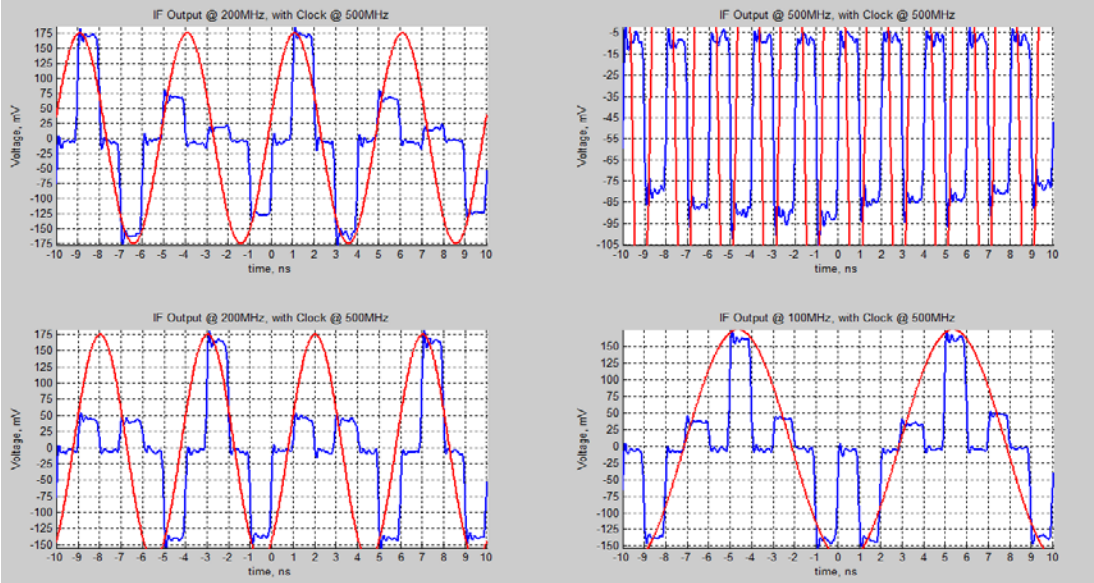

Figure 30: Device 1 with a clock of 500MHz recombined track and hold samples (Blue), ideal IF sine-wave (Red)

Looking at Equation 14, we can see how the device determines what the output frequency will be. The round function simply takes the nearest integer from the division whether it is rounding up or down. However, in cases where the division is already an integer, the output frequency equation can be reduced to Equation 15.

$$f_{IF} = \frac{f_{signal} * f_{clk}}{f_{clk}} - f_{signal} \longrightarrow f_{IF} = f_{signal} - f_{signal} \quad (15)$$

When the division of the signal frequency and clock frequency is an integer, then the output freqency is 0. This was the instabiity that we saw in that one channel where the signal frequency divided by the clock frequency was an integer was caused by the output having a frequnecy of 0 Hz. Now that we can predict and prove why this is occuring we can try to come up with a way around this problem.

The way we decided to accomplish stability across all channels is to choose our clock frequency so that none of the RF frequencies are whole number multiples. Using a clock frequency of 900 MHz will accomplish this process for us which can be seen in the following images. Figure 31 and Figure 32 show the output of the track-and-hold amplifier and the ideal sine-wave that it is trying to produce. Both devices are stable and reform the sine-wave as expected, with a lower frequency. From here we went on to measure the receiver parameters.

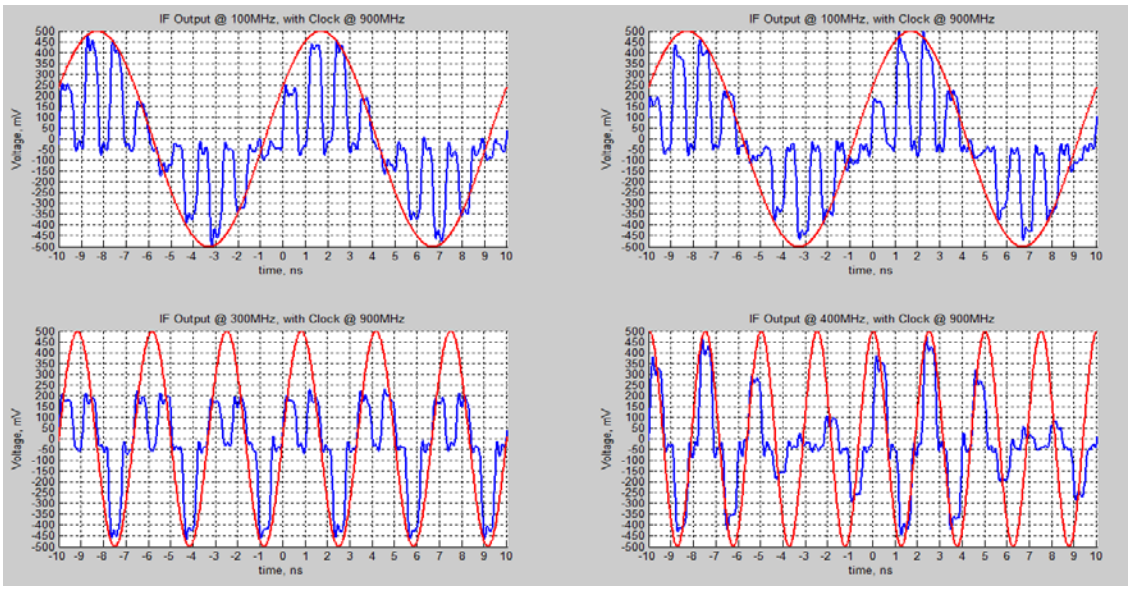

Figure 31: Device 1 with a clock of 900MHz recombined track and hold samples (Blue), ideal IF sine-wave (Red)

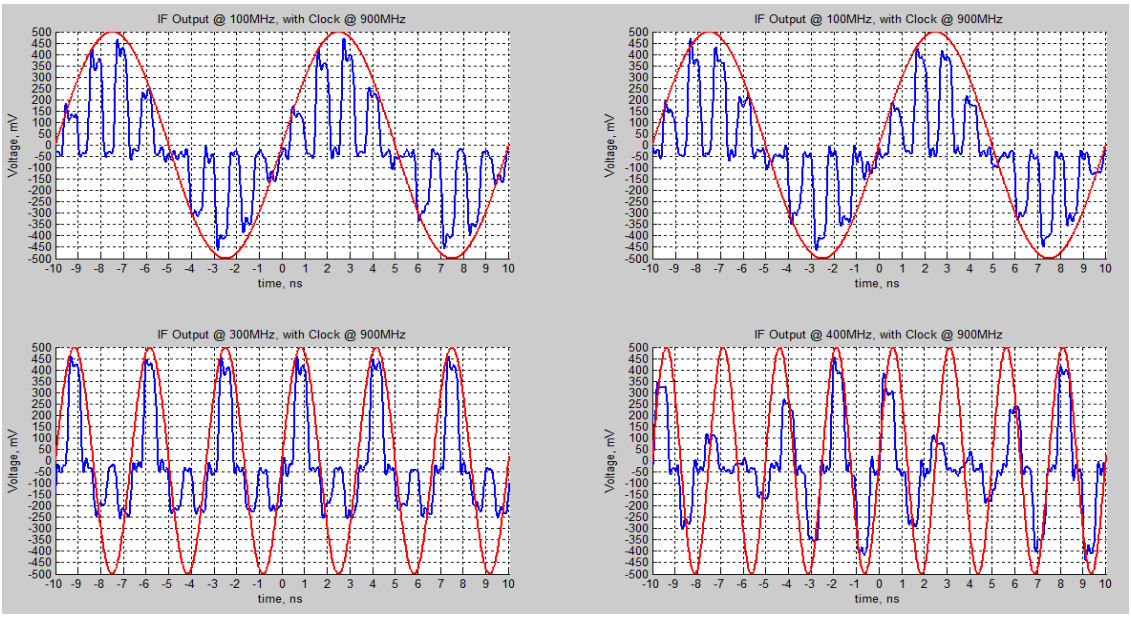

Figure 32: Device 2 with a clock of 900MHz recombined track and hold samples (Blue), ideal IF sine-wave (Red)

5.2 : Noise Figure (NF)

The noise figure is a measurement that quantifies the degradation of the signal through the device. The input SNR of the device will be degraded and have a smaller output SNR. The noise figure takes the ratio of these two items to determine how much degradation takes place in the chain. The following is the procedure we used to calculate the noise figure and the results that we got from our measurements.

5.2.1 : Procedure

The procedure for how we setup our test bench is listed below. An image of the entire test arrangement can be seen in Figure 33 and Figure 34.

1. Requires the following instruments:
    a. Kepco MSK 10-10M Power Supply
    b. Anritsu MG3692B 20 GHz Signal Generator
    c. Agilent N8973A Noise Figure Meter and Noise Source
    d. 6 inch SMA-SMA cable
    e. Balun
    f. 50Ω termination
    g. Band-pass filter
    h. Low Noise Amplifier (LNA)
2. Calibrate noise figure meter to span the range of noise figure meter. Set measure setup to down convert with 101 points.
3. Connect noise source to input of LNA and output of LNA to noise figure meter.
4. Measure NF and Gain of LNA.
5. Connect output of LNA to input of band-pass filter. Connect output of band-pass filter to positive input of Eval Board. Terminate negative input with 50Ω. Set power level to +8 dBm and signal to channel 0 frequency
6. Connect signal generator to single-ended input of balun. Connect I_+/Q_+ output of balun to positive clock input and I_-/Q_- to negative clock input. Set power level of clock to +6 dBm and frequency to 900MHz.
7. Connect positive output of Eval Board to noise figure meter. Terminate negative output with 50 Ω. Figure 33 displays the specific setup used for this test.
8. Save Trace.
9. Repeat steps 9-12 with a second LNA connected between band-pass filter and THA. Figure 34 demonstrates our test bench setup when a second LNA is used.

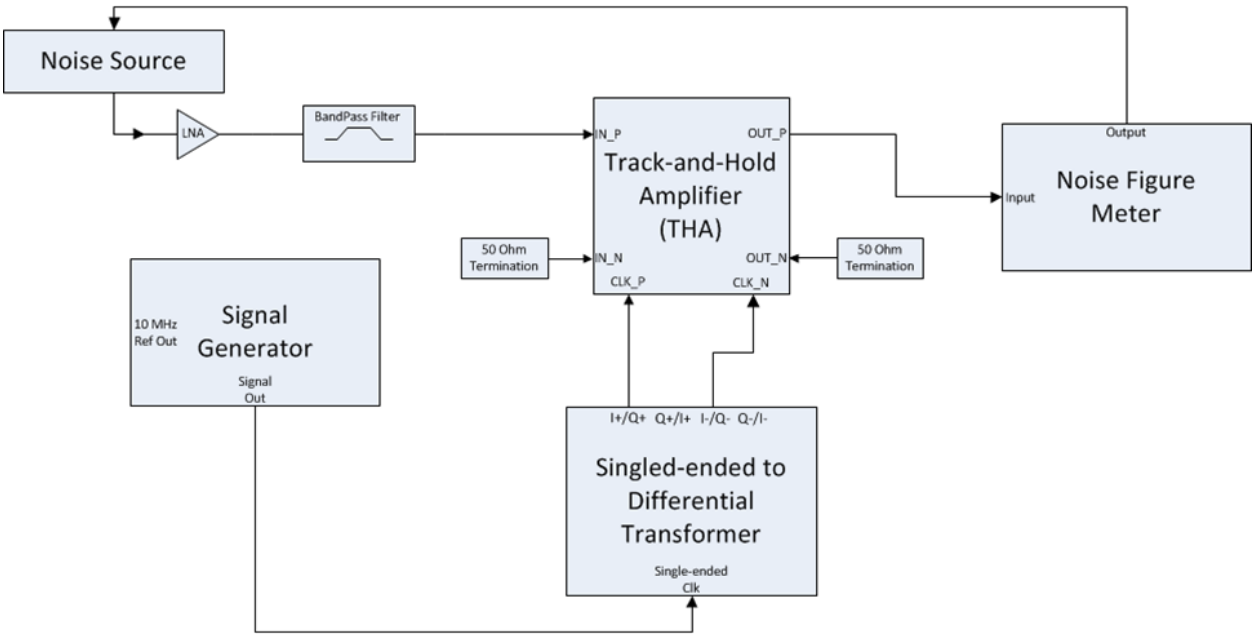

Figure 33: Original noise figure test bench

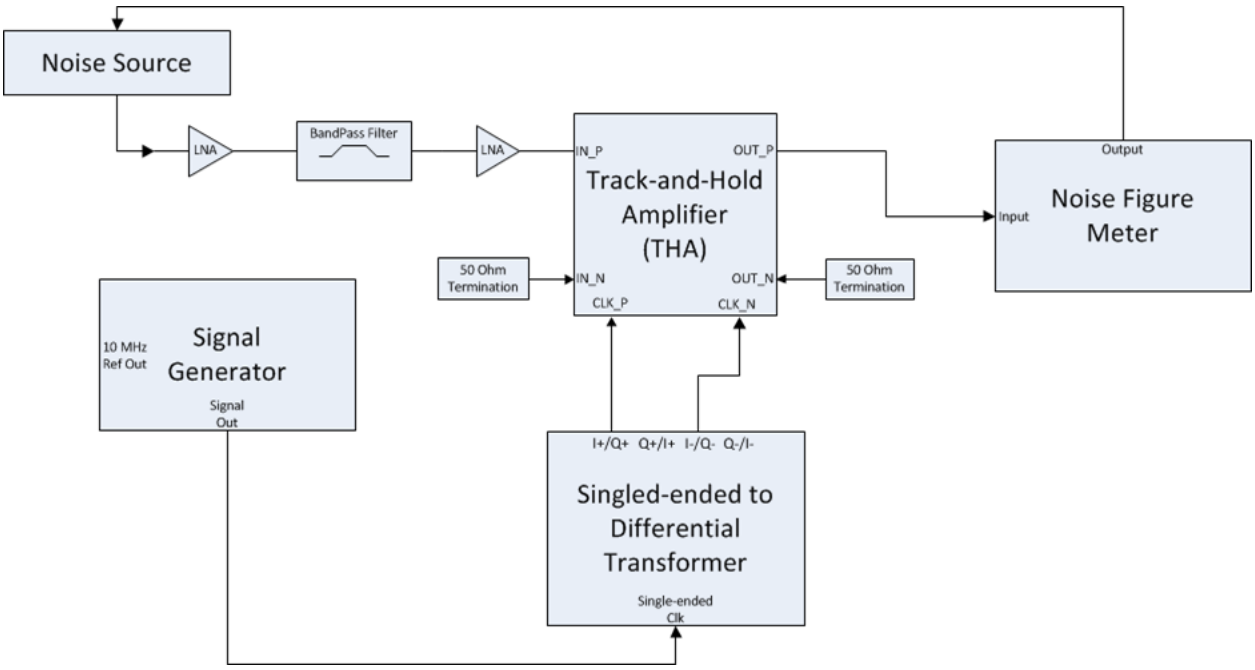

Figure 34: Adapted noise figure test bench

5.2.2 : Results

For our measurements, we used an LNA preceding the THA; thus we investigated its noise figure first. The NF for the LNA was about 0.9dB with a gain of ~26dB. Using both an LNA and band-pass filter at the input of the THA led to a NF of 15.8dB and gain of ~13dB at our IF. Figure 35 (Figure 57 for device 2) illustrates the results of the setup with an LNA and

band-pass filter at the input. After inputting a second LNA at the input of the THA, we observed a greater drop in NF. The NF for this setup was observed to be about 1.7dB with a gain of ~39dB. Figure 36 (Figure 58 for device 2) demonstrates this drop in NF with a second LNA at the input of the THA. This drop in NF can be explained using the noise figure formula for cascaded devices shown in Equation 16.

$$F = F_1 + \frac{F_2 - 1}{G_1} + \frac{F_3 - 1}{G_1 G_2} + \frac{F_4 - 1}{G_1 G_2 G_3} + \cdots + \frac{F_n - 1}{G_1 G_2 G_3 \ldots G_{n-1}} \tag{16}$$

The formula seen above demonstrates how the NF is heavily influenced by the first few stages of a given system [14]. Therefore, the addition of another LNA led to a large decrease in NF. Our initial design with one LNA did not contain a sufficiently low NF. Due to the second LNA lowering the noise figure to a sufficiently low result, our current design for this system contains two LNAs.

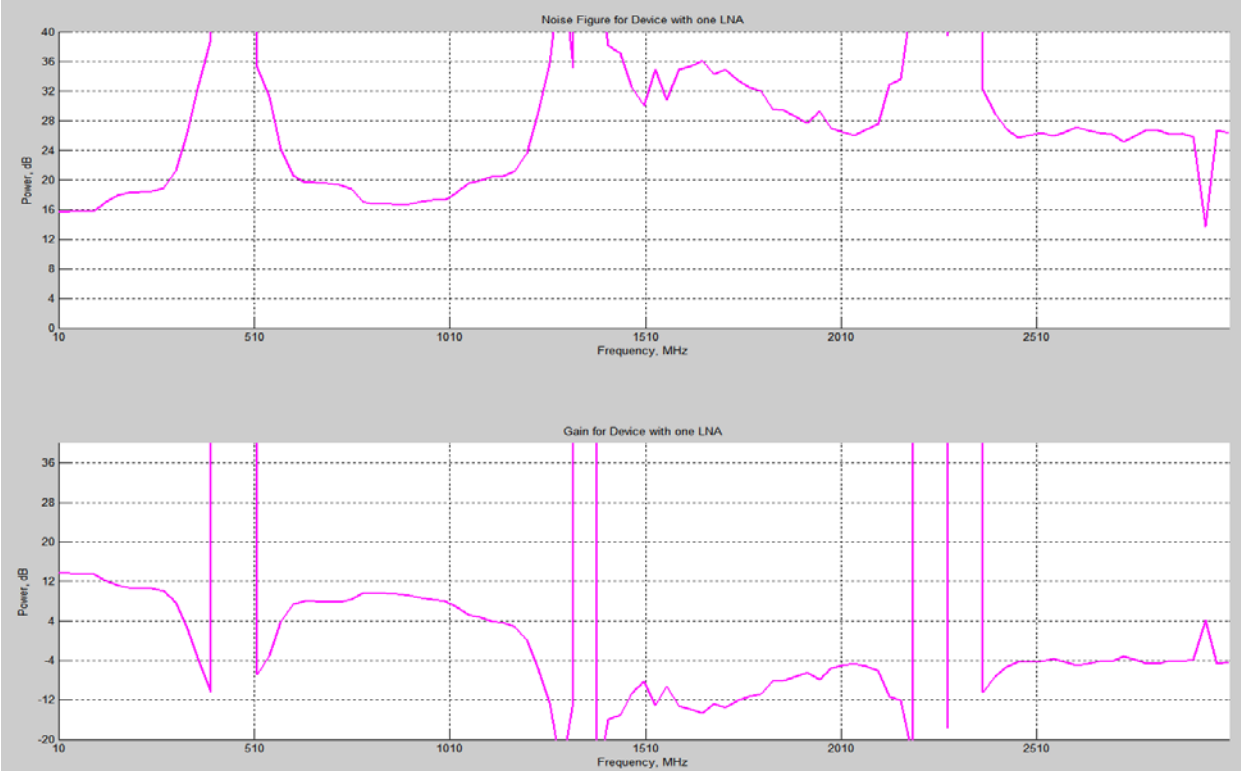

Figure 35: THA noise figure and gain with one LNA for device 1

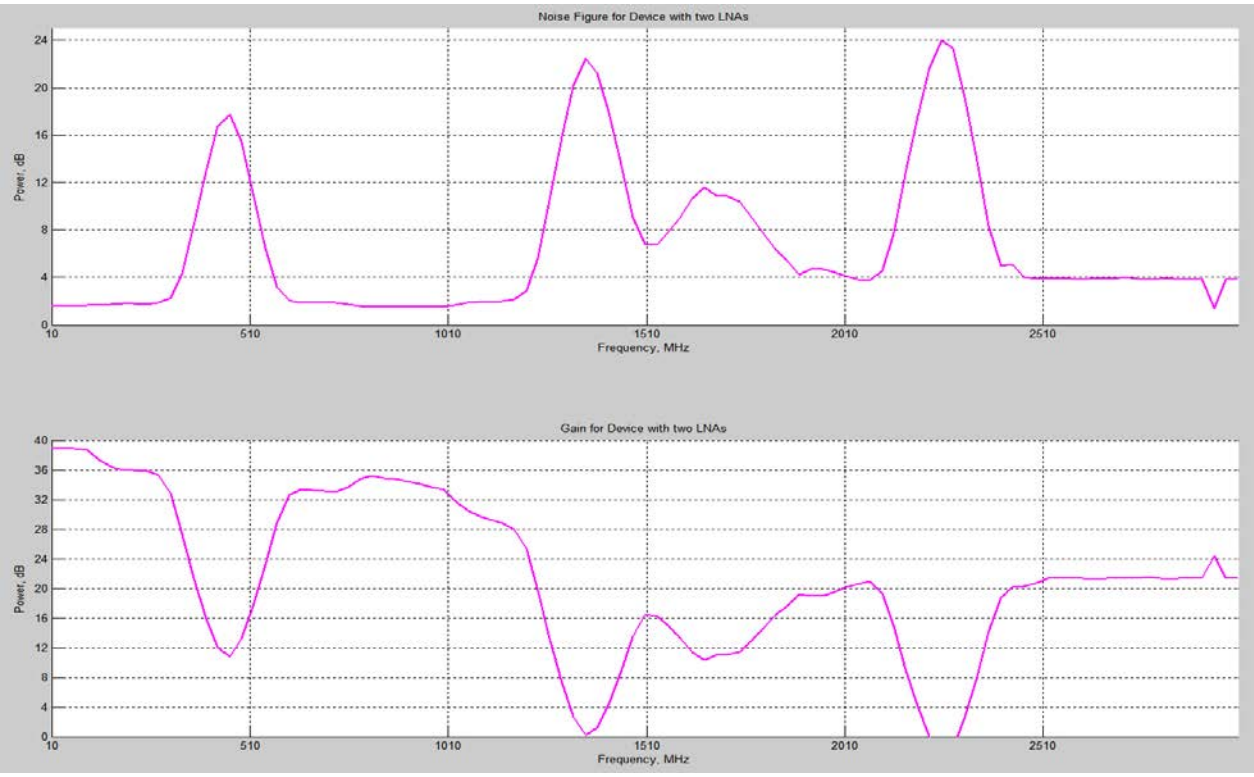

Figure 36: THA noise figure and gain with two LNAs for device 1

5.3 : Signal to Noise Ratio (SNR)

In this section we measured the signal to noise ratio of the track and hold amplifier. The signal to noise ratio determines how much more power your wanted signal has versus the noise in the system. The gain and noise figure of the system has to be factored in to the calculation dude to them both affecting the noise and signal equally.

5.3.1 : Procedure

The procedure for how we setup our test bench is listed below. An image of the entire test arrangement can be seen in Figure 37.

1. Requires the following instruments:
    a. Kepco MSK 10-10M Power Supply
    b. Anritsu MG3692B 20 GHz Signal Generator
    c. Agilent 8564EC 30 Hz – 40 GHz Spectrum Analyzer
    d. 6 inch SMA-SMA cable
    e. Balun
    f. 50Ω termination
    g. Splitter 2:1
    h. BNC-BNC cables
2. Connect signal generator to input of THA system. Terminate negative input with 50 Ω. Set power level to -38 dBm and signal to channel 0 frequency
3. Connect signal generator to single-ended input of balun. Connect I_+/Q_+ output of balun to positive clock input and I_-/Q_- to negative clock input. Set power level of clock to +6 dBm and frequency to 900MHz.
4. Connect positive output of Eval Board to spectrum analyzer. Terminate negative output with 50 Ω.
5. Connect 10MHz Reference Out from signal generator being used as a clock to the source of a splitter.
6. Connect outputs from splitter to 10MHz Reference In on the signal generator being used as the RF signal and to spectrum analyzer. Figure 37 demonstrates how our test bench was organized for this measurement.
7. Set center frequency on spectrum analyzer to IF (100 MHz for Channel 0) with frequency span of 200MHz.
8. Repeat for all channels. IF is 100MHz, 300MHz, and 400 MHz for Channels 1, 2, and 3, respectively.

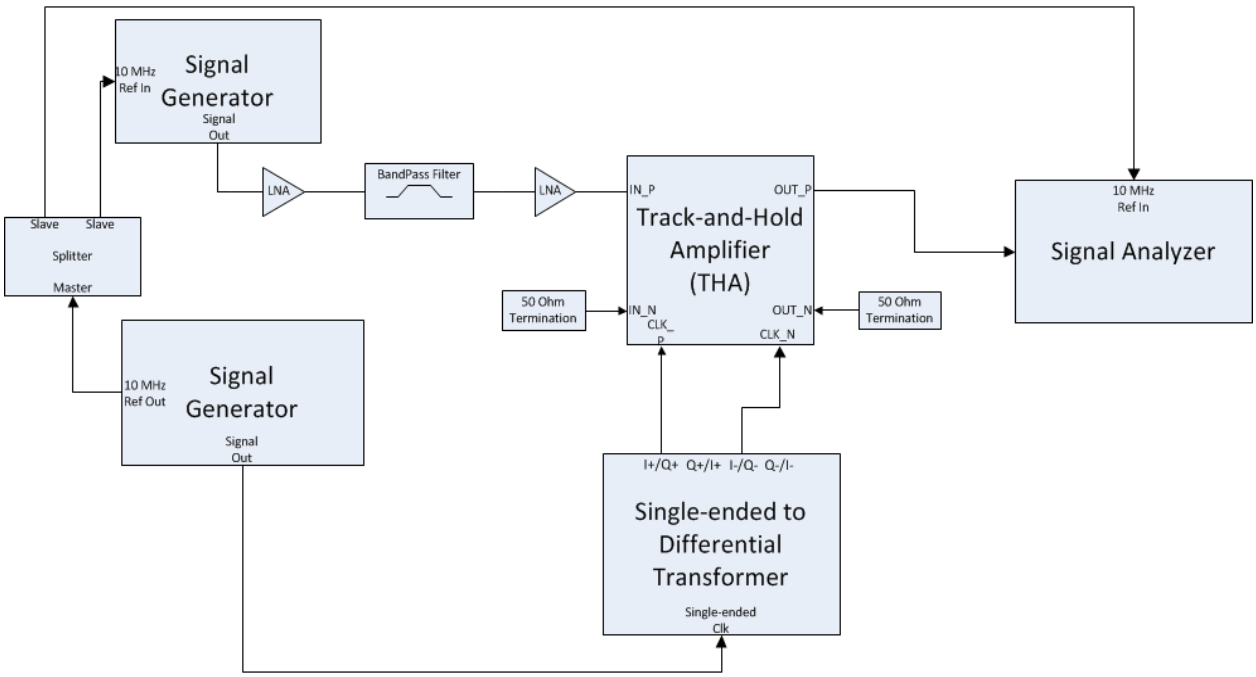

Figure 37: SNR test bench configuration

5.3.2 : Results

Signal to Noise Ratio (SNR) is a parameter that measures the relative strength of the signal power in relation to the noise power. This parameter describes the ability for the signal to be processed despite the amount of noise in the system. SNR can be calculated using Equation 17.

$$SNR = 10 * \log \frac{Pout}{Pout_{noise}} \tag{17}$$

Figure 38 (Figure 59 for device 2) provides an example of the IF signal at 300MHz. Using the power level of the signal as well as the noise power, we were able to determine the SNR. The noise floor is defined by Equation 18 where k is the Boltzmann constant, 1.3806e-23 J/K and T is the temperature of the device, which is about 300K. Using a bandwidth, BW, of 200MHz, the noise floor was found to be about –56.14 dBm. Our measurements for SNR are shown in Table 12. Our results show the device having a good output power level with respect to the noise floor.

$$P_{out_{noise}} = 10 * \log(k * T * BW * G * NF) \tag{18}$$

Table 12: SNR measurements for THA

SNR	Device 1 (dBm)	Device 2 (dBm)
Ch0	17.686	17.363
Ch1	17.150	17.255
Ch2	16.714	16.443
Ch3	15.879	15.341

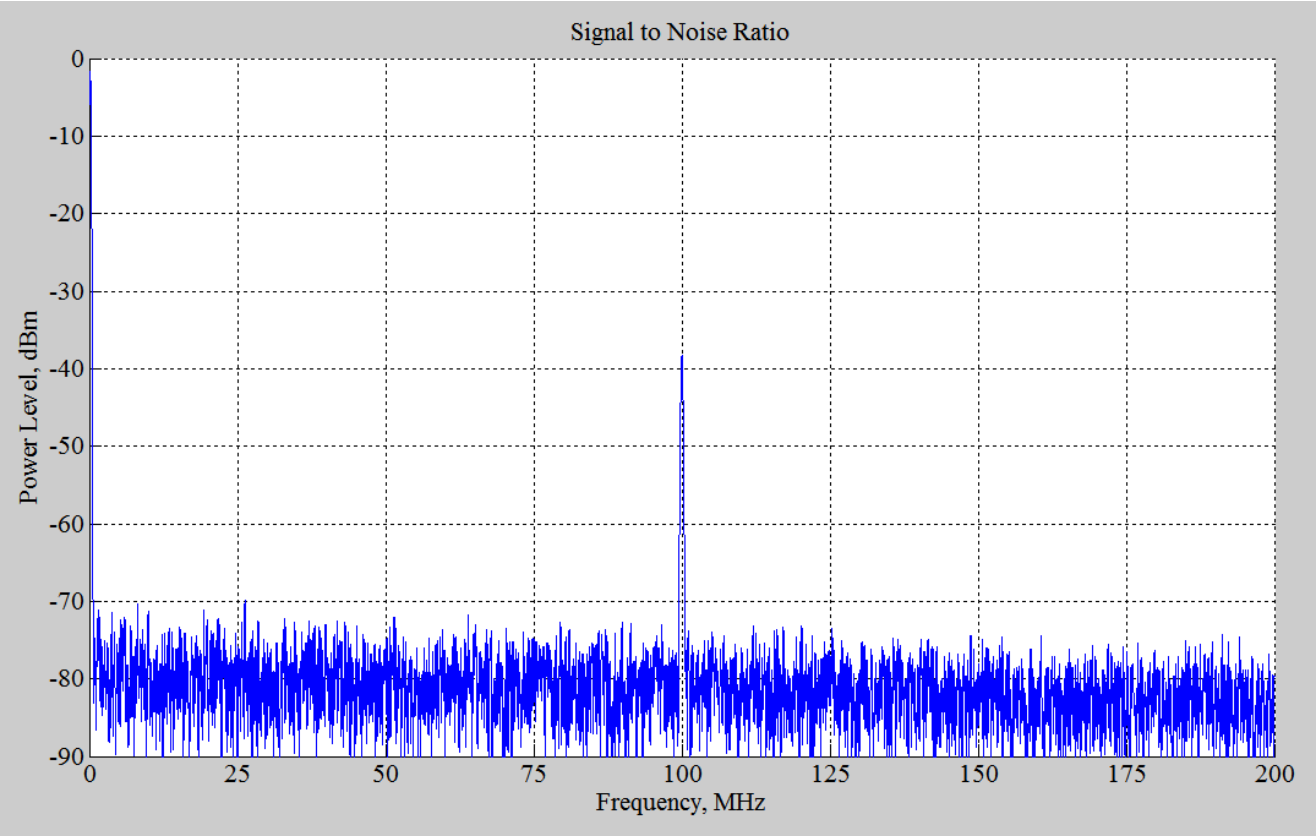

Figure 38: Signal power level with IF = 300 MHz and clock at 900 MHz for device 1

5.4 : 1-dB Compression

The procedure for how we calculated the 1dB compression point is discussed in the following section.

5.4.1 : Procedure

The procedure for how we setup our test bench is listed below. An image of the entire test arrangement can be seen in Figure 39.

1. Requires the following instruments:
    a. Kepco MSK 10-10M Power Supply
    b. Anritsu MG3692B 20 GHz Signal Generator
    c. Agilent 8564EC 30 Hz – 40 GHz Spectrum Analyzer
    d. 6 inch SMA-SMA cable
    e. Balun
    f. 50Ω termination
    g. Splitter 2:1
    h. BNC-BNC cable
2. Connect signal generator to positive input of Eval Board. Terminate negative input with 50 Ω. Set power level to +2 dBm and signal to channel 0 frequency
3. Connect signal generator to single-ended input of balun. Connect I_+/Q_+ output of balun to positive clock input and I_-/Q_- to negative clock input. Set power level of clock to +6 dBm and frequency to 900MHz.
4. Connect positive output of Eval Board to spectrum analyzer. Terminate negative output with 50 Ω.
5. Connect 10MHz Reference Out from signal generator being used as a clock to the source of a splitter.
6. Connect outputs from splitter to 10MHz Reference In on the signal generator being used as the RF signal and to spectrum analyzer. Figure 39 demonstrates how our test bench was organized for this measurement.
7. Set center frequency on spectrum analyzer to IF (100 MHz for Channel 0).
8. Increase power level in increments of 0.5 dBm and record signal power level. Continue until 1-dB compression point is measured.
9. Repeat for all channels. IF is 100MHz, 300MHz, and 400 MHz for Channels 1, 2, and 3, respectively.

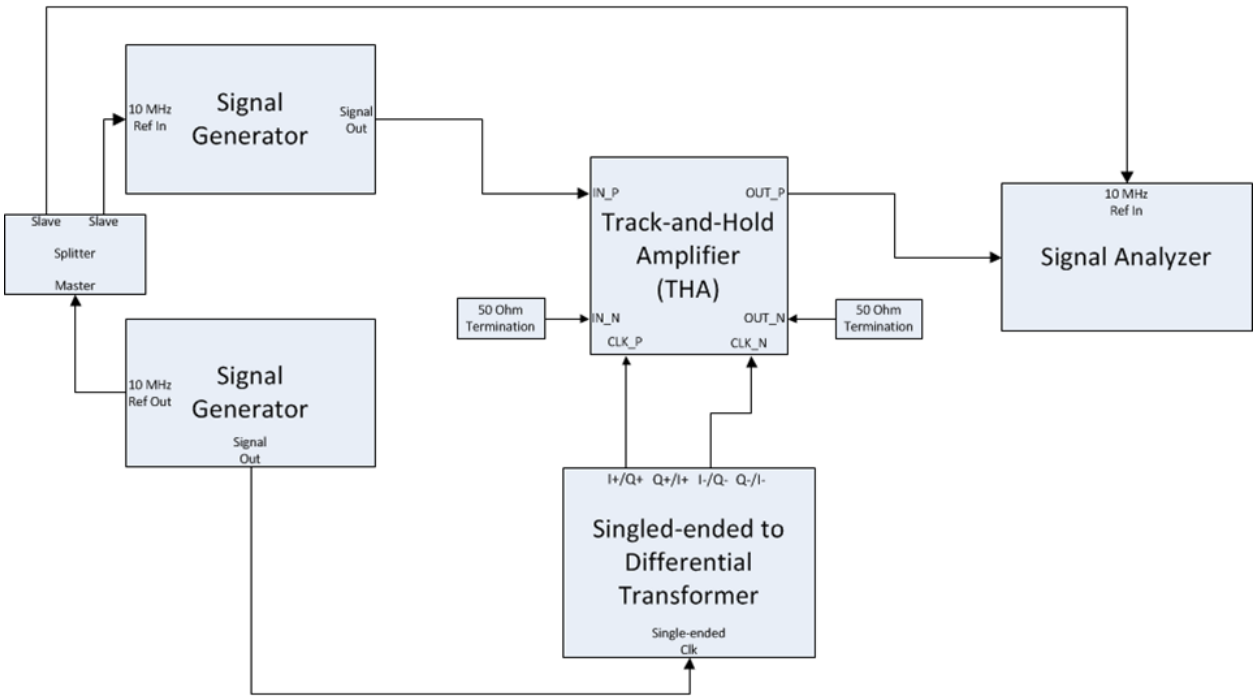

Figure 39: 1-dB compression test bench

5.4.2 : Results

The 1dB compression point is the point where the output signal power is approximately 80% of its ideal output signal power within the linear extrapolation. The compression of device occurs due to the device being railed or maxed out. The results for 1dB compression can be found in Table 13. The compression started to begin past +8 dBm input power which is consistent with the data sheet as we determined +8 dBm input power to be our full scale range. Figure 40 (Figure 60 for device 2) displays the graph of the output power versus the input power for both devices. These figures illustrate the devices working in the linear range before compressing as the input power becomes greater than +8 dBm (full-scale range).

Table 13: 1-dB compression point measurements for THA

1-dB Compression	Device 1 In (dBm)	Device 1 Out (dBm)	Device 2 In (dBm)	Device 2 Out (dBm)
Ch0	9.578	-3.689	8.967	-3.567
Ch1	8.106	-6.239	9.263	-3.607
Ch2	8.615	-5.774	8.948	-5.741
Ch3	8.856	-6.767	9.022	-7.011

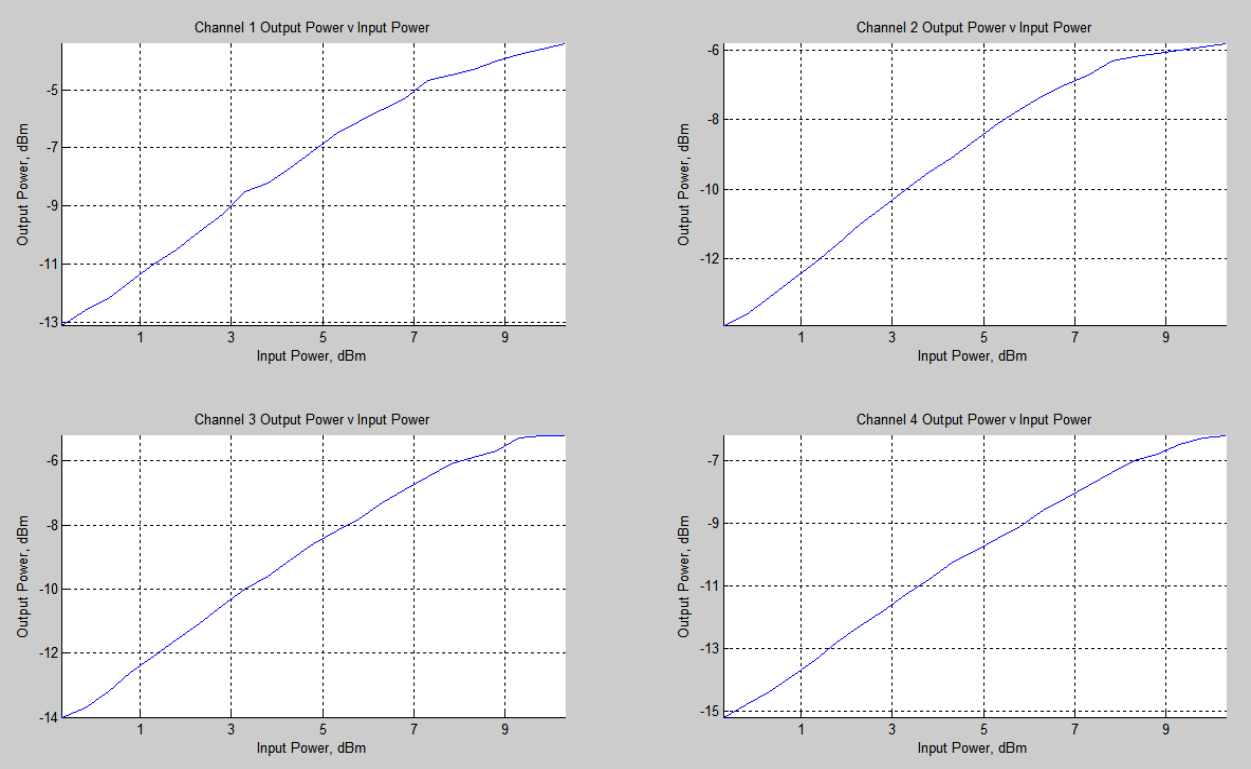

Figure 40: Output versus input power for device 1

5.5 : Third-Order Intercept Point (IP3)

To measure the linearity of the receiver, we investigated the third-order intercept point, or IP3. By injecting two closely spaced signals at the input, we can examine their third order intermodulated products at the output. As you increase the fundamental tone, the third order product should increase by a factor of three. By taking measurements at multiple points, one can perform a linear regression for the two lines. One will exhibit a slope of 1 while the other will exhibit a slope of 3. The 'y' coordinate of where these two lines cross is the output IP3 values that we are looking for.

5.5.1 : Procedure

The procedure for how we setup our test bench is listed below. An image of the entire test arrangement can be seen in Figure 41.

1. Requires the following instruments:
    a. Kepco MSK 10-10M Power Supply
    b. Anritsu MG3692B 20 GHz Signal Generator
    c. Agilent 8564EC 30 Hz – 40 GHz Spectrum Analyzer
    d. 6 inch SMA-SMA cable
    e. Splitter
    f. Isolator
    g. Balun
    h. 50Ω termination
    i. Splitter 3:1
    j. BNC-BNC cable
2. Connect two signal generators to isolators. Connect isolators to inputs of splitter with current flowing into splitter.
3. Connect source of splitter to input of THA system. Terminate negative input with 50 Ω. Set power level to -38 dBm and signal to channel 0 frequency
4. Connect signal generator to single-ended input of balun. Connect I_+/Q_+ output of balun to positive clock input and I./Q. to negative clock input. Set power level of clock to +6 dBm and frequency to 900MHz.
5. Connect positive output of Eval Board to spectrum analyzer. Terminate negative output with 50 Ω.
6. Connect 10MHz Reference Out from signal generator being used as a clock to the source of a splitter.
7. Connect outputs from splitter to 10MHz Reference In on the two signal generators being used as the RF signals and to spectrum analyzer. Figure 41 illustrates how our test bench was setup for this parameter measurement.

8. Set center frequency on spectrum analyzer to IF (100 MHz for Channel 0) with frequency span of 15MHz.
9. Repeat for all channels. IF is 100MHz, 300MHz, and 400 MHz for Channels 1, 2, and 3, respectively.

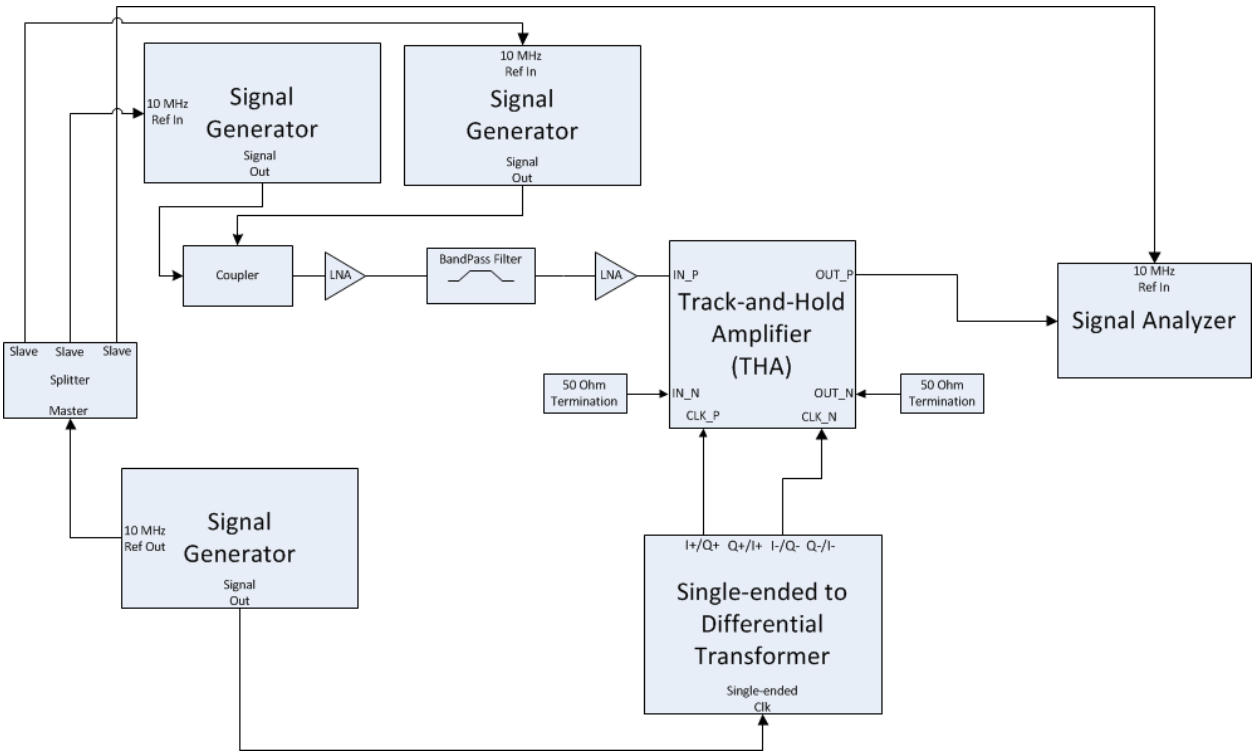

Figure 41: Third-order intercept point measurement arrangement

5.5.2 : Results

As stated before, the IP3 parameter is a measurement that describes the linearity of an electronic system or device. This parameter is dependent on the idealized output power as this value lies beyond the 1dB compression point. Our results for IP3 are shown in Table 14. These results demonstrate that the THA does not exhibit acceptable linearity. The IP3 was calculated based on the following equation:

$$\frac{3*P_{out}-P_{third-order}}{2} \quad (10)$$

Another issue that was observed in our measurements was the presence of even order harmonics for Channel 2. This channel revealed the presence of second and fourth order intermodulated products along with third and fifth order while Channels 0, 1, and 3 only

demonstrated third and fifth order intermodulated products. Figure 42 (Figure 61 for device 2) illustrates our measurement for this parameter on device 1.

Table 14: IP3 measurements for THA

IP3	Device 1 (dB)	Device 2 (dB)
Ch0	2.370	1.808
Ch1	2.030	1.653
Ch2	1.143	0.778
Ch3	-0.345	-0.728

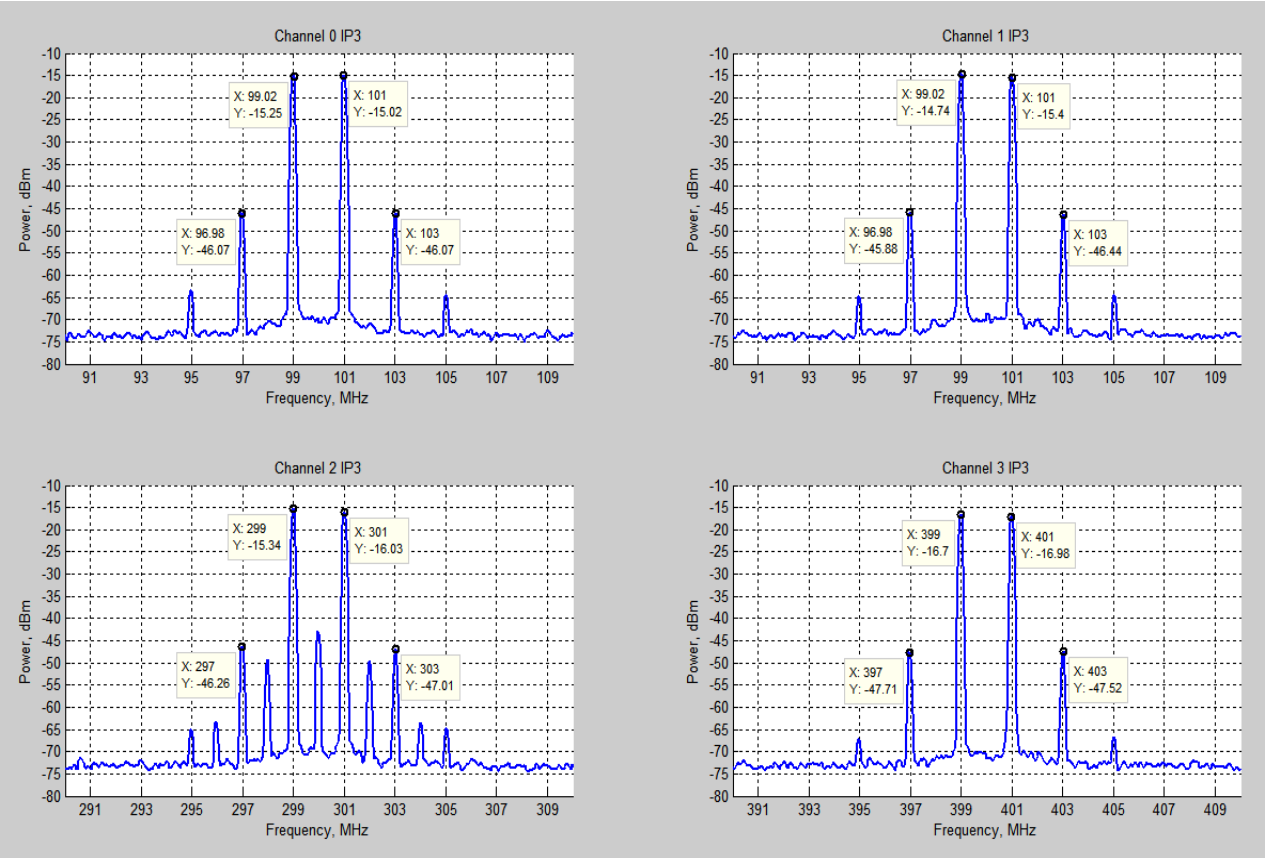

Figure 42: IP3 for device 1 for all four channels

Chapter 6 : Comparison

The following sections investigate the overall comparison between the two designs. Some of the issues brought up are the following: performance, cost, and size. Using these three characteristics, we made a list of recommendations and a final decision on which design performs better.

6.1 : Performance

Hittite's Wideband Track and Hold Amplifier may be used in the design of an RF receiver. However, this device contains various issues and concerns that must also be addressed. Some of the issues that this device posed were a moving IF, a large noise figure, referencing clocks required very high precision, and amplitude modulation at certain frequencies. Choosing our clock for the THA was difficult as we needed to verify that none of our channel frequencies were integer number multiples of the clock which caused amplitude modulation in the IF stage. This led us to choose 900MHz as our clock since none of the frequencies used in X-band were an integer number multiple of 900MHz. However, since our frequencies could not be changed, the IF would differ between each channel. For Channels 0 and 1, the IF was 100MHz while Channels 2 and 3 would have an IF of 300MHz and 400MHz, respectively. The formula to determine the IF for the THA is shown in Equation 14 where f_{clk} is the clock frequency and f_{signal} is the frequency of the input signal.

$$f_{IF} = \left| round\left(\frac{f_{signal}}{f_{clk}}\right) * f_{clk} - f_{signal} \right| \quad (14)$$

Phase-locking the reference clocks was another concern when evaluating the THA. Referencing the clocks required a precision of about 159fs for a 10 GHz signal to be accurate within +/- 10mV at full scale range. Several attempts were required until we could verify that our reference clocks were locked within 1ps. We could not verify even further due to the constraints of our oscilloscope. The formulas used to determine the slew rate (SR) of our signal is given in Equation 12, where f is the signal frequency and A is amplitude of the signal.

$$SR = 2 * \pi * f * A \quad (12)$$

The equation used to determine the accuracy necessary for proper phase locking is seen in Equation 13.

$$Sample\ accuracy = 10mV/SR \tag{13}$$

Another issue for our device was the large noise figure. To reduce this noise figure our device required two LNAs. The superheterodyne receiver contained much lower NF than the THA until a second LNA was implemented in the THA design. If the THA were to be implemented in receiver architecture, methods such as cascading more LNAs or gain blocks would be needed to suppress this very large noise figure.

In regards to IP3, the superheterodyne receiver displayed highly linear results as all the measurements exceeded +20 dB. However, the THA system demonstrated significantly lower linearity as several values were near 0 dB. While taking those measurements, we also observed second and fourth order intermodulated products being present in Channel 2. None of the channels in the superheterodyne receiver displayed the presence of second or fourth order intermodulated products.

Implementing a receiver using the THA would not result in fewer components when compared to a traditional superheterodyne due to the need of several band-pass filters to address the different IF among each channel. Our current design for a receiver consisting of the THA is shown in Figure 43. The design will become simpler if different operating frequencies can be used or if the clock frequency being injected into the THA could adjust. This simpler design is shown in Figure 44. The simplified THA-based receiver architecture could essentially be used as an RF front end if the previously mentioned concerns are addressed and overcome.

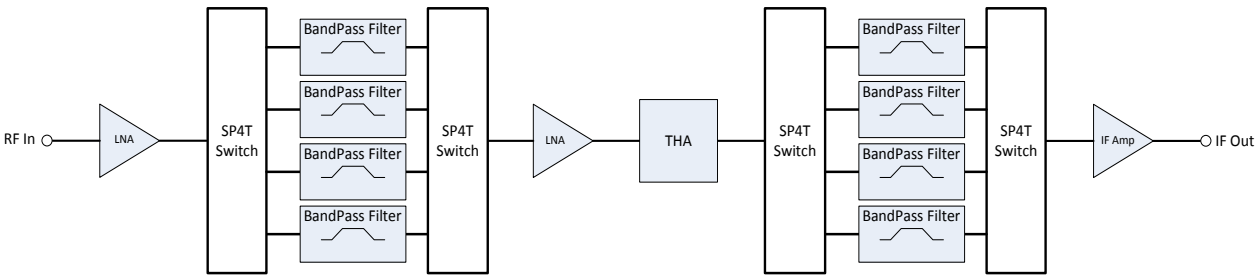

Figure 43: Current THA receiver design

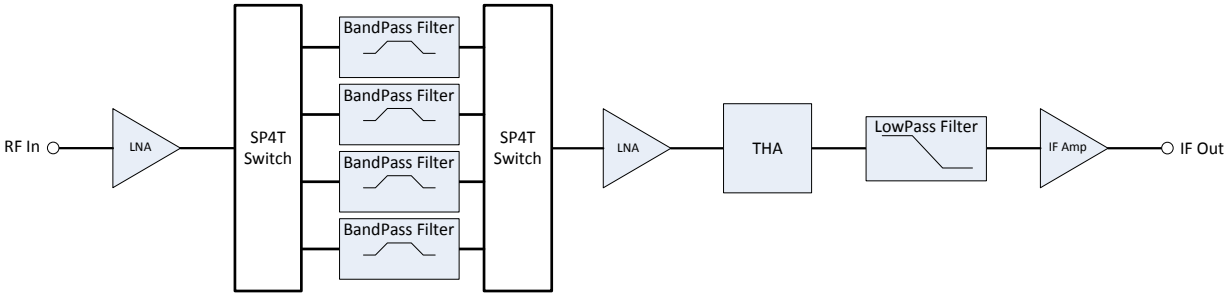

Figure 44: simplified THA receiver design

6.2 : Cost Analysis

We performed an approximate cost analysis between both receiver designs to help determine whether the receiver model with the THA would be more cost effective. Figure 45 illustrates the section of the superheterodyne design that we would replace with our THA design.

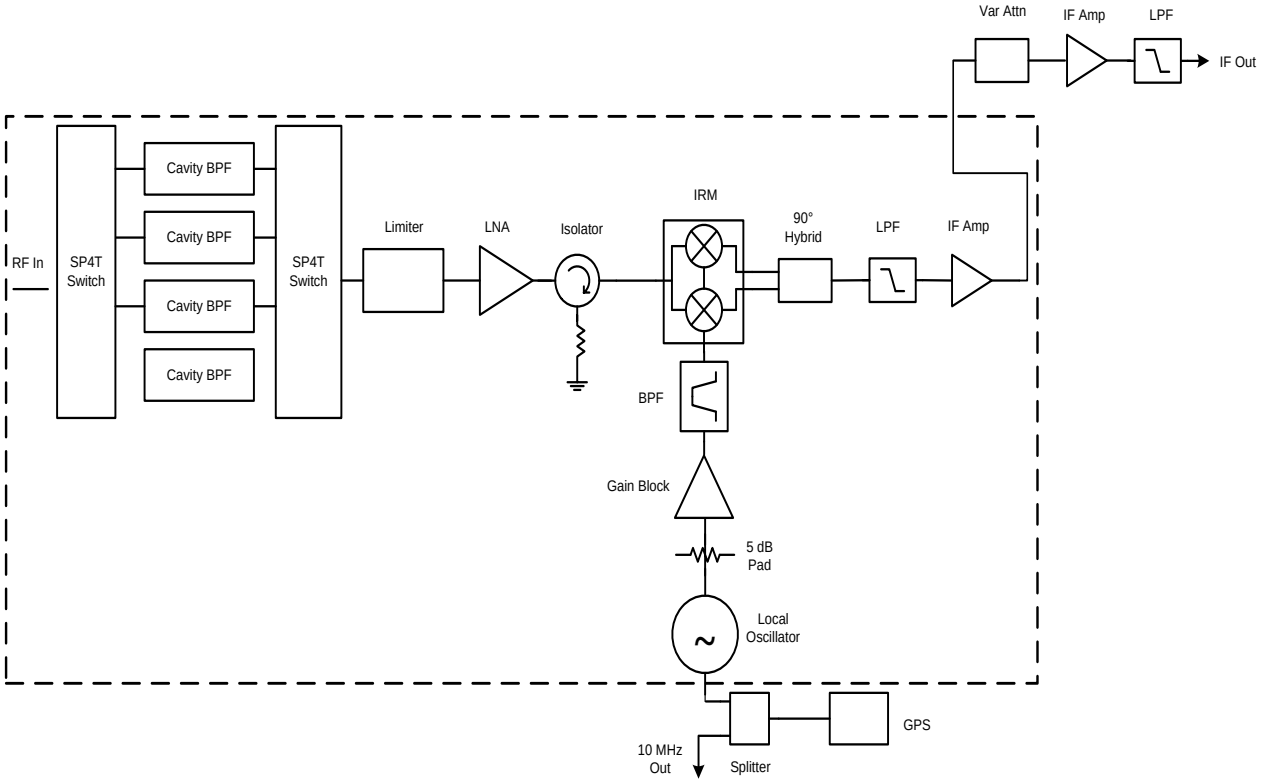

Figure 45: Segment of superheterodyne that would be replaced with THA design

Table 15 and Table 16 both reveal a list of components and the price for each part for the superheterodyne and the THA, respectively. The cost between both designs favors the THA as

the total cost for the superheterodyne is $14,075 while the THA is $10,468.90. This difference can be explained through the elimination of an image rejection mixer and an LO. The price of the LO itself accounted for $5,625 of the superheterodyne design. Although the cost for the THA design was cheaper, the overall design may not necessarily be more simplistic. The overall component count for the THA is greater as another two 4:1 switches and another 4 IF band-pass filters were required due to each channel containing a different IF. If the issue of a moving IF can be resolved either through using different operating frequencies or having the internal LO change, our current design of the THA receiver can be simplified.

Table 15: Price list for traditional superheterodyne setup

Rx components	Amount	Price	Total
RF 4:1 switch	2	$465	$930
BPF	4	$586	$2344
Limiter	1	$200	$200
LNA	1	$1650	$1650
Isolator	1	$178	$178
Image Rejection Mixer	1	$1000	$1000
Gain Block	1	$940	$940
LO filter	1	$576	$576
LO	1	$5625	$5625
Quadrature hybrid	1	$200	$200
LPF	1	$432	$432
	15		$14075

Table 16: Price list for current design of THA receiver

THA components	Amount	Price	Total
RF 4:1 switch	2	$465	$930
IF 4:1 Switch	2	$20	$40
BPF	4	$586	$2344
LNA	2	$1650	$3300
IF BPF	4	$594	$2376
IF Amp	1	$150	$150
THA	1	$534	$534
IF Balun	2	$29.95	$59.90
X-band Balun	1	$735	$735
	19		$10468.90

Table 13 contains a price list for the components of the simplified THA design if the previously mentioned moving IF could be addressed. The price of this design was calculated to

be $5,428.10 cheaper than the superheterodyne design and $1,822 cheaper than our current THA design. This significant price drop is attributed to the reduction of three IF band-pass filters, which reduced the price by $1,782. Although this design is much cheaper than the superheterodyne, it does not significantly reduce the total component count as this simpler THA design requires only one less component versus the superheterodyne.

Table 17: Price list for simplified THA design

THA components	Amount	Price	Total
RF 4:1 switch	2	$465	$930
BPF	4	$586	$2344
LNA	2	$1650	$3300
IF BPF	1	$594	$594
IF Amp	1	$150	$150
THA	1	$534	$534
IF Balun	2	$29.95	$59.90
X-band Balun	1	$735	$735
	14		$8646.90

6.3 : List of Recommendations

1. Need to isolate to one IF:

   Due to the IF being dependent on the clock, having a similar clock for all channels poses some difficulty in providing a constant IF among all channels. We suggested some possible methods for addressing this issue. One method would be to change the operating X-band frequencies to all be equidistant to the clock. Using a pre-selector to change clocks for each channel would be another method to manually set the IF. We could also ask Hittite if a register can be added in order to adjust the clock when the channels change. Being able to manually set our IF to one specific frequency may be a difficult task; however, this would provide greater simplicity in our design involving the THA.

2. Stay away from unstable frequencies:

   Instability was a major issue for the THA design. When taking initial measurements in order to determine our clock frequency, we noticed greater amplitude modulation on channels where the signal frequency was an integer number multiple of

the clock. When the outputs of these channels were viewed under an oscilloscope in the time domain, we realized that the system was unstable at these frequencies and would not be able to reconstruct a sine wave. This issue led us to choose a clock frequency of 900MHz as none of the X-band signals were integer number multiples of that frequency. We recommend verifying that the system is stable at all input frequencies with respect to the clock.

3. Poor linearity needs to be addressed:

   When measuring the IP3 parameter, we noticed the device containing a high power level for the third order intermodulated products. Due to the device being less linear than the superheterodyne model, the IP3 measurements were significantly lower for the THA. However, other implementations can be used to increase the linearity of the system.

4. Suppress the large noise figure:

   When measuring the noise figure for the device, we observed the device having significantly large noise figure. In order to reduce the large noise figure, an LNA and a bandpass filter were inputted into the device. Despite the use of an LNA, the noise figure of the system was still fairly high at about 16dB. We decided to input a second LNA into our system to further reduce the noise figure. The addition of a second LNA caused the noise figure to drop to a sufficiently low result of 1.6dB. Although we chose to add a second LNA in order to suppress the noise figure, there may also be other implementations that would also provide low noise figure such as using a gain block.

5. Precise phase-locking between clock and signal:

   The THA design requires very precise phase-locking between the clock and signal due to the large slew rate of X-band signals. For a 10GHz input signal at $1V_{pp}$ to be accurate within +/-10mV, the absolute sample accuracy must be 159fs. We verified our system to have an absolute sample accuracy within 1ps but could not measure a more precise value due to the constraints of our oscilloscope.

Chapter 7 : Conclusion

In many ways, a direct connection of a wideband and high dynamic range analog to digital converter to the output of an antenna represents the ultimate goal in receiver simplification. In order to move the digital interface closer to the antenna output, the Hittite wideband THA was implemented in an effort to evaluate the possibility of reducing the complexity of many RF receivers. While the THA design did not allow for a direct connection between the antenna and the ADC, this new design did reduce the cost for the RF front end of a receiver and does eliminate several components found in a superheterodyne such as the image rejection mixer and the LO. We evaluated several parameters such as SNR, IP3, 1dB compression, and NF to gain valuable insight about the performance between the two designs. Our goal for this project was to implement the new Hittite THA design and determined whether or not it is a viable addition to the superheterodyne architecture.

After we implemented and evaluated both designs, we observed that the THA design raised many issues that affected its performance. The problems that the THA design posed include a differing IF among each channel, instability if the input frequencies are integer number multiples of the clock, a large noise figure, poor linearity, and phase-locking the reference clocks. Due to this instability, we chose to have a clock of 900MHz in order to avoid these unstable frequencies. However, as the IF is dependent on the clock, the clock being constant among all channels resulted in each channel containing a different IF. We could not implement our original design as the system contained an excessively large noise figure. In order to suppress this large noise figure, a second LNA was needed at the input of the THA. This setup allowed for the NF to be lowered to an acceptable level. Our system also contained very poor linearity which needed to be addressed. While the superheterodyne model contained high linearity with IP3 measurements of +20 dB, the THA design yielded very low IP3 measurements. Phase-locking between clock and signal was difficult due to the large slew rate requirement at X-band frequencies. The very high slew rate required our system to contain very precise sample accuracy. For our system to be accurate within +/-10mV at full scale range with a 10GHz input signal, our absolute sample accuracy must be within 159fs.

Although many technical issues were rasied with our THA design, the cost comparison clearly favored the THA. The superheterodyne design cost $3,606.10 more expensive than the

THA design. This price difference is attributed to the elimination of the LO and the image rejection mixer in the THA design. Those two components cost a total of $6,625 which accounted for approximately 47% of the entire superheterodyne design. Although this design is cheaper, it may not reduce the complexity of an RF receiver as it contains a total of 19 components compared to the 15 components found in the superheterodyne model. However, if the issue of a shifting IF between each channel is overcome, our current design can be further simplified, leading to a total price difference of 5,428.10 between the superheterodyne model and the THA model. This price drop is attributed to the removal of three IF bandpass filters which accounted for $1,782. The removal of several components would also provide a simpler design compared to the superheterodyne. The total component count of the superheterodyne model was 15 components whereas the simplified THA model would provide a total of 14 components.

Based on our performance comparison and cost analysis, we developed a list of recommendations relative to the THA design. The issue of a changing IF between channels needs to be addressed. Some plausible methods for overcoming this issue include changing the RF operating frequencies or providing a pre-selector to change the clock between each channel in order to maintain a constant IF. The next recommendation is to avoid unstable frequencies. Instability of the system would occur at input frequencies being integer number multiples of the clock. These input frequencies led to an IF of 0 Hz, which would not be able to reconstruct the input signal. Another issue was the poor linearity of the THA system. While the superheterodyne demonstrated high linearity, the THA provided relatively low IP3 results. Other implementations may be needed in order to mitigate the low linearity of the THA system. Our next recommendation is to develop ways to suppress the large noise figure of the device. We used two LNAs and a bandpass filter at the input of the THA in order to cascade the noise figure resulting in a low noise figure at the output. Other methods for reducing the noise figure include the addition of gain blocks along with LNAs. We also recommend that there is precise phase-locking verification between the clock and signal. The large slew rate of X-band signals requires that the absolute sample accuracy be very precise. Our system required a precision of approximately 159 fs between the clock and signal.

References

[1] "The Superhet or Superheterodyne Radio Receiver." *Superhet or Superheterodyne Radio Receiver*. N.p., n.d. Web. 04 Sept. 2012.

[2] "DACs and ADCs Assist RF Communications." *Microwaves and RF*. N.p., n.d. Web. 04 Sept. 2012.

[3] Armstrong, E.H. "The Super-Heterodyne-Its Origin, Development, and Some Recent Improvements." *Proceedings of the IRE* 12.5 (1924): 539-552. Print.

[4] Kester, Walt. "Understand SINAD, ENOB, SNR, THD, THD + N, and SFDR so You Don't Get Lost in the Noise Floor." *Tutorials*. Analog Devices, 2009. Web. 25 June 2012. <http://www.analog.com/static/imported-files/tutorials/MT-003.pdf>.

[5] Hittite Microwave. "Hittite's 18 GHz Ultra Wideband Track-and-Hold Amplifier Enhances High Speed ADC Performance." Hittite Microwave, 2011. Web. 14 June 2012

[6] Pozar, D. M. "Chapter 3.7, Dynamic Range." *Microwave and RF Wireless Systems*. New York: John Wiley & Sons, 2001. 102-103. Print.

[7] Rohde, Ulrich L., and David P. Newkirk. "1-7 System Specifications and Their Relationship to Circuit Design." *RF/microwave Circuit Design for Wireless Applications*. New York: John Wiley, 2000. 92-96. Print.

[8] Pozar, David M. *Microwave Engineering*. Hoboken, NJ: J. Wiley, 2005. Print.

[9] Gu, Qizheng. "4.2.4. Influence of Antenna VSWR to Receiver Noise Figure." *RF System Design of Transceivers for Wireless Communications*. New York: Springer, 2005. 241-242. Print.

[10] Gu, Qizheng. "3.1.3.1 Receiver Sensitivity, Linearity, and Selectivity." *RF System Design of Transceivers for Wireless Communications*. New York: Springer, 2005. 133. Print.

[11] Pozar, D. M. "Chapter 7.1, Mixer Characteristics." *Microwave and RF Wireless Systems*. New York: John Wiley & Sons, 2001. 227-228. Print.

[12] Pozar, D. M. "Chapter 3.7, Dynamic Range." *Microwave and RF Wireless Systems*. New York: John Wiley & Sons, 2001. 101-102. Print.

[13] "Mixers." - *Microwave Encyclopedia*. P-N Designs, Inc., 9 June 2012. Web. 02 July 2012. <http://www.microwaves101.com/encyclopedia/mixers.cfm>.

[14] Pozar, D. M. "Chapter 3.5, Noise Temperature and Noise Figure." *Microwave and RF Wireless Systems*. New York: John Wiley & Sons, 2001. 91-93. Print.

Acknowledgements

We would like to thank the following people whose help and assistance was invaluable in this project:

Eric Renda Jr., who selflessly helped get our project functional even though he wasn't a project advisor and humbly fixed every problem we had in under a minute, while making deride comments like, "Don't worry, I used to do stupid things all the time when I was an intern."

Naomi Marcus, who suffered our tedious, unending questions for the last five and a half months and took time to show us how to use extremely expensive equipment properly so we didn't blow up any of our devices… again.

Chris Serrano, who helped us build a superheterodyne receiver and showed us how to characterize it with different receiver parameters.

John Putnam, the one who hired us to work on this project, and read over all of our papers and presentations.

Professor Reinhold Ludwig, who took time every week to read over our work, help guide us to the correct solution, and taught us the basics of RF and Microwave engineering.

Professor Sergey Makarov, who constructed our project with the MITRE Corporation and got us transportation to and from work every day.

And of course the people at Border Café on 128 Middlesex Turnpike, Burlington M.A., who served us delicious dishes that kept us full and sane during the dark times.

Appendices

The following section contains the research that was gathered in preparation of the Major Qualifying Project (MQP) with MITRE. The first section contains information on receivers and their performance parameters. Topics discussed include signal to noise ratio, dynamic range, input/output VSWR, receiver selectivity, image rejection and IP3.

Appendix I: Receiver Performance Parameters

There are numerous parameters that must be considered when building a receiver for an RF/Microwave application. Understanding the relationship between all these parameters is important so that tradeoffs and compromises can be made to ensure the receiver meets performance requirements. This section offers an introductory view of these parameters and how they pertain to receiver design.

Signal to Noise Ratio and Noise Figure

Noise in a receiver is very important to consider when receiving a signal. By comparing the desired signal power to the noise power in a particular system, one can determine whether the noise in the system will allow the desired signals to be processed. The parameter used to define the ratio is called the signal to noise ratio (SNR). The SNR is defined as the root-mean-square (RMS) signal amplitude divided by the average root-sum-square (RSS) of the noise, excluding DC, harmonics and other spurious signals. Noise power is defined over a certain frequency range or bandwidth. The exact formula for calculating SNR can be seen in Equation (2), where Pout and $Pout_{noise}$ are in Watts.

$$SNR = 10 * \log \frac{Pout}{Pout_{noise}} \tag{2}$$

In general, SNR for a receiver degrades as the bandwidth increases. Figure 2 below shows a typical receiver output at an IF frequency of 1.05 GHz. Assuming we are operating at room temperature with a bandwidth of 200 MHz, the SNR of the figure below is approximately 70 dB. Our noise floor is defined in Equation (3) where k is the Boltzmann constant, which is 1.3806e-23JK^{-1}, and T is the room temperature in Kelvin. Using a bandwidth (BW) of 100kHz, the noise floor will be -120 dBm. The signal in Figure 3 is contained in an ideal system where all the harmonics and intermodulated products are filtered out. Otherwise, these distorted products would affect the SNR.

$$Pout_{noise} = 10 * \log(k * T * BW) = -174 + 10 * \log(BW) \quad (3)$$

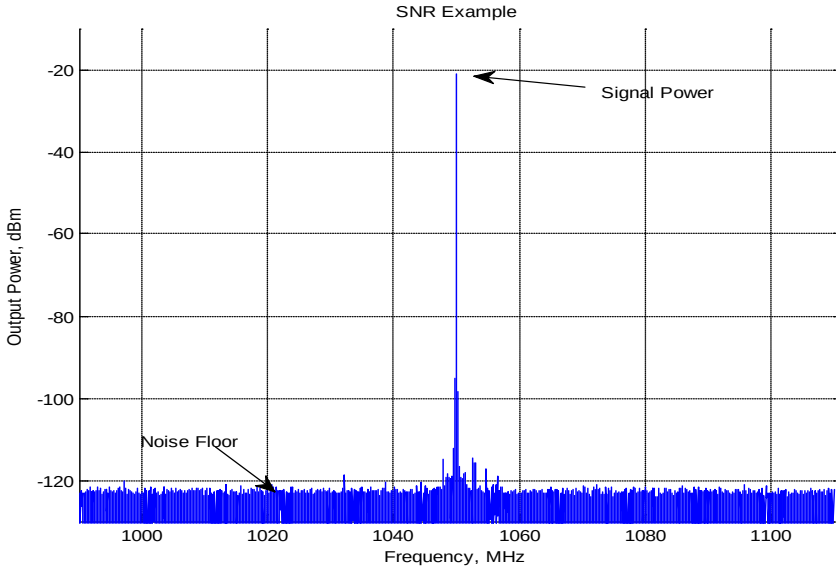

Figure 46: Typical output for receiver at IF stage

SNR is not the only parameter that determines relative strength of the signal versus the noise. One of the other parameters to consider is the signal to noise and distortion ratio (SINAD). This test takes into account the harmonics and other distortion products that could exist in the system and includes them in the noise calculations. When two signals at frequencies f_1 and f_2 pass through a non-linear component in a receiver, the non-linear characteristic produces frequencies at nf_1 +/- mf_2 where n and m are integers. Harmonics are the nf_1 or mf_2 integer multiples of f_1 and f_2, while other distortion products where both n and m $\neq$ 0, are referred to as intermodulation products. The two-tone third order intermodulation products $2f_1 - f_2$ or $2f_2 - f_1$ are particularly troublesome, since they can fall directly within the IF passband and cannot easily be filtered out. The power ratio of harmonic or intermodulation distortion products to the desired signal is in units of decibels with respect to the carrier (dBc). While SNR disregards distortion products when calculating the signal to noise ratio, SINAD does not and is therefore a more accurate representation of the system performance. The formula for calculating the SINAD ratio in decibels can be seen in Equation (4) [4].

SNR is used in calculating the noise figure (NF) of a receiver. Noise figure is a ratio of the signal to noise ratio at the input of a receiver divided by the signal to noise ratio at the output of a receiver, which is seen in Equation (5). Note that the signal, noise, and distortion values in

Equation (4) and Equation (5) are all power levels while SINAD and NF are recorded in decibels.

$$SINAD = 10 * \log \frac{Pout + Pout_{noise} + Pout_{distortion}}{Pin_{noise} + Pin_{distortion}} \quad (4)$$

$$NF = 10 * \log \frac{SNR_{in}}{SNR_{out}} \quad (5)$$

The dynamic range (DR) of a receiver is the ratio between the maximum input signal level and the minimum detectable signal level. For a receiver system, the dynamic range is bounded by the noise floor ($P_{out_{noise}}$) on the lower side and the 1dB compression point of the RF amplifier (P_{1dB}) on the upper side. If these two values are calculated in decibels (dB or dBm) then the formula for calculating the dynamic range of the system can be seen in Equation (6).

$$DR = P_{1dB} - Pout_{noise} \quad (6)$$

While this is useful, most RF receiver designers use another formula that is called spurious free dynamic range (SFDR). The definition for spurious free dynamic range is the ratio between the maximum output signal power and the highest spur which is generally the third-order intermodulated products [6]. This dynamic range calculation takes into account the undesired intermodulation products or spurs in the system that might be due to undesired, random spurs and are greater than the noise floor. SFDR is calculated as the output power ($P_{\omega 1}$) for a desired signal frequency divided by the output power of the third-order intermodulation products ($P_{2\omega 1-\omega 2}$). Equation (7) shows the formula for calculating the SFDR, note that everything is calculated in dB. As noted earlier, intermodulation distortion (IMD) involves the generation of new signals that are not just at harmonics. "Third-order IMD (IM_3) results, for an input consisting of two signals ω_1 and ω_2, in the production of new signals at $2\omega_1 \pm \omega_2$ and $2\omega_2 \pm \omega_1$ [7]." The third-order IMD products at $2\omega_1 - \omega_2$ and $2\omega_2 - \omega_1$ can be quite troublesome, since for two signals ω_1 and ω_2 that are closely spaced and within the input signal range, the IMD products can appear within the IF passband and cannot easily be filtered out.

$$SFDR = P_{\omega 1} - P_{2\omega 1-\omega 2} \quad (7)$$

Input and Output Voltage Standing Wave Ratio

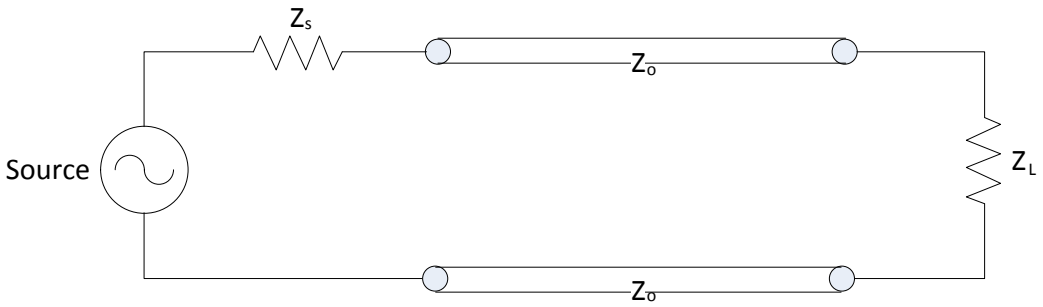

Figure 47: Example circuit for VSWR circuit

The voltage standing wave ratio (VSWR) is a parameter that can have a significant impact on the noise figure and selectivity of any receiver. Figure 70 seen above shows a simplistic transmission line circuit, which will be used for an example calculation. VSWR in the simplest terms measures the impedance mismatch at the input and output of the receiver. While this mismatch can be overcome through impedance matching or matching networks, perfectly matching a system is impossible when tolerances are considered. Every real world system will have some VSWR that is above 1, so theoretical formulas must be used to understand the effects. The formula for calculating the input or output VSWR can be seen in Equation (24) and Equation (25) [8].

$$VSWR_{In} = \frac{1+|\Gamma_S|}{1-|\Gamma_S|} \; where \; \Gamma_S = \frac{Z_S - Z_0}{Z_S + Z_0} \tag{24}$$

$$VSWR_{Out} = \frac{1+|\Gamma_L|}{1-|\Gamma_L|} \; where \; \Gamma_L = \frac{Z_L - Z_0}{Z_L + Z_0} \tag{25}$$

Ideally, a VSWR of 1 means that there is no mismatch, since Γ_s or Γ_L is equal to zero, and all the power is delivered from the source to the load. However, it is impossible to get a perfect impedance match since everything is made with an impedance tolerance, so compromises must be made when designing a receiver. The mismatch between source and load has even greater implications when noise figure (NF) is taken into account. As stated before, noise figure is the degradation of the signal to noise ratio when comparing the input to the output of any device. To show how all of these parameters are intertwined, the relationship between VSWR and NF will be shown, while excluding SNR. Equation (26) shows the rather complicated relationship between NF and VSWR. Note that $F_{Rx,o}$ is the receiver noise figure under perfectly matched conditions. The total NF of the receiver increases as VSWR increases as shown in Figure 71. To understand how much of an impact this can have, one can look at standard cell

phone users as an example. On average, the VSWR of the antenna in a cell phone can vary anywhere from 1.1 to 6. By making a small extrapolation from the graph seen in Figure 71, one can say that on average the NF will vary by approximately 4 dB while talking on a cell phone. That amount of power loss due to mismatch can easily disrupt the receiver by causing too much noise in the SNR and the NF.

$$NF_{Rx} = 10 * \log\{1 + \frac{F_{Rx,o}-1}{2}(\frac{1}{VSWR} + VSWR)\}\ [dB] \quad (26)$$

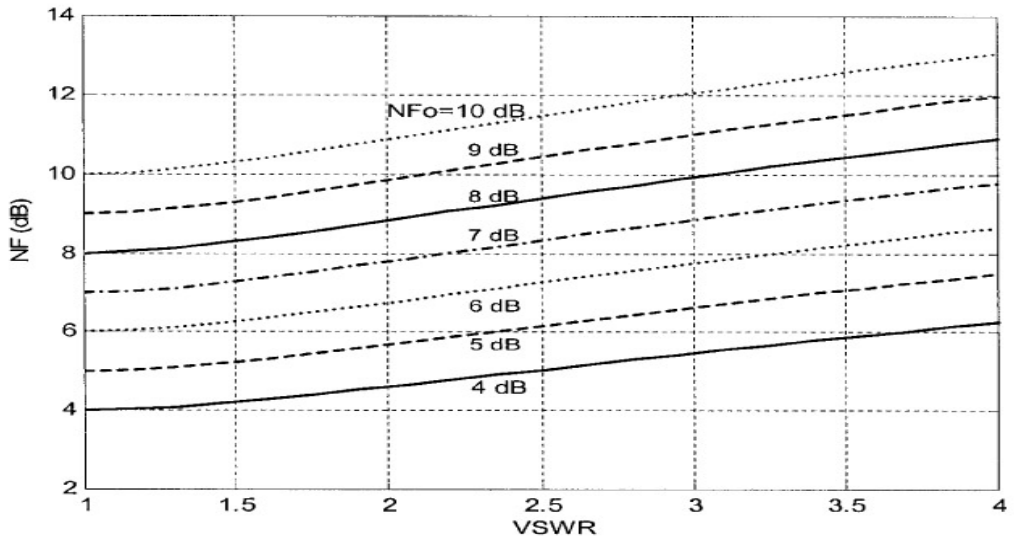

Figure 48: Noise figure versus VSWR with initial NFo Values 4-10 dB [9]

Receiver Selectivity and Image Rejection

Receiver Selectivity consists of the ability to remove any unwanted signals and obtain any wanted signals. Proper filtering allows for the desired signals to be received and the rejection of unwanted signals. Receiver selectivity is measured by using a ratio of the wanted signal versus a different signal from another frequency. This ratio is described in Equation (27).

$$Selectivity = \frac{P_{out}}{P_{spur}} \tag{27}$$

One issue caused during the mixing process in a receiver is the spurious signals, or spurs, that are formed. Earlier, we noted the general production of harmonic or intermodulation signals in a non-linear component at frequencies nf_1 +/- mf_2, given input signals at frequencies f_1 and f_2. Mixer spurs are undesired output frequencies due to the multiplication of desired input signal and the mixer LO. They are a subset of the general set of spurious signals that can be due to undesired input signals. The mathematical definition of these mixer spurs is represented in Equation (28). The desired responses include M=1 and N=-1 for low-side injection and M=-1 and N=1 for high-side injection. For certain combinations of f, f_{LO}, M and N it is possible for the mixer spurs to appear in the desired IF passband. Mixer spur calculators are available to determine the presence of these spurs in a receiver.

$$IF = M * f + N * f_{LO} \tag{28}$$

An example of receiver selectivity includes adjacent channel selectivity. Channel selectivity defines the receiver's ability to receive the desired signal while there are other adjacent channels near the desired frequency. High filter attenuation will help reduce these interfering signals. The selectivity ratio for adjacent channel selectivity is known as the adjacent-channel rejection ratio (ACRR) where the other signal level is represented by an adjacent signal. ACRR is defined in Equation (29). Note that $Padj_{channel}$ is the power level of the adjacent channel and Pout is the power level of the current channel.

$$ACRR = \frac{P_{out}}{Padj_{channel}} \tag{29}$$

The superhet receiver has a major issue with image frequency. The image frequency is a frequency other than the original RF signal that produces the same IF when multiplied with the LO frequency within the mixing stage. The image frequency is considered to be an example of a

spur where the M and N from Equation (28) would be inversed from the IF to represent the image frequency. For example, if an input signal contains a frequency of 5GHz and the local oscillator with a frequency of 3GHz, then the IF is 2GHz. However, if a frequency of 7GHz is inputted into the mixer, then the difference of this frequency with the LO frequency is also 2GHz leading to two interfering signals. This difference is shown in Figure 72. The image frequency can be found using Equation (30) [10].

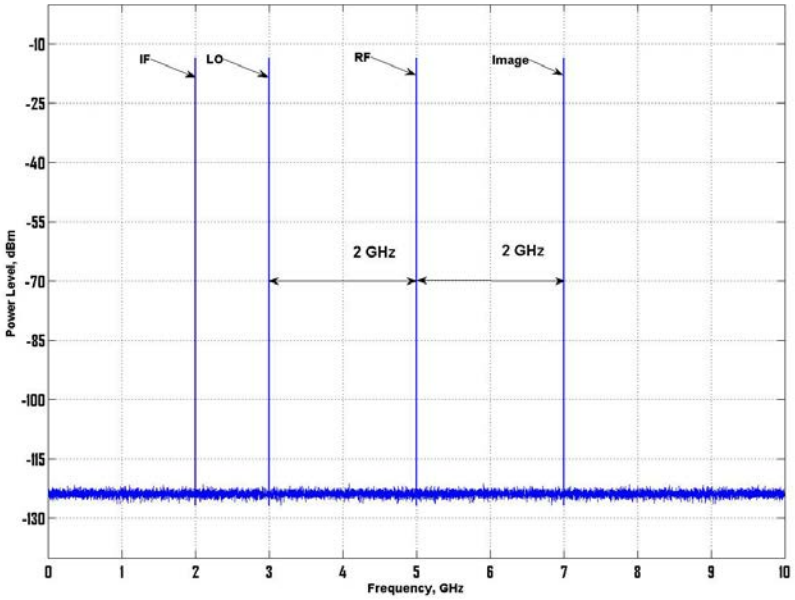

Figure 49: Output mixing image frequency

$$f_{img} = \begin{cases} f + 2 * f_{IF}, & if\ f_{LO} < f \\ f - 2 * f_{IF}, & if\ f_{LO} > f \end{cases} \tag{30}$$

If the receiver can be designed with a filter to reject the image frequency, then potential interference by signals within the image band can be reduced or eliminated. A higher IF produces a greater chance of easily filtering out the image frequency. The image rejection ratio (IRR) is the ratio between the desired signal level and the image signal level. A receiver with a larger IRR demonstrates better performance than receivers with a lower IRR. Those receivers with low IRR are far more likely to run into greater levels of interference than those with a higher IRR. In an ideal receiver, the IRR would be infinity as the image signal level would be zero. Equation (31) quantifies the IRR [11].

$$IRR = \frac{P_{out}}{Pimage_{out}} \tag{31}$$

Third-Order Intercept Point (IP3)

Figure 73 is a graph of the output power for a receiver given a first-order or fundamental signal (such as our desired signal at frequency f_1) and a third-order signal such as the $2f_1 - f_2$ two-tone third order product produced by our desired signal at f_1 and an undesired signal at f_2 as the input voltage V_0 increases, the third-order response increases cubically. This would lead to first-order responses with a slope of 1 and third-order responses with a slope of 3. For a third order response, the output power increases by 3dB for every 1dB increase from the input power. This increase demonstrates that the third order response contains a slope of 3 which is due to the output power containing third order products. A graphical comparison on a logarithmic scale of the first order and third order responses are seen in Figure 73.

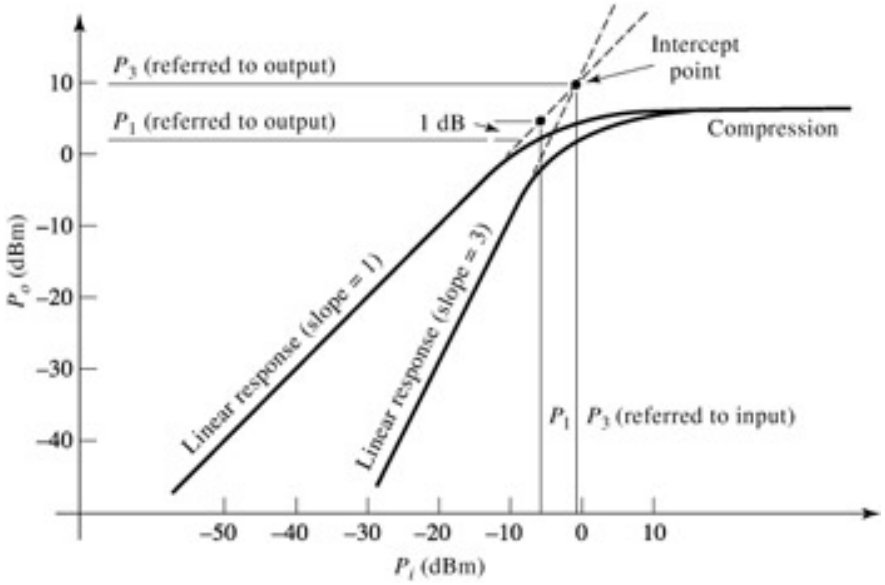

Figure 50: Input versus output power graph for first-order and third-order response [12]

$$P_{dB} = 10 * \log\left(\frac{P_o}{P_i}\right) = 10 * \log(P_O) - 10 * \log(P_i) \tag{32}$$

$$P_{dB\ (third-order)} = 10 * \log\left(\frac{{P_O}^3}{P_i}\right) = 30 * \log(P_O) - 10 * \log(P_i) \tag{33}$$

As can be seen in Equation (32) and Equation (33), the slope for the output power in the third-order response is three times greater than the slope of the first-order response. These responses will both display compression at higher input power with the 1dB compression point noted in the first-order response. The 1dB compression point demonstrates the point where the actual output power, affected by compression, is exactly one decibel in difference from the

idealized output power. The third-order intercept point (IP3) generally occurs past the 1dB compression point and is a theoretical point only found using the idealized output power. The dotted lines in Figure 73 demonstrate the ideal first and third-order responses. The point in which they intersect is considered to be the IP3. The IP3 can be divided into both the output third-order intercept point (OIP3) which relates to the rise of the IP3 and input third-order intercept point (IIP3), which relates to the run of the IP3. The IIP3 is more commonly preferred for receiver design while the OIP3 is more frequently used for transmitter design. The IP3 parameter is important since a greater IP3 demonstrates a more linear component. This parameter is used by many system designers in order to help approximate the spurious free dynamic range. This system for measuring third-order components provides more information about their performance [13].

Proof of IP3 Equation

The following walks through the proof of how we get Equation 10 from the traditional IP3 meaurements.

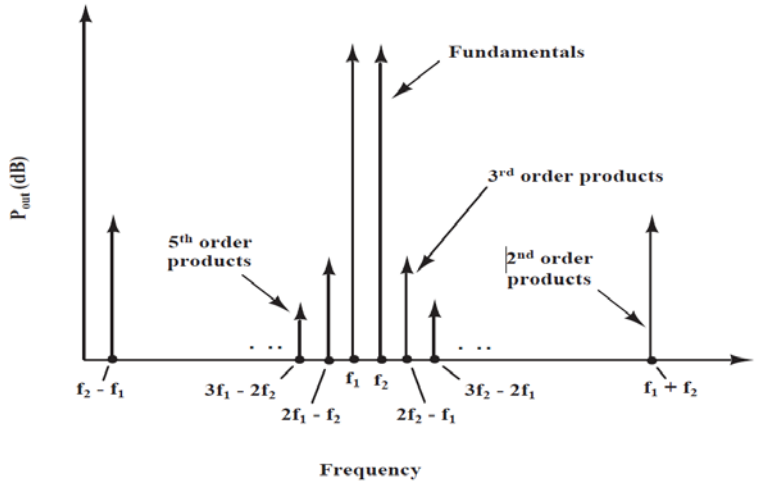

Figure 51: Frequency domain of two-tone IP3 measurement

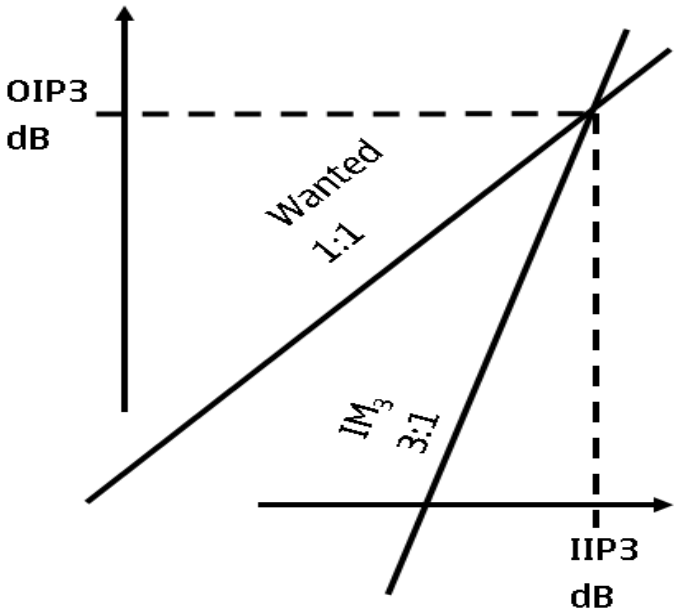

Figure 52: Graph of input power versus output power of fundamental and third-order tone

First we put two tones into the input of the device to calculate the nonlinearity using OIP3. Figure 74 shows a replica of what we see on a signal analyzer. Knowing that the input tone is linear and has a slope of 1 and the 3rd order product has a slope of 3, we can calculate the point at which they cross, which is seen in Figure 75.

Assumption:

Knowing that IP3 can be calculated using Equation 10, where P_1= fundamental tone power and P_3= third-order tone power, we set out to proof this formula.

$$OIP3 = \frac{3P_1 - P_3}{2} \tag{10}$$

Derivation:

First, we will use the point-slope formula seen in Equation 34 to calculate the formula of both the lines seen in Figure 75.

$$y - y_o = m(x - x_o) \tag{34}$$

$$y - P_1 = 1(x - P_{in}) \tag{35}$$

$$y - P_3 = 3(x - P_{in}) \tag{36}$$

Using the point-slope formula, we can see that the equation of the fundamental tone line is Equation 35 and the equation of the third-order tone line is Equation 36. All points are arbitrarily chosen. Next we well solve both equations for x.

$$\text{Fundamental: } y - P_1 = 1(x - P_{in}) \xrightarrow{yields} x = 1(y - P_1) + P_{in} \tag{37}$$

$$\text{Third-Order; } y - P_3 = 3(x - P_{in}) \xrightarrow{yields} x = \frac{1}{3}(y - P_3) + P_{in} \tag{38}$$

Using these two equations we set them equal to each other and solve for y.

$$1(y - P_1) + P_{in} = \frac{1}{3}(y - P_3) + P_{in} \tag{39}$$

$$3y - 3P_1 = (y - P_3) \tag{40}$$

$$3y - y = 3P_1 - P_3 \tag{41}$$

$$2y = 3P_1 - P_3 \tag{42}$$

$$y = \frac{3P_1 - P_3}{2} \tag{43}$$

However, due to the variation in measuring by hand, this formula assumes that all measurements lie directly on the line. To account for error within measurement, a couple of points should be taken and then averaged together to get the best result, which makes the final formula:

$$\sum_{n=1}^{\infty} y = \frac{3P_1^n - P_3^n}{2n} \tag{44}$$

Appendix II: Superheterodyne Rx02 and THA device two parameter measurements

In the following sections we list all of the data for Rx02. Since the majority of the reported data was similar to Rx01, we moved it into the appendix. The point of having two devices was to ensure that the first functional model was not operating by random chance and that the model can be verified. The current section only displays the graphs: please proceed to the results section for an in-depth analysis of each parameter measurement.

Superheterodyne 1dB Compression

Section 4.1.2 discusses the 1dB compression point of the superheterodyne receiver and how this data was collected.

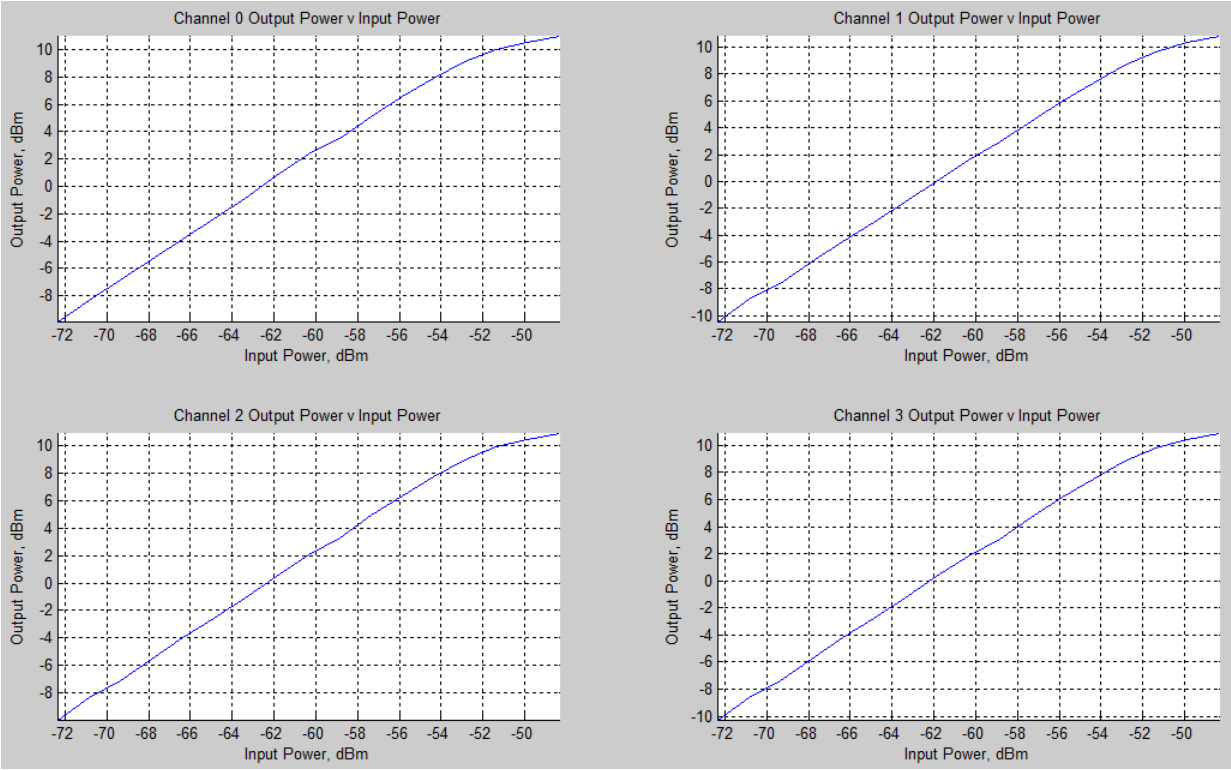

Figure 53: Output power versus input power for Rx02

Superheterodyne Group Delay

Section 4.2.2 discusses the group delay of the superheterodyne receiver and how this data was collected.

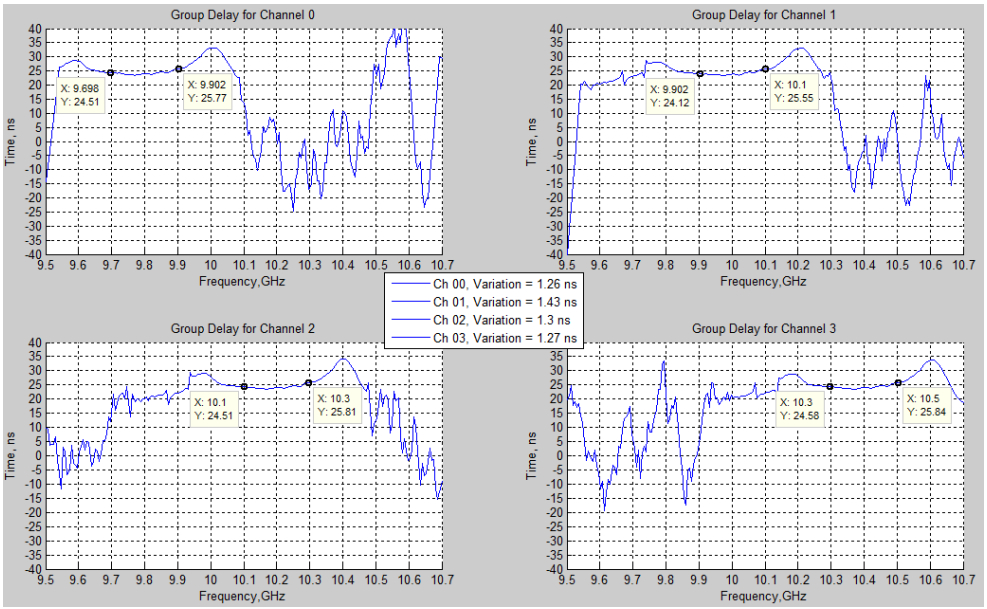

Figure 54: S21 parameter measuring delay across all four channels for Rx02

Superheterodyne In-band Spurs

Section 4.3.2 discusses the in-band spurs of the superheterodyne receiver and how this data was collected.

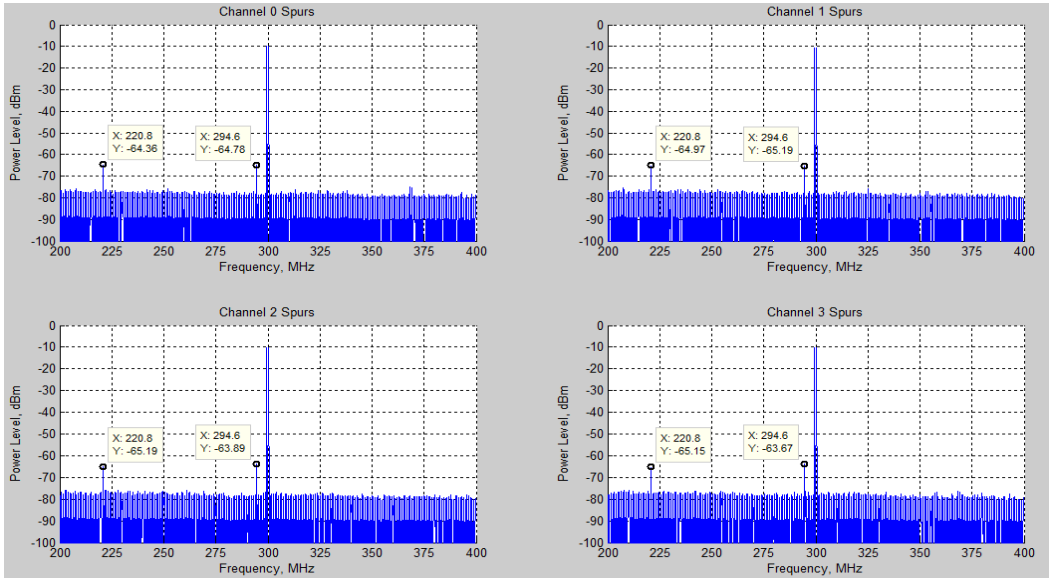

Figure 55: Output power level versus frequency for the In-band spurs of Rx02

Superheterodyne Input VSWR

Section 4.4.2 discusses the input VSWR of the superheterodyne receiver and how this data was collected.

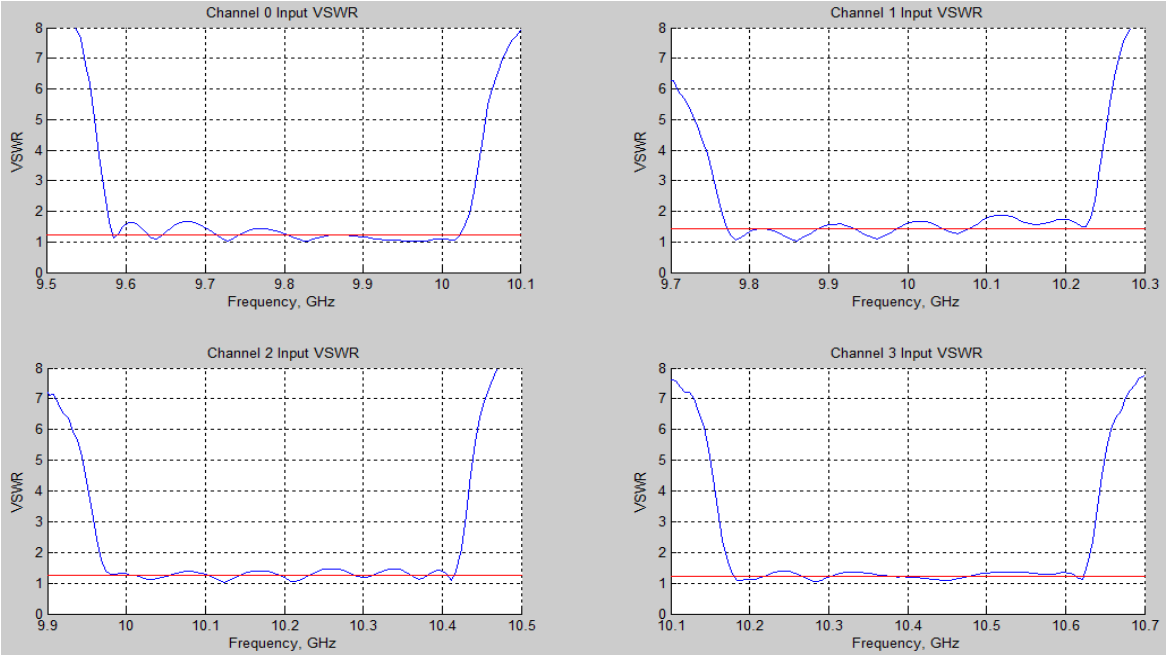

Figure 56: Input VSWR versus frequency for Rx02

Superheterodyne Noise Figure

Section 4.5.2 discusses the noise figure of the superheterodyne receiver and how this data was collected.

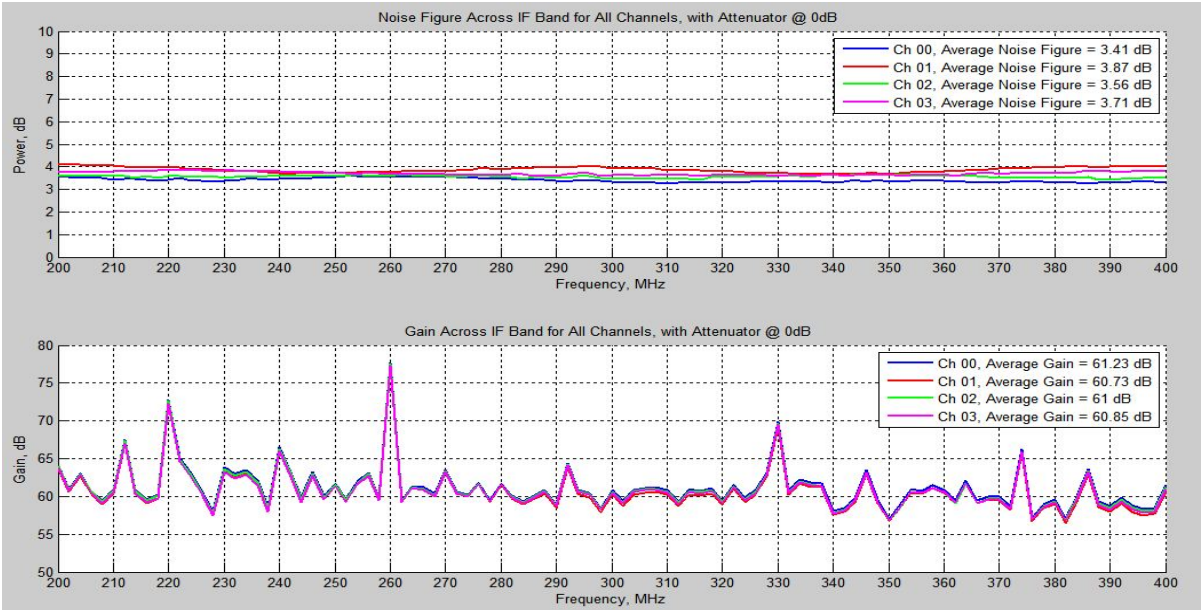

Figure 57: Rx02 noise figure and gain with variable attenuator at 0 dB

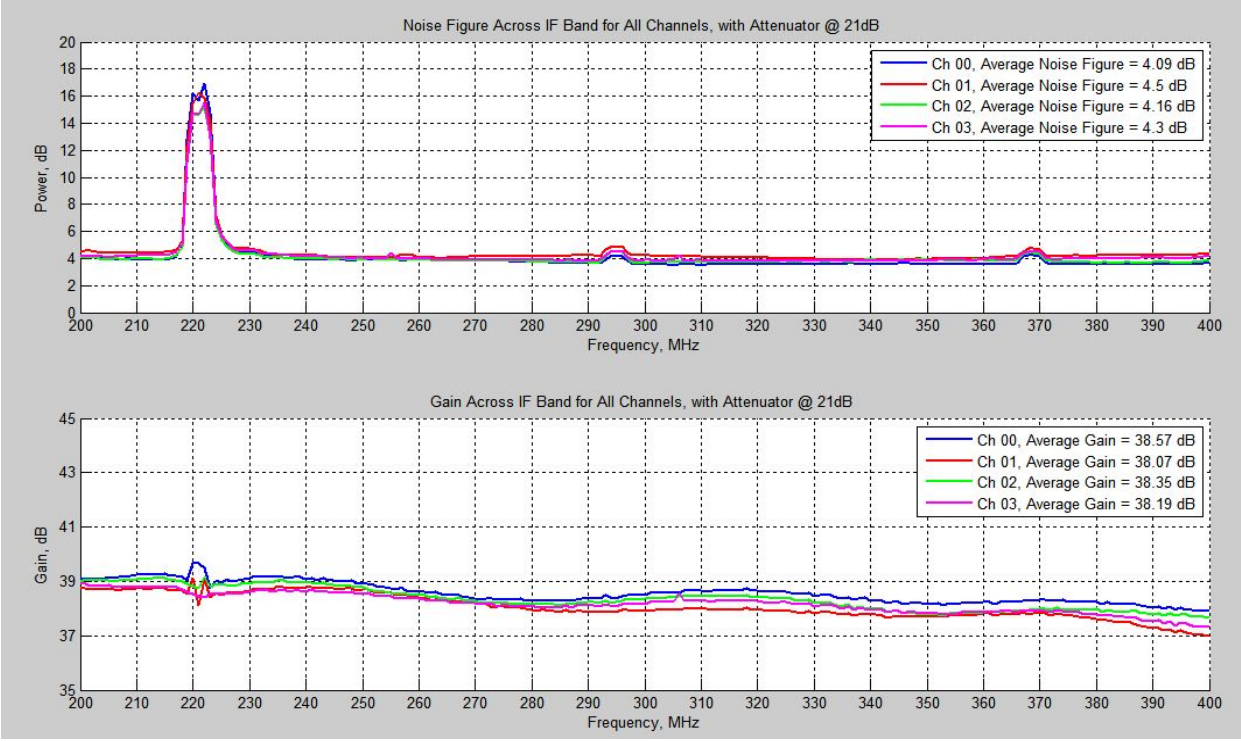

Figure 58: Rx02 noise figure and gain with variable attenuator at 21 dB

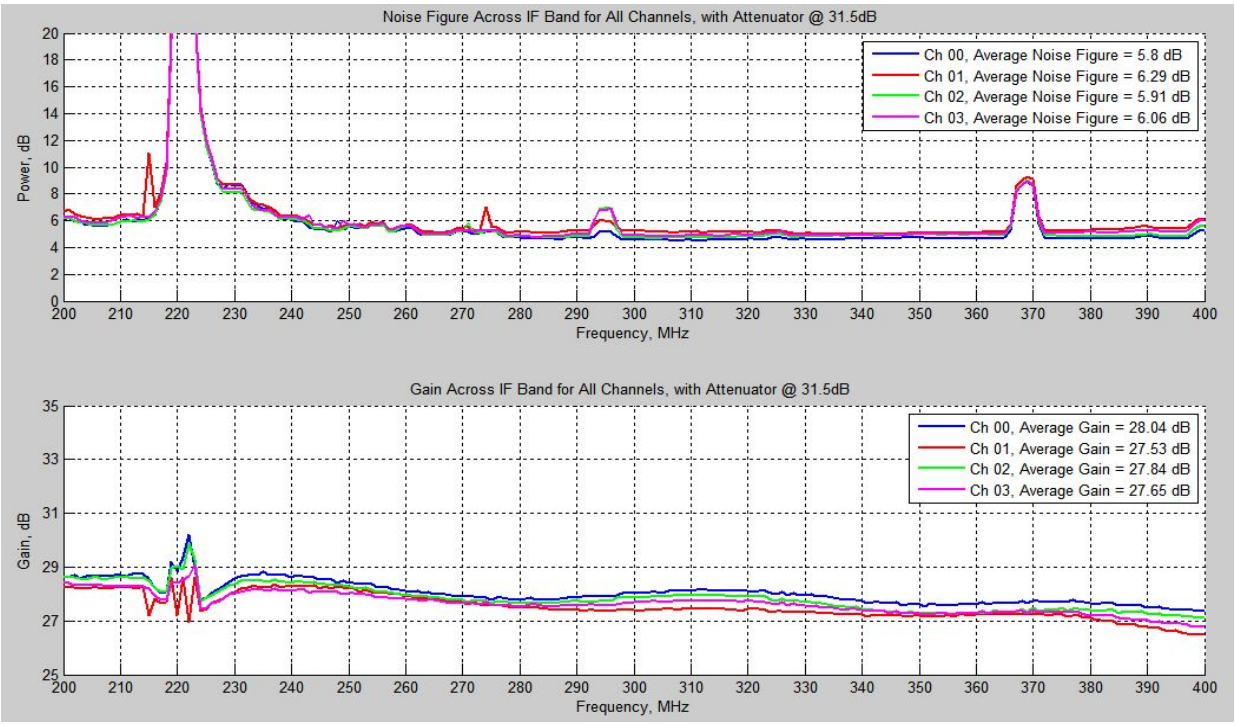

Figure 59: Rx02 noise figure and gain with variable attenuator at 31.5 dB

Superheterodyne Third-Order Intercept Point

Section 4.6.2 discusses the IP3 of the superheterodyne receiver and how this data was collected.

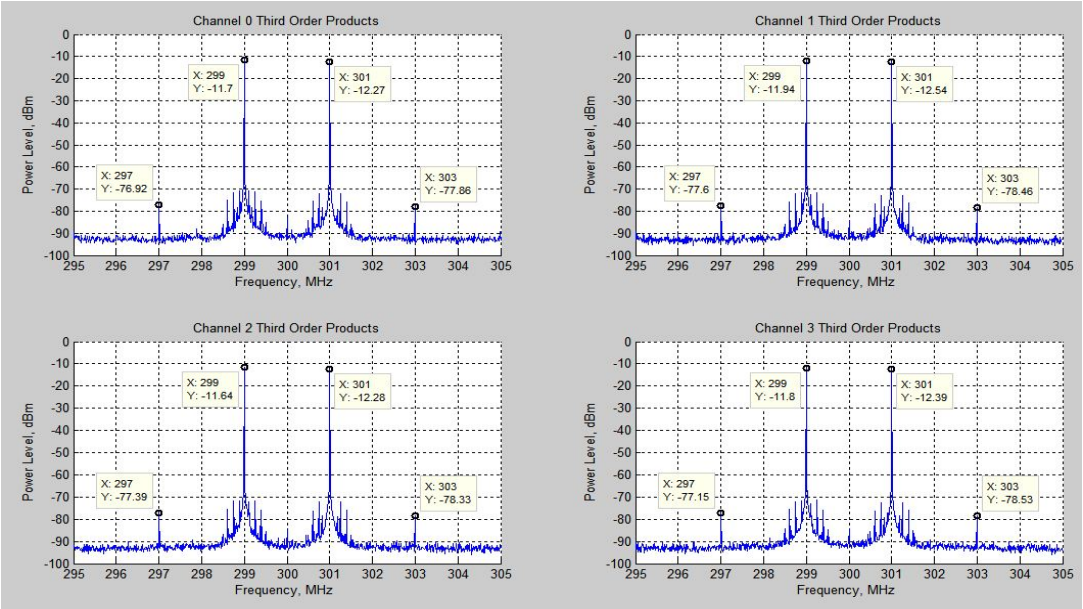

Figure 60: Output third-order intermodulated products versus frequency for Rx02

Superheterodyne Out of Band Rejection

Section 4.7.2 discusses the out of band rejection of the superheterodyne receiver and how this data was collected.

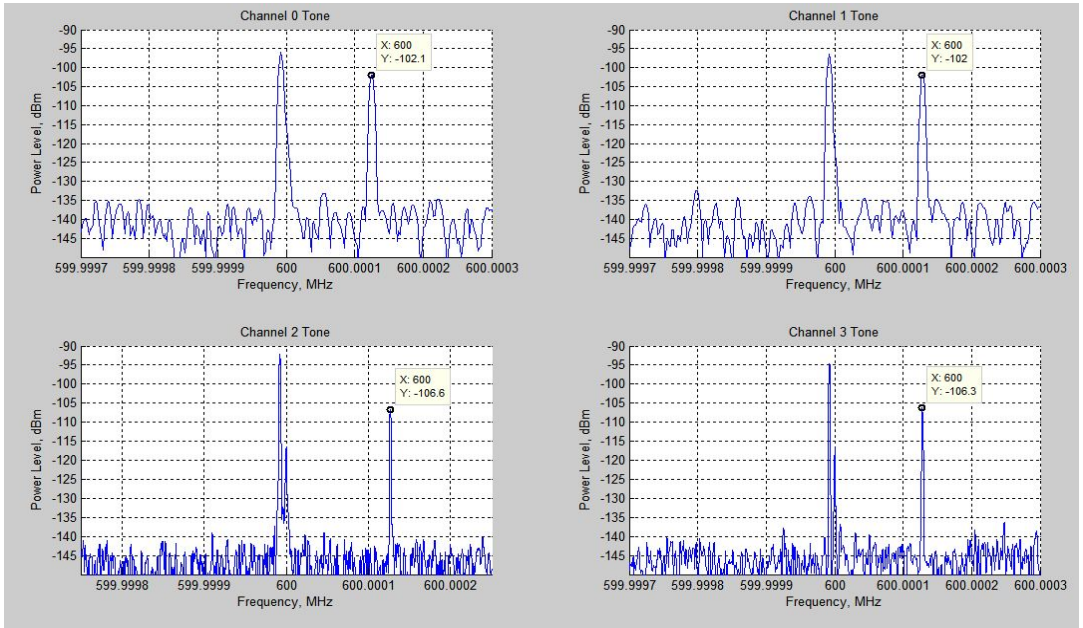

Figure 61: Out of band rejection versus frequency for Rx02

Superheterodyne Output VSWR

Section 4.8.2 discusses the output VSWR of the superheterodyne receiver and how this data was collected.

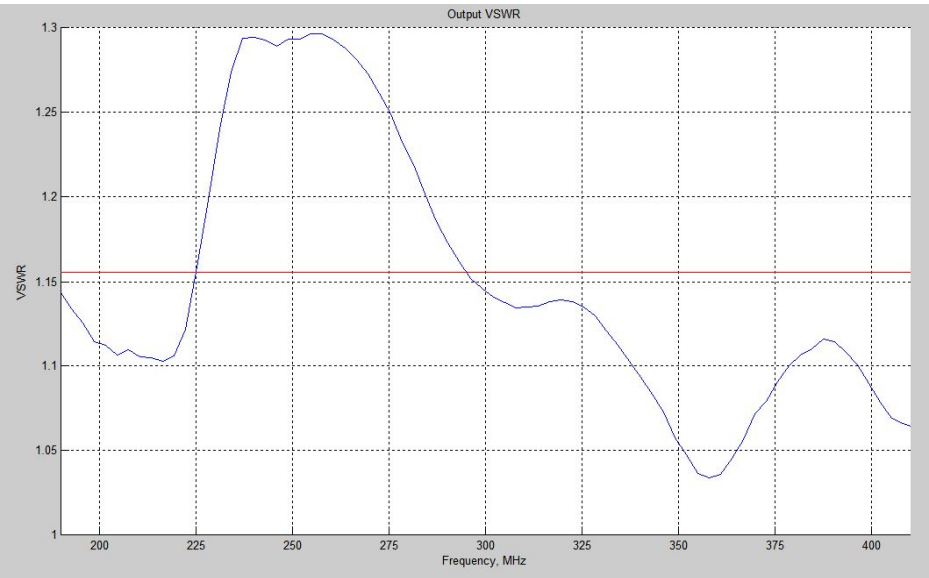

Figure 62: Output VSWR versus frequency for Rx01

Superheterodyne RF to IF Gain

Section 4.9.2 discusses the RF to IF gain of the superheterodyne receiver and how this data was collected.

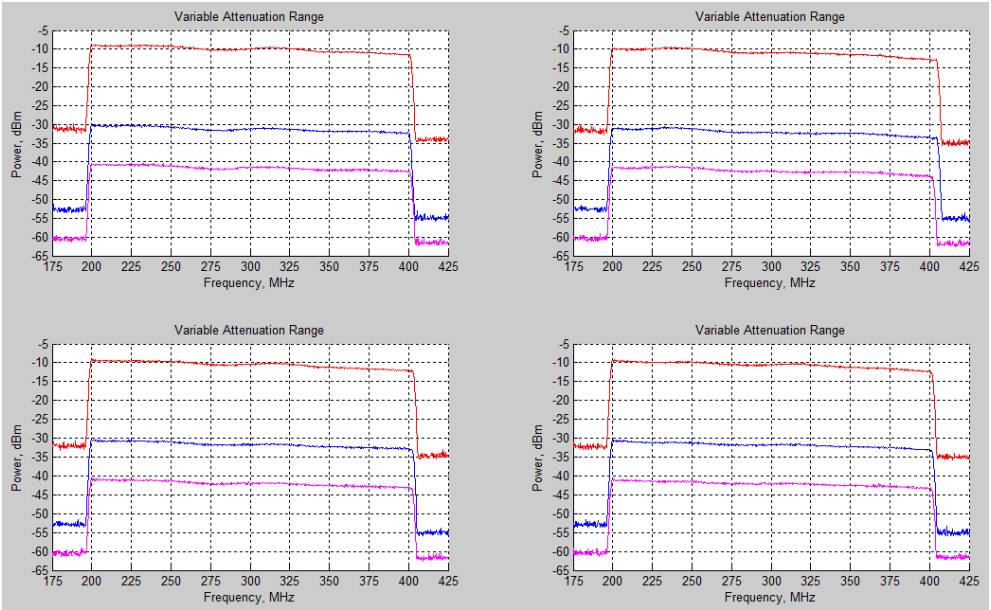

Figure 63: RF to IF Gain for Rx02

Track and Hold Noise Figure

Section 5.2.2 discusses the noise figure of the track and hold receiver and how this data was collected.

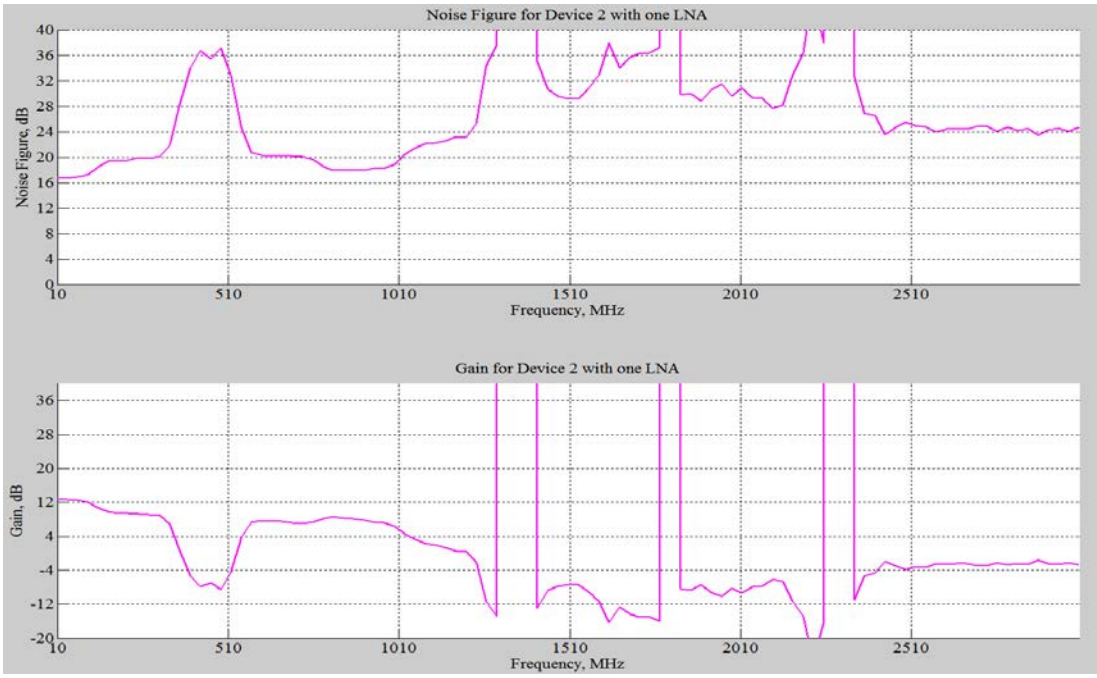

Figure 64: THA noise figure and gain with one LNA for device 2

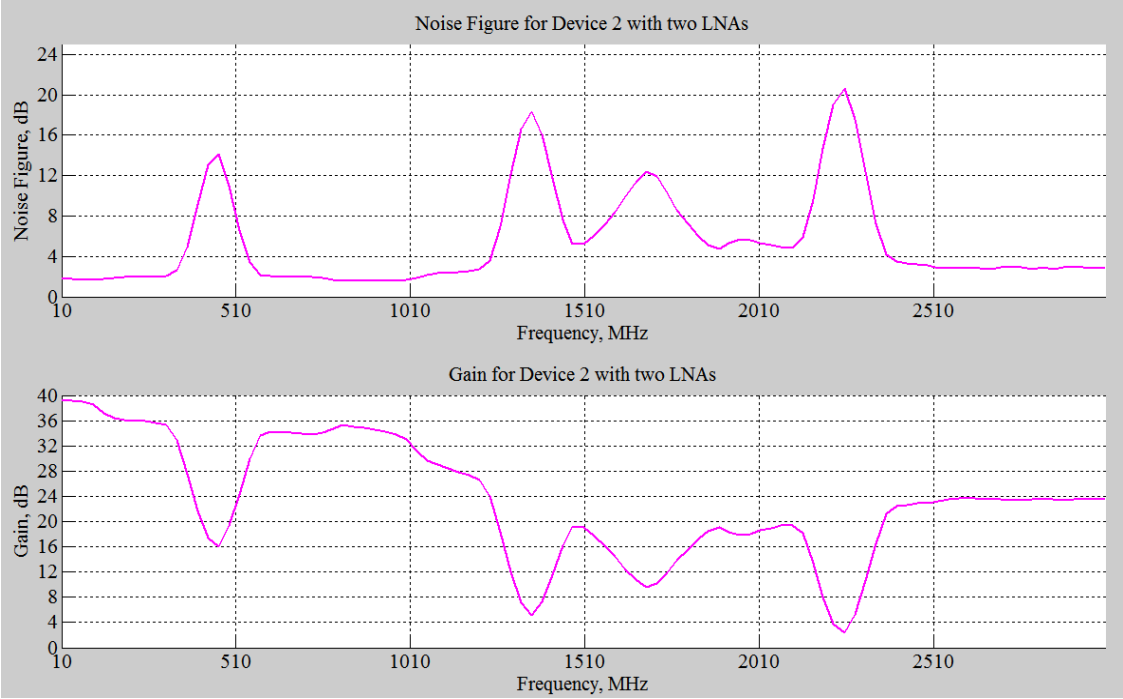

Figure 65: THA noise figure and gain with two LNAs for device 2

Track and Hold Signal to Noise Ratio

Section 5.3.2 discusses the signal to noise ratio of the track and hold receiver and how this data was collected.

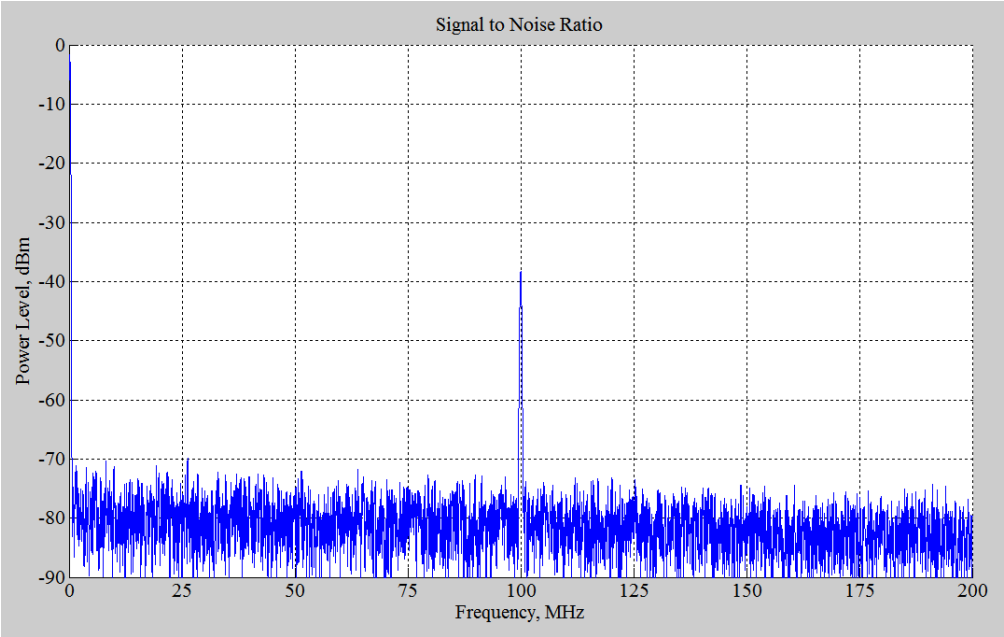

Figure 66: Signal power level with IF = 300 MHz and clock at 900 MHz for device 2

Track and Hold 1dB Compression

Section 5.4.2 discusses the 1dB compression of the track and hold receiver and how this data was collected.

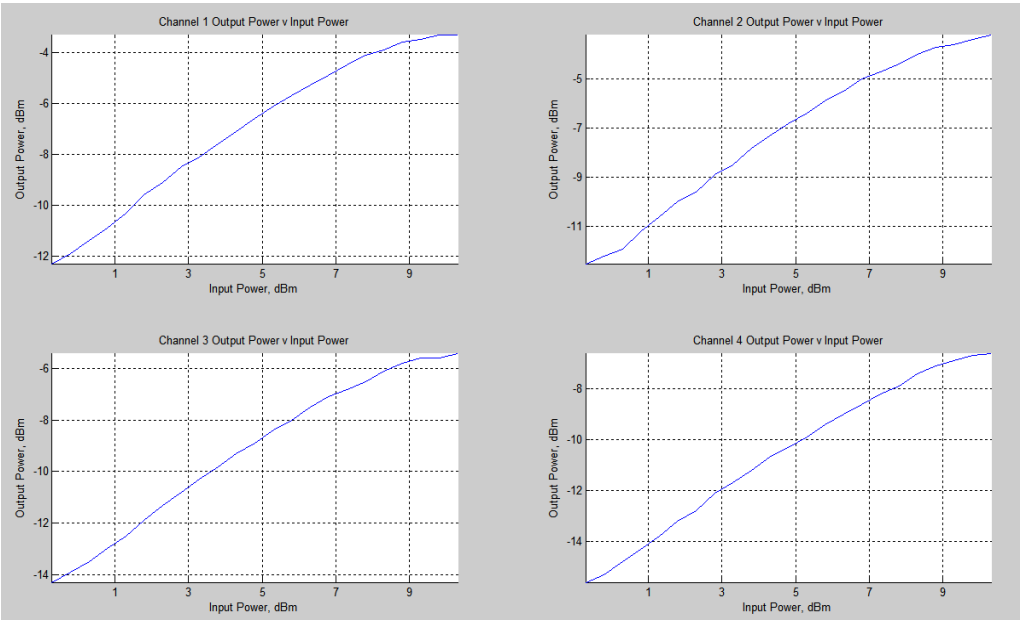

Figure 67: Output versus input power for device 2

Track and Hold Third-Order Intercept Point

Section 5.5.2 discusses third-order intercept point of the track and hold receiver and how this data was collected.

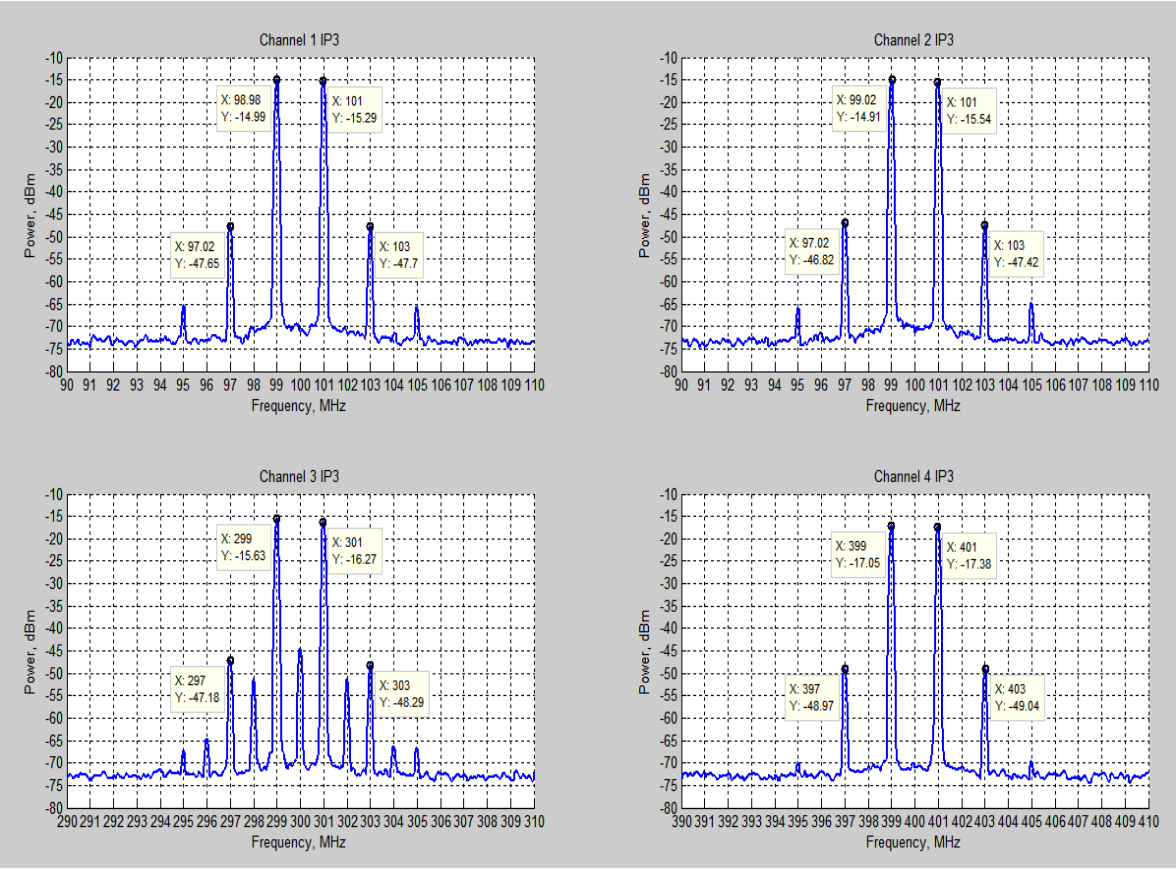

Figure 68: IP3 for device 2 for all four channels